

THE USE OF FIVE AND SIX BOND LONG-RANGE  $^1\text{H}$ - $^1\text{H}$  AND  $^1\text{H}$ - $^{19}\text{F}$   
COUPLING CONSTANTS IN THE DETERMINATION OF  
CONFORMATIONAL PREFERENCES IN SOME SUBSTITUTED  
DERIVATIVES OF TOLUENE AND THE DETERMINATION OF THE  
NATURE OF THE ROTATIONAL BARRIER IN  
 $\alpha,\alpha$ -DIACETOXYTOLUENE DERIVATIVES.

by



CRAIG S. TAKEUCHI

A thesis submitted to the  
Faculty of Graduate Studies  
in partial fulfillment  
of the requirements of the degree

Master of Science

Winnipeg, Manitoba,

July, 1988

Permission has been granted to the National Library of Canada to microfilm this thesis and to lend or sell copies of the film.

The author (copyright owner) has reserved other publication rights, and neither the thesis nor extensive extracts from it may be printed or otherwise reproduced without his/her written permission.

L'autorisation a été accordée à la Bibliothèque nationale du Canada de microfilmer cette thèse et de prêter ou de vendre des exemplaires du film.

L'auteur (titulaire du droit d'auteur) se réserve les autres droits de publication; ni la thèse ni de longs extraits de celle-ci ne doivent être imprimés ou autrement reproduits sans son autorisation écrite.

ISBN 0-315-47983-3

THE USE OF FIVE AND SIX BOND LONG-RANGE  $^1\text{H}$ - $^1\text{H}$  AND  $^1\text{H}$ - $^{19}\text{F}$   
COUPLING CONSTANTS IN THE DETERMINATION OF CONFORMATIONAL PREFERENCES  
IN SOME SUBSTITUTED DERIVATIVES OF TOLUENE AND THE DETERMINATION OF THE  
NATURE OF THE ROTATIONAL BARRIER IN  $\alpha,\alpha$ -DIACETOXYTOLUENE DERIVATIVES

BY

CRAIG S. TAKEUCHI

A thesis submitted to the Faculty of Graduate Studies of  
the University of Manitoba in partial fulfillment of the requirements  
of the degree of

MASTER OF SCIENCE

© 1988

Permission has been granted to the LIBRARY OF THE UNIVER-  
SITY OF MANITOBA to lend or sell copies of this thesis. to  
the NATIONAL LIBRARY OF CANADA to microfilm this  
thesis and to lend or sell copies of the film, and UNIVERSITY  
MICROFILMS to publish an abstract of this thesis.

The author reserves other publication rights, and neither the  
thesis nor extensive extracts from it may be printed or other-  
wise reproduced without the author's written permission.

## ACKNOWLEDGEMENTS

I wish to thank my supervisor Dr. Ted Schaefer for his encouragement, guidance and advice relating to this work and to other matters. His patience with me is greatly appreciated.

I thank Mr. Rudy Sebastian for his invaluable instruction with the use of many computer programs used and in running and analyzing high-resolution nmr spectra during the course of this work.

I also thank Mr. Kirk Marat for his help with the Bruker AM300 spectrometer. His high standards in maintaining the AM300 have enabled me to obtain some excellent high resolution spectra.

I am grateful to Dr. N.R. Hunter, Dr. J.L. Charlton and Dr. D.M. McKinnon for their advice regarding organic syntheses in this project and in other work. I would also like to thank Dr. A.F. Janzen for his advice regarding synthesis of some fluorinated compounds.

I thank my friends and colleagues Glenn Penner, Rudy Sebastian, Potlaki Tseki, Mike Sowa, Dr. Jim Peeling, Kirk Marat and Andre Silvanovich for some interesting and helpful discussions.

I would also like to thank my family, whose support and encouragement throughout my undergraduate years enabled me to pursue a career in chemistry.

## TABLE OF CONTENTS

	<u>Page</u>
PART I The Use of Five and Six Bond Long-Range $^1\text{H}$ - $^1\text{H}$ and $^1\text{H}$ - $^{19}\text{F}$ Coupling Constants in the Determination of Conformational Preferences in Some Substituted Derivatives of Toluene .....	1
A) INTRODUCTION .....	2
1) Experimental Investigations .....	3
2) Introduction to the Problem .....	13
B) EXPERIMENTAL METHODS .....	15
1) Materials and Syntheses .....	16
A) preparation of 3,5-difluorotoluene .....	16
B) preparation of 3,5-difluoroethylbenzene .....	17
C) preparation of 3,5-difluoroisopropylbenzene .....	18
D) preparation of 2,3-difluorotoluene .....	21
E) preparation of 2,3-difluoro- $\alpha,\alpha$ -diacetoxytoluene .....	22
F) preparation of 2-bromo-5-fluoro- $\alpha,\alpha$ -diacetoxytoluene .....	23
2) Sample Preparation .....	24
3) Spectroscopic Method .....	25
4) Computations .....	26
C) EXPERIMENTAL RESULTS .....	27
1) 3,5-difluorotoluene .....	28
a) determination of the relative sign of $^5J_m(\text{F},\text{CH}_3)$ by double resonance experiments .....	31
2) 3,5-difluoroethylbenzene .....	37
a) determination of the relative sign of $^5J_m(\text{F},\text{CH}_2)$ by double resonance experiments .....	40
3) 3,5-difluoroisopropylbenzene .....	45
a) determination of the relative sign of $^5J_m(\text{F},\text{CH})$ by double resonance experiments .....	48
4) 2,3-difluorotoluene .....	51

	<u>Page</u>
5) 2,3-difluoro- $\alpha,\alpha$ -diacetoxytoluene .....	58
a) determination of the relative sign of $^5J_m(\text{F,CH})$ .....	62
6) 2-bromo-5-fluoro- $\alpha,\alpha$ -diacetoxytoluene .....	69
 D) DISCUSSION .....	 77
 E) SUMMARY AND CONCLUSIONS .....	 86
 F) REFERENCES .....	 88

	<u>Page</u>
PART II The Determination of the Nature of the Rotational Barrier in $\alpha,\alpha$ -Diacetoxytoluene Derivatives .....	92
A) INTRODUCTION .....	93
B) EXPERIMENTAL METHODS .....	97
1) Materials and Syntheses .....	98
A) preparation of $\alpha,\alpha$ -diacetoxytoluene .....	98
B) preparation of 2,6-dibromo- $\alpha,\alpha$ -diacetoxytoluene .....	99
2) Sample Preparation .....	100
3) Spectroscopic Method .....	101
4) Computations .....	102
C) EXPERIMENTAL RESULTS .....	103
1) 2,6-dibromotoluene .....	104
2) 2,6-dibromo- $\alpha,\alpha$ -diacetoxytoluene .....	108
a) determination of the relative sign of ${}^6J_p(\text{H,CH})$ by double resonance experiments .....	111
3) $\alpha,\alpha$ -diacetoxytoluene .....	115
D) DISCUSSION .....	122
E) SUMMARY AND CONCLUSIONS .....	129
F) REFERENCES .....	131

## LIST OF FIGURES

### PART I

<u>Figure</u>		<u>Page</u>
1	Definition of the dihedral angle for the four-bond coupling, ${}^4J_o(\text{H}, \text{CH}_3)$ ; the dihedral angle is $\text{H}_\alpha\text{-C}_\alpha\text{-C}_1\text{-C}_2$ .....	5
2	${}^5J_m(\text{H}, \text{CH}_3)$ coupling paths in a symmetrical benzene derivative where $\text{H}_\alpha$ is in the plane of the benzene ring .....	6
3	A plot of the INDO MO FPT values of ${}^4J_o(\text{F}, \text{CH}_3)$ for 2-fluorotoluene as a function of the dihedral angle $\Theta$ . The empirical couplings are determined by Schaefer et al <sup>27</sup> as shown in the upper curve .....	10
4	Benzal compounds which are "locked" into <i>cis</i> and <i>trans</i> conformers with the appropriate <i>ortho</i> substituents .....	11
5	Compounds with a reduction in the three-fold symmetry of the sidechain (side-view) using $\alpha$ -substituents .....	13
6	A first-order representation of the line spectra for the methyl protons and the <i>para</i> proton $\text{H}_4$ in 3,5-difluorotoluene .....	32
7	Sign determination of ${}^5J_m(\text{F}, \text{CH}_3)$ in 3,5-difluorotoluene .....	33
	A) the spectral region of the <i>para</i> proton $\text{H}_4$ of 3,5-difluorotoluene .....	33
	B) with irradiation of line 15 of the methyl group (low frequency peak) .....	33
	C) with irradiation of line 1 of the methyl group (high frequency peak) .....	33



<u>Figure</u>		<u>Page</u>
8	A) the methyl proton region of 3,5-difluorotoluene ..... B) computer simulation of the methyl proton region using the parameters from Table 1 assuming a linewidth of 0.08 Hz .....	34 34
9	NMR spectrum of the <i>para</i> proton H <sub>4</sub> for 3,5-difluorotoluene .....	35
10	Fluorine-19 spectrum for the <i>meta</i> fluorines in 3,5-difluorotoluene .....	36
11	Sign determination of $^5J_m(\text{F}, \text{CH}_2)$ in 3,5-difluoroethylbenzene ..... A) a low frequency multiplet with no irradiation ..... B) a low frequency multiplet with irradiation of the low frequency peak in the methyl proton region ..... C) predicted low frequency multiplet with irradiation of the low frequency peak in the methyl proton region .....	41 41 41 41
12	The proton nmr regions for the ethyl sidechain in 3,5-difluoroethylbenzene .....	42
13	Fluorine-19 nmr spectrum for the <i>meta</i> fluorines in 3,5-difluoroethylbenzene .....	43
14	NMR spectrum for the <i>para</i> proton H <sub>4</sub> region in 3,5-difluoroethylbenzene .....	44
15	Sign determination of $^5J_m(\text{F}, \text{CH})$ in 3,5-difluoroisopropylbenzene ..... A) <i>meta</i> fluorine region with no irradiation of peaks in the methyl region .....	49 49

<u>Figure</u>		<u>Page</u>
	B) with irradiation of the low frequency peak of the methyl doublet .....	49
	C) with irradiation of the high frequency peak of the methyl doublet .....	49
16	NMR spectrum for the <i>para</i> proton H <sub>4</sub> in 3,5-difluoroisopropylbenzene .....	50
17	Methyl proton region of 2,3-difluorotoluene .....	54
18	Ring proton region of 2,3-difluorotoluene .....	55
19	<sup>19</sup> F nmr spectrum for the <i>meta</i> fluorine F <sub>5</sub> region in 2,3-difluorotoluene .....	56
20	The <i>ortho</i> fluorine F <sub>6</sub> region of 2,3-difluorotoluene .....	57
21	Sign determination of <sup>5</sup> J <sub>m</sub> (F,CH) in 2,3-difluoro- $\alpha,\alpha$ -diacetoxytoluene .....	63
	A) experimental <i>meta</i> fluorine-19 region .....	63
	B) simulated <i>meta</i> fluorine-19 region with <sup>5</sup> J <sub>m</sub> (F,CH) < 0 .....	63
	C) simulated <i>meta</i> fluorine-19 region with <sup>5</sup> J <sub>m</sub> (F,CH) > 0 .....	63
22	The methyl and methine regions of 2,3-difluoro- $\alpha,\alpha$ -diacetoxytoluene .....	64
23	The <i>meta</i> ring proton region of 2,3-difluoro- $\alpha,\alpha$ -diacetoxytoluene .....	65
24	The <i>ortho</i> and <i>para</i> proton regions of 2,3-difluoro- $\alpha,\alpha$ -diacetoxytoluene .....	66

<u>Figure</u>		<u>Page</u>
25	The <i>ortho</i> fluorine region of 2,3-difluoro- $\alpha,\alpha$ -diacetoxytoluene .....	67
26	The <i>meta</i> fluorine region of 2,3-difluoro- $\alpha,\alpha$ -diacetoxytoluene .....	68
27	The methyl and methine proton regions of 2-bromo-5-fluoro- $\alpha,\alpha$ -diacetoxytoluene .....	72
28	The <i>meta</i> proton ring region of 2-bromo-5-fluoro- $\alpha,\alpha$ -diacetoxytoluene .....	73
29	The <i>ortho</i> proton ring region of 2-bromo-5-fluoro- $\alpha,\alpha$ -diacetoxytoluene .....	74
30	The <i>para</i> proton region of 2-bromo-5-fluoro- $\alpha,\alpha$ -diacetoxytoluene .....	75
31	$^{19}\text{F}$ nmr spectrum of the <i>meta</i> fluorine in 2-bromo-5-fluoro- $\alpha,\alpha$ -diacetoxytoluene .....	76
32	A plot of the angle dependence of $^5J_{\text{m}}(\text{F},\text{CH}_3)$ for 3,5-difluorotoluene from INDO MO FPT calculations .....	80
33	Equilibrium showing two different conformers of 2-bromo-5-fluoro- $\alpha,\alpha$ -diacetoxytoluene .....	85

## PART II

<u>Figure</u>		<u>Page</u>
1	Definition of the dihedral angle for the six-bond coupling, ${}^6J_p(\text{CH}_3, \text{H}_4)$ ; the dihedral angle is defined by $\text{H}_\alpha\text{-C}_\alpha\text{-C}_1\text{-C}_2$ .....	95
2	A diagram showing the different substituted toluene derivatives studied in part II .....	96
3	Proton nmr spectrum for the methyl group in 2,6-dibromotoluene. The linewidth at half-height is estimated to be 0.04 Hz .....	107
4	Sign determination of ${}^6J_p(\text{H}, \text{CH}_3)$ in 2,6-dibromo- $\alpha, \alpha$ -diacetoxytoluene using partial decoupling experiments .....	112
	A) <i>para</i> proton region with no decoupling .....	112
	B) with partial decoupling of the high frequency peak of the <i>meta</i> doublet .....	112
5	The methyl and methine proton regions in 2,6-dibromo- $\alpha, \alpha$ -diacetoxytoluene .....	113
6	The <i>meta</i> and <i>para</i> ring proton regions in 2,6-dibromo- $\alpha, \alpha$ -diacetoxytoluene .....	114
	A) <i>meta</i> proton nmr spectrum .....	114
	B) <i>para</i> proton nmr spectrum .....	114
7	The methyl and methine proton regions in $\alpha, \alpha$ -diacetoxytoluene .....	119
	A) methyl proton region .....	119
	B) methine proton region .....	119

<u>Figure</u>		<u>Page</u>
8	The <i>ortho</i> ring proton region of $\alpha,\alpha$ -diacetoxytoluene .....	120
9	Spectrum of the <i>meta para</i> ring proton region of $\alpha,\alpha$ -diacetoxytoluene .....	121

# LIST OF TABLES

## PART I

<u>Table</u>	<u>Page</u>
1      Proton and fluorine spectral parameters for a 2.5 mole% solution of 3,5-difluorotoluene in CS <sub>2</sub> /C <sub>6</sub> D <sub>12</sub> at 300 K .....	29
2      Proton and fluorine spectral parameters for a 2.5 mole% solution of 3,5-difluoroethylbenzene in CS <sub>2</sub> /C <sub>6</sub> D <sub>12</sub> at 300 K .....	38
3      Proton and fluorine spectral parameters for a 1.0 mole% solution of 3,5-difluoroisopropylbenzene in CS <sub>2</sub> /C <sub>6</sub> D <sub>12</sub> at 300 K .....	46
4      Proton and fluorine spectral parameters for a 3.9 mole% solution of 2,3-difluorotoluene in CS <sub>2</sub> /C <sub>6</sub> D <sub>12</sub> at 300 K .....	52
5      Proton and fluorine spectral parameters for a 2.0 mole% solution of 2,3-difluoro- $\alpha,\alpha$ -diacetoxytoluene in CS <sub>2</sub> /C <sub>6</sub> D <sub>12</sub> and a 2.1 mole% solution of 2,3-difluoro- $\alpha,\alpha$ -diacetoxytoluene in acetone-d <sub>6</sub> at 300 K .....	59
6      Proton and fluorine spectral parameters for a 3.2 mole% solution of 2-bromo-5-fluoro- $\alpha,\alpha$ -diacetoxytoluene in CS <sub>2</sub> /C <sub>6</sub> D <sub>12</sub> at 300 K .....	70
7      INDO and CNDO/2 MO FPT values in Hz for $^5J_m(\text{F,CH})$ in 3,5-difluorotoluene for a standard geometry .....	79

## PART II

<u>Table</u>	<u>Page</u>
1      Proton spectral parameters for a 2.5 mole% solution of 2,6-dibromotoluene in CS <sub>2</sub> /C <sub>6</sub> D <sub>12</sub> and a 3.0 mole% solution of 2,6-dibromotoluene in acetone-d <sub>6</sub> at 300 K .....	105
2      Proton spectral parameters for a 3.0 mole% solution of 2,6-dibromo- $\alpha,\alpha$ -diacetoxytoluene in CS <sub>2</sub> /C <sub>6</sub> D <sub>12</sub> and a 3.1 mole% solution of 2,6-dibromo- $\alpha,\alpha$ -diacetoxytoluene in acetone-d <sub>6</sub> at 300 K .....	109
3      Proton spectral parameters for a 2.0 mole% solution of $\alpha,\alpha$ -diacetoxytoluene in CS <sub>2</sub> /C <sub>6</sub> D <sub>12</sub> and a 2.1 mole% solution of $\alpha,\alpha$ -diacetoxytoluene in acetone-d <sub>6</sub> at 300 K .....	116

# ABSTRACT

In part I, the CNDO/2 and INDO MO FPT values for  ${}^5J_m(\text{F}, \text{CH}_3)$  in 3-fluoro and 3,5-difluorotoluene are exactly reproduced by  $A + B\sin^2\Theta + C\sin^2(\Theta/2)$ . Here  $\Theta$  is the angle by which the  $\alpha$  C-H bond twists out of the plane of the benzene ring. Adjustment of A, B and C to give agreement with experiment for 3,5-difluorotoluene yields an empirical equation which is tested by  ${}^5J_m(\text{F}, \text{CH})$  in 3,5-difluoroethylbenzene and 3,5-difluoroisopropylbenzene. The equation reproduces  ${}^5J_m(\text{F}, \text{CH})$  in these two compounds, the values of  $\langle \sin^2\Theta \rangle$  being derived from  ${}^6J_p(\text{H}, \text{CH})$ , the spin-spin coupling constant over six bonds between the  $\alpha$  and *para* ring protons.  ${}^5J_m(\text{F}, \text{CH})$  is obtained for the asymmetrical compounds, 2,3-difluoro- $\alpha, \alpha$ -diacetoxytoluene and 2-bromo-5-fluoro- $\alpha, \alpha$ -diacetoxytoluene. It is shown how  ${}^5J_m(\text{F}, \text{CH})$  in the latter compound can discriminate between two conformers, each of which, on the basis of  ${}^6J_p(\text{H}, \text{CH})$ , will be characterized by a large degree of torsion about the  $\text{Csp}^2\text{-Csp}^3$  bond.

In part II, the  ${}^1\text{H}$  nmr spectral parameters are given for  $\alpha, \alpha$ -diacetoxytoluene in  $\text{CS}_2$  and acetone- $\text{d}_6$  solutions. The long-range spin-spin constant over six bonds,  ${}^6J(\text{H}, \text{CH})$ , is used to derive apparent twofold barriers to rotation about the exocyclic  $\text{Csp}^2\text{-Csp}^3$  bond in the two solutions. The conformation of lowest energy has the  $\alpha$  C-H bond in the plane of the benzene ring. The barrier is higher in  $\text{CS}_2$  than in acetone- $\text{d}_6$  solution, in contrast to a molecule like benzyl chloride. In 2,6-dibromo- $\alpha, \alpha$ -diacetoxytoluene, the free energy of activation for rotation about the  $\text{Csp}^2\text{-Csp}^3$  bond is 36 kJ/mole at 165 K in dimethyl ether solution. Such a high barrier implies a very small six-bond proton-proton coupling constant for this compound because  ${}^6J_p(\text{H}, \text{CH})$  is proportional to the expectation value of  $\sin^2\Theta$ . The angle  $\Theta$  is zero when the  $\alpha$  C-H bond lies in the plane of the benzene ring. The observed  ${}^6J_p(\text{H}, \text{CH})$  coupling is -0.051 Hz in acetone- $\text{d}_6$  solution; its sign is determined by double resonance experiments. The question of an angle-independent component of  ${}^6J$  that



is, whether  ${}^6J$  is finite at  $\Theta = 0^\circ$ , is addressed. A maximum magnitude of 0.02 Hz may be present at  $\Theta = 0^\circ$  for 2,6-dibromo- $\alpha,\alpha$ -diacetyltoluene, although a zero magnitude is also compatible with the experimental data. In a compound with a higher internal barrier,  $\alpha,\alpha,2,6$ -tetrachlorotoluene, the experimental results are most compatible with a negligibly small  ${}^6J_p(\text{H,CH})$  at  $\Theta = 0^\circ$ .

## PART I

The Use of Five and Six Bond Long-Range  
 $^1\text{H}$ - $^1\text{H}$  and  $^1\text{H}$ - $^{19}\text{F}$  Coupling Constants in the  
Determination of Conformational Preferences  
In Some Substituted Derivatives of Toluene

## A. INTRODUCTION

# FIGURE 1

Definition of the dihedral angle for the four-bond coupling,  ${}^4J_o(\text{H}, \text{CH}_3)$ ;  
the dihedral angle is defined by  $\text{H}_\alpha - \text{C}_\alpha - \text{C}_1 - \text{C}_2$

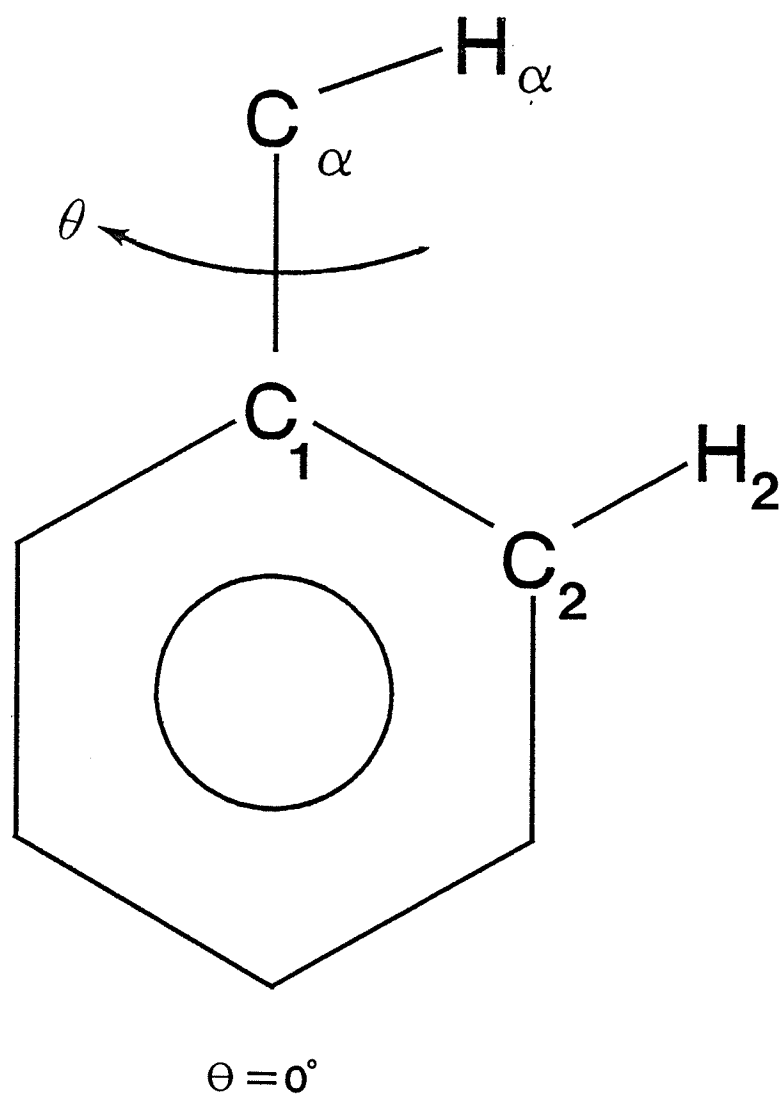
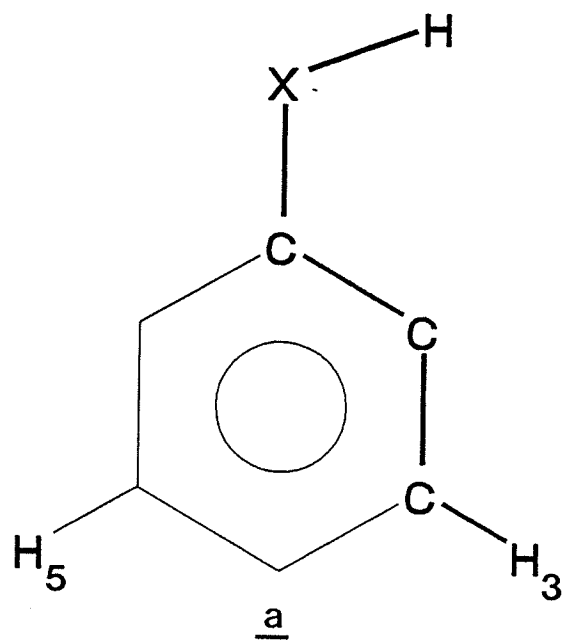


FIGURE 2

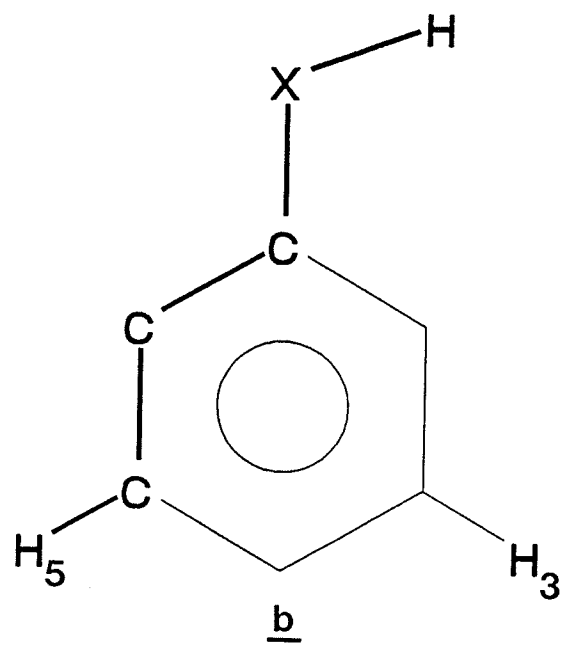
$^5J_m(\text{H}, \text{CH}_3)$  coupling paths in a symmetrical benzene derivative where  $\text{H}_\alpha$  is in the plane of the benzene ring

- a) the *cis* coupling path
- b) the *trans* coupling path

The appropriate coupling paths over five bonds are illustrated by the bold lines



$$\theta = 0^\circ$$



$$\theta = 180^\circ$$

It has been proposed<sup>5</sup> for toluene that  $^5J_m(H,CH_3)$  is described by equation 3

$$^5J_m(H,CH_3) = ^5J_{90}^{\pi} \sin^2\Theta + ^5J_{180}^{\sigma} \sin^2(\Theta/2) \quad (3)$$

where  $^5J_{90}^{\pi}$  is the magnitude of the  $\sigma$ - $\pi$  component for  $\Theta = 90^\circ$  and  $^5J_{180}^{\sigma}$  is the magnitude of the  $\sigma$ -component for  $\Theta = 180^\circ$ , or the all-*trans* bond arrangement (b in figure 2).  $^5J_{90}^{\pi}$  vanishes for conformations where the  $\alpha$  C-H bond lies in the molecular plane while  $^5J_{180}^{\sigma}$  vanishes only at  $\Theta = 0^\circ$ .

A detailed INDO MO FPT approach to toluene suggests that the  $^5J_m(H,CH_3)$  is a composite of a  $\sigma$ - $\pi$  electronic interaction<sup>4a</sup> which varies as  $\sin^2\Theta$  and a  $\sigma$  electronic interaction which varies as  $\sin^2(\Theta/2)$ . Evidence for the  $\sigma$ - $\pi$  component<sup>17-20</sup> has been provided via the methyl group replacement technique<sup>21</sup> where the coupling over six formal bonds between the methyl groups in *meta*-xylene is taken as the negative of the  $\sigma$ - $\pi$  component of  $^5J(H,CH_3)$ . This means that in toluene the  $\sigma$ - $\pi$  electron contribution is given by 0.336 Hz<sup>4a</sup> while the  $\sigma$  electron component is 0.322 Hz, providing a basis for equation 4 and

$$^5J_m(H,CH_3) = 0.336\langle\sin^2\Theta\rangle + 0.322\langle\sin^2(\Theta/2)\rangle \quad (4)$$

where brackets indicate expectation values.

A  $\sigma$  component of  $^5J_m(H,SH)$  varying as  $\sin^2(\Theta/2)$  was postulated for thiophenol and its *para*-substituted derivatives.<sup>22</sup> In these molecules, it is independent of the twofold barrier to rotation about the C-S bond, always being 0.5, while  $\langle\sin^2\Theta\rangle$  shows a dependence on the twofold barrier, allowing a decomposition of the observed couplings into their two components.

In addition, it is well understood that in toluene the coupling over six bonds between  $\alpha$  and ring protons,  $^6J_p(H,CH_3)$ , is proportional to  $\sin^2\Theta$  and arises from a  $\sigma$ - $\pi$  mechanism.<sup>6</sup> The  $\pi$ -electrons transmit the spin information and the  $\sigma$ - $\pi$  spin polarization acts at both ends of the coupling path to complete the interaction between the protons and the  $\sigma$  electron framework. Unlike  $^5J_m(H,CH_3)$ , the coupling over six bonds is insensitive to intrinsic (electronic) perturbations by ring substituents, therefore allowing



${}^6J_p(\text{H}, \text{CH}_3)$  to be an useful indicator of conformational preferences.

The change in sign expected for a  $\pi$ -electron dominated coupling, according to the methyl group replacement, was observed by Kotowycz and Schaefer<sup>24</sup> in a toluene derivative. They found a negative sign for  ${}^6J_p(\text{H}, \text{CH}_3)$  as opposed to that of the  ${}^5J_p(\text{H}, \text{H})$  coupling. Using substituted xylenes, MacDonald and Reynolds determined  ${}^6J_p(\text{H}, \text{CH}_3)$  to be  $-0.61(3)$  Hz and  $-0.57(3)$  Hz; they found  ${}^7J_p(\text{CH}_3, \text{CH}_3)$  to be  $+0.62(3)$  Hz.<sup>17</sup> These results indicate a dominant  $\sigma$ - $\pi$  mechanism.<sup>18</sup>

Wasylishen and Schaefer<sup>2</sup> calculated  ${}^6J_p(\text{H}, \text{CH}_3)$  in toluene and  ${}^7J_p(\text{CH}_3, \text{CH}_3)$  in *para*-xylene using INDO FPT molecular orbital theory. They performed a calculation of the six-bond coupling from an  $\alpha$  proton to the *para* ring proton in toluene as a function of the dihedral angle  $\Theta$  defined in figure 1, and found that the coupling followed a  $\sin^2\Theta$  dependence very closely. Assuming that the INDO values for a  $90^\circ$  dihedral angle arise entirely from a  $\sigma$ - $\pi$  mechanism, one obtains equation 5

$${}^6J_p(\text{H}, \text{CH}_3) = {}^6J_{90}\pi \sin^2\Theta \quad (5)$$

where  ${}^6J_{90}\pi$  is the value of  ${}^6J_p(\text{H}, \text{CH}_3)$  when the  $\alpha$  C-H bond lies in the plane perpendicular to the benzene plane.<sup>2,6</sup> Since the barrier to methyl group rotation is small<sup>9</sup>, then  $\langle \sin^2\Theta \rangle$  is assumed to be 0.5 and the rotationally averaged coupling,  $\langle J^\pi \rangle$ , for this mechanism can be estimated as

$$\langle J^\pi \rangle = 1/2 {}^6J_{90}\pi \quad (6)$$

In toluene,  $\langle {}^6J_p^\pi(\text{H}, \text{CH}_3) \rangle$  is calculated as  $-0.61$  Hz, and  $\langle {}^7J_p^\pi(\text{CH}_3, \text{CH}_3) \rangle$  as  $0.72$  Hz in *para*-xylene. These compare well with the experimental values of  $-0.62(2)$  Hz<sup>25</sup> and  $+0.62(3)$  Hz<sup>17</sup>, respectively. Also, assuming relatively free rotation of the methyl group, the average INDO value for  ${}^6J_p(\text{H}, \text{CH}_3)$  in toluene is calculated as  $-0.64$  Hz, which is very similar to  $\langle {}^6J_p^\pi(\text{H}, \text{CH}_3) \rangle$ . This is a good indication of an almost pure  $\sigma$ - $\pi$  electron mechanism for this coupling.

Although proton-proton couplings from  $\alpha$  protons to ring protons have been examined thoroughly, couplings from  $\alpha$  protons to ring fluorine have not been studied as

extensively. The majority of the studies have been on toluene<sup>26,27</sup>, phenol<sup>28,29</sup>, and benzaldehyde<sup>30</sup> derivatives, with fluorotoluenes receiving the most attention.

In a recent investigation of 2-fluorotoluene<sup>27</sup>  ${}^4J_o(\text{F},\text{CH}_3)$  was found to be relatively large and positive, attributable to a dominant  $\sigma$ - $\pi$  mechanism with additional contributions from  $\sigma$  and/or proximate mechanisms. The two mechanisms are not easily distinguishable. In figure 3, INDO MO FPT values for  ${}^4J_o(\text{F},\text{CH}_3)$  are illustrated as a function of the dihedral angle  $\Theta$ . The couplings determined experimentally are also plotted in figure 3. The INDO curve shows a dominant positive  $\sigma$ - $\pi$  component and a through-space component is inherent. Even though the empirical curve contains a large  $\sigma$ - $\pi$  component, a positive interaction is present as  $\Theta$  approaches  $0^\circ$ , suggested to arise from positive  $\sigma$  and/or through-space mechanisms. The standard INDO MO FPT approaches fail to reproduce the conformational dependence of  ${}^4J_o(\text{H},\text{CH}_3)$ .

For 4-fluorotoluene, INDO MO FPT calculations indicate that  ${}^6J_p(\text{F},\text{CH}_3)$  may be transmitted by a  $\sigma$ - $\pi$  mechanism. In fact,  ${}^6J_p(\text{F},\text{CH}_3)$  is computed to have an angular dependence which can be written as

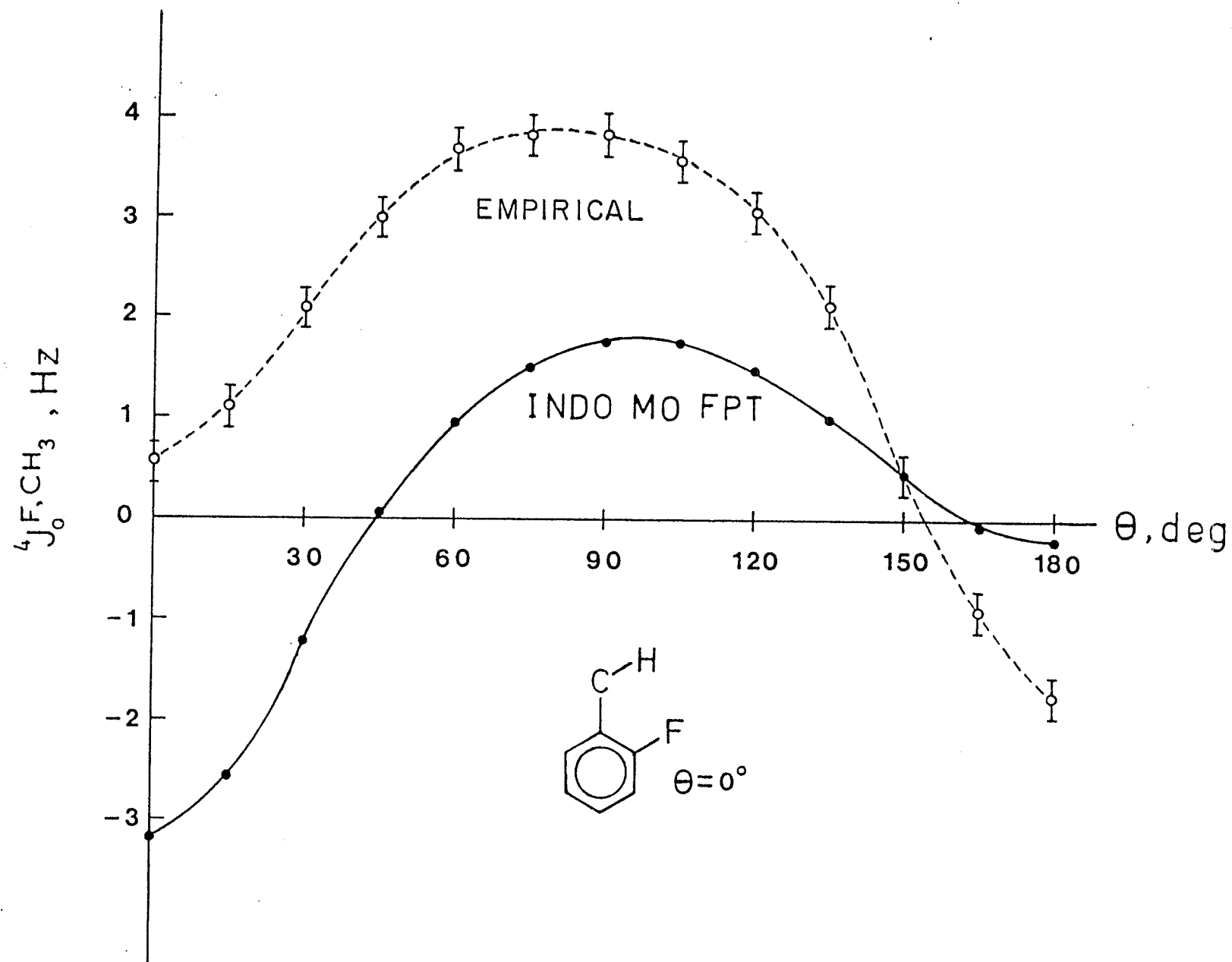
$$\begin{aligned} {}^6J_p(\text{Hz}) &= -0.008 + 1.872\sin^2\Theta \\ &= 1.87\sin^2\Theta \end{aligned} \quad (7)$$

Since the barrier to methyl group rotation in 4-fluorotoluene is relatively low<sup>31</sup>, only 57.7 J/mole,  $\langle\sin^2\Theta\rangle$  is effectively 0.5 and subsequently predicts  ${}^6J_p(\text{F},\text{CH}_3)$  as 0.94 Hz. Experimentally,  ${}^6J_p(\text{F},\text{CH}_3)$  is found to be 1.12 Hz.<sup>32</sup>

Evidence for the  $\sin^2\Theta$  dependence of  ${}^6J_p(\text{F},\text{CH})$  allows subsequent use of the J method<sup>6</sup> to determine small (<20 kJ/mole) twofold barriers to internal rotation about the ring carbon to methylene carbon bond in 4-fluorobenzyl derivatives. Schaefer, Danchura, Niemczura and Peeling<sup>32</sup> determined barriers for some 4-fluorobenzyl compounds and found fair agreement with more reliable barriers derived from  ${}^6J_p(\text{CH}_2\text{X},\text{H})$  values in 3,5-dihalobenzyl derivatives. For other *para*-fluorobenzene derivatives, the six-bond  $\alpha$  proton to ring fluorine coupling has not been examined extensively. In

### FIGURE 3

A plot of the INDO MO FPT values of  ${}^4J_o(\text{CH}_3, \text{F})$  for 2-fluorotoluene as it varies with the dihedral angle  $\Theta$ . The empirical couplings as determined by Schaefer et al<sup>27</sup> as shown in the upper curve.



4-fluorothiophenol, the barrier is small, 2.1(8) kJ/mole, and the observed value of  ${}^6J_p(\text{F,SH})$  is 1.00 Hz. In the case of 2,6-dibromo-4-fluorophenol, the hydroxyl group is held coplanar with the benzene ring by intramolecular hydrogen bonding to bromine and the observed  ${}^6J_p(\text{F,OH})$  coupling is -0.27 Hz.<sup>28</sup> In 4-fluorobenzaldehyde where planar conformations are suggested to dominate, the observed  ${}^6J_p(\text{F,CHO})$  value is found to be -0.44 Hz.<sup>29</sup> The negative sign is a puzzle<sup>29a</sup>.

An investigation by Schaefer, Danchura and Niemczura of the coupling mechanism of  ${}^5J_m(\text{F,CH}_3)$  in 3-fluorotoluenes has been done recently.<sup>26</sup> Their INDO FPT calculations are reproduced by the equation

$${}^5J_m(\text{Hz}) = 0.57 - 2.60\sin^2\Theta + 1.68\sin^2(\Theta/2) \quad (8)$$

The  $\sin^2\Theta$  term originates from a  $\sigma$ - $\pi$  mechanism while the  $\sin^2(\Theta/2)$  term originates from a  $\sigma$  mechanism. Because the barrier<sup>34</sup> to methyl group rotation is a mere 175 J/mole, thirteen calculated couplings can be averaged to give a value of +0.11 Hz. This is fairly close to an observed value of -0.23 Hz in 3-fluorotoluene. It is possible that the constant term, 0.57 Hz, is an artifact of the INDO FPT calculations and the expectation values of  $\langle \sin^2\Theta \rangle$  and  $\langle \sin^2(\Theta/2) \rangle$  are very close to 0.5. Then a value of -0.46 Hz for  ${}^5J_m(\text{F,CH}_3)$  is predicted. The validity of equation 8 could be tested using benzal compounds which are "locked" into *cis* (1) and *trans* (2) conformers with the appropriate

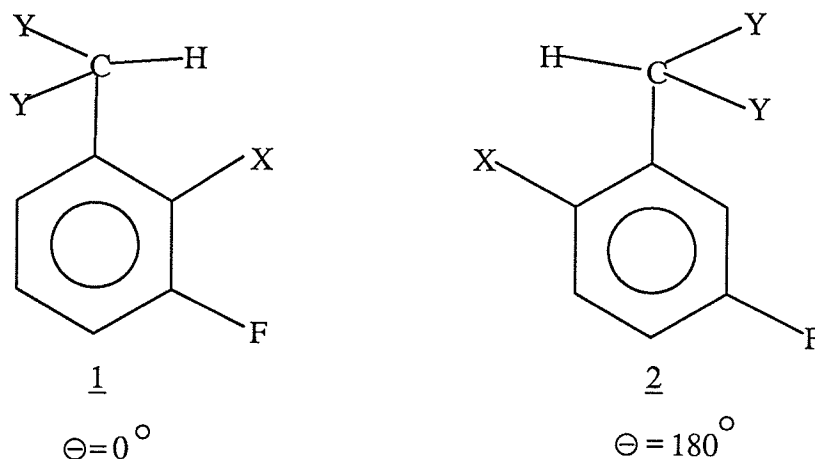


Figure 4

ortho substituents. This method is feasible only if the substitution at the  $\alpha$  and *ortho*

positions do not significantly perturb the  $^5J_m(\text{F,CH})$  coupling mechanism.

Unpublished INDO MO FPT data for 3-fluorophenol show a similar angular dependence

$$^5J_m(\text{F,OH}) = 0.31 - 2.76\sin^2\Theta + 2.62\sin^2(\Theta/2) \quad (9)$$

Experimentally, values of  $^5J_{\text{trans}}(\text{F,OH}) = 1.56$  Hz and  $^5J_{\text{cis}}(\text{F,OH}) = -0.35$  Hz are obtained. Since the INDO method usually overestimates  $^5J_{\text{trans}}$  in benzene derivatives, it is not unreasonable that, in this case, the all-*trans* coupling is overestimated. Moreover, phenols have a planar ground state conformation and a reasonably high barrier to internal rotation and subsequently, a *cis-trans* equilibrium<sup>11,28,35</sup> can be used to predict a value for the  $^5J_m(\text{F,OH})$  for pentafluorophenol. The average of *cis* and *trans* couplings,  $(1.56-0.35)/2 = 0.61$  Hz, agrees with the observed value for  $^5J_m(\text{F,OH})$  of 0.59 Hz.<sup>28</sup>

## Introduction to the problem

A disentanglement of the  $\sigma$ - $\pi$  components of  ${}^5J_m(\text{F}, \text{CH}_3)$  requires a reduction of the threefold symmetry in the sidechain. This situation is achieved by substitution at the methyl site, preferably with substituents which do not significantly perturb the coupling mechanisms nor their magnitude. Methyl groups may be used as these substituents. Furthermore, a range of  $\langle \sin^2 \Theta \rangle$  and  $\langle \sin^2(\Theta/2) \rangle$  values is required in order to have a set of well-conditioned equations of the type

$${}^5J_m(\text{F}, \text{CH}_3) = {}^5J_{90} \pi \langle \sin^2 \Theta \rangle + {}^5J_{180} \sigma \langle \sin^2(\Theta/2) \rangle \quad (10)$$

This requirement is met by the introduction of  $\alpha$ -substituents to give preferred conformations as in 3 and 4

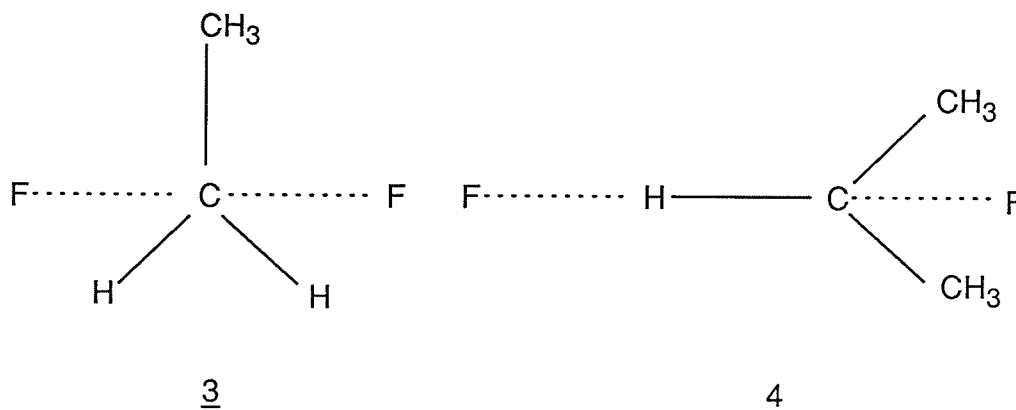


figure 5

The intent of this work was to investigate the five-bond stereospecific long-range nmr spin-spin coupling  ${}^5J_m(\text{F}, \text{CH})$  between the sidechain  $\alpha$ -proton and the *meta* ring fluorine in some symmetrically and unsymmetrically substituted benzyl and benzal compounds both experimentally and by application of the INDO method. All

derivatives that were prepared and studied include 3,5-difluorotoluene, 3,5-difluoroethylbenzene, 3,5-difluoroisopropylbenzene, 2,6-dibromotoluene, 2,3-difluoro- $\alpha,\alpha$ -diacetoxytoluene and 2-bromo-5-fluoro- $\alpha,\alpha$ -diacetoxytoluene.

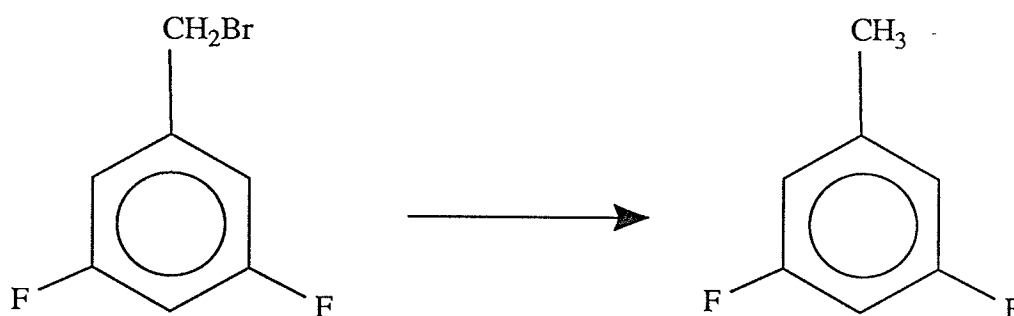


## B. EXPERIMENTAL METHODS

## 1. Materials and Syntheses

### A. Preparation of 3,5-difluorotoluene\*

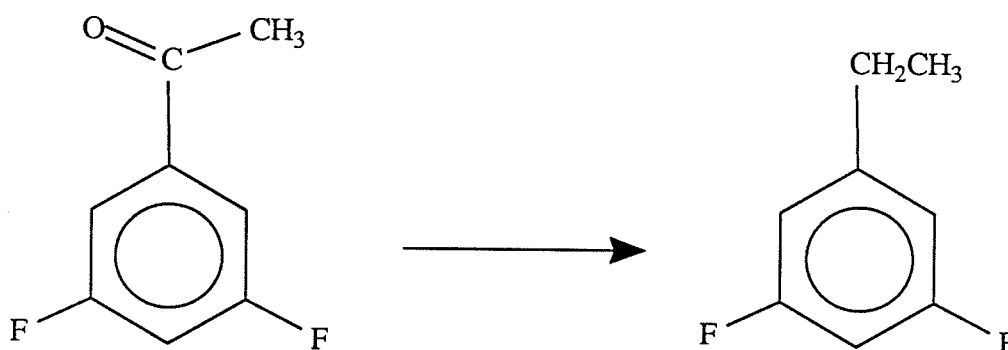
The 3,5-difluorotoluene was prepared using the method as described below.



The benzyl bromide (1.0 g/4.83 mmole) obtained from Fluorochem was added via a dropping funnel over a period of 15 minutes to a mixture of crushed magnesium turnings (0.13 g/5.35 mmole) and anhydrous ether (40 ml) in a round bottomed flask. A crystal of iodine was required to initiate the reaction. After approximately 2 hours, concentrated hydrochloric acid was added to the mixture. The ether layer was separated, washed with water and dried over magnesium sulfate. The solvent was removed under reduced pressure to yield the toluene. This product was confirmed by NMR. (\*synthesis was done by Eric Sveinson)

## B. Preparation of 3,5-difluoroethylbenzene

The 3,5-difluoroethylbenzene was prepared using a modified Wolff-Kishner reduction known as the Huang-Minlon method<sup>36</sup> and the description of the procedure is given below.



The acetophenone (1.75g/0.011 mole), obtained from Fluorochem, diethylene glycol (100 ml), hydrazine hydrate (10 ml) and potassium hydroxide pellets (2.00g/0.036 mole) were placed into a three-necked round bottomed flask (200 ml) fitted with a reflux condenser, a thermometer with a rubber septum in the sideneck and a drying tube in the remaining neck. The bulb of the thermometer was immersed in the reaction mixture. The flask was warmed using a heating mantle until the potassium hydroxide dissolved and then heated under reflux for 1 hour. The flask was then cooled and the reflux condenser was replaced with a still-head and condenser for downward distillation. The temperature of the liquid was allowed to rise to 175°C and the distillate was collected. The upper hydrocarbon layer was separated and the aqueous layer was extracted twice with 20 ml portions of anhydrous ether. The combined upper layer and ethereal extracts were dried over magnesium sulfate and the solvent was removed under reduced pressure. The remaining residue was then distilled and the ethylbenzene (0.84g) was collected at 125-135°C. The 3,5-difluoroethylbenzene was identified by NMR (300 MHz).

### C. Preparation of 3,5-difluoroisopropylbenzene

The 3,5-difluoroisopropylbenzene was synthesized using the method of Veregin<sup>37</sup> as shown in Scheme 1.

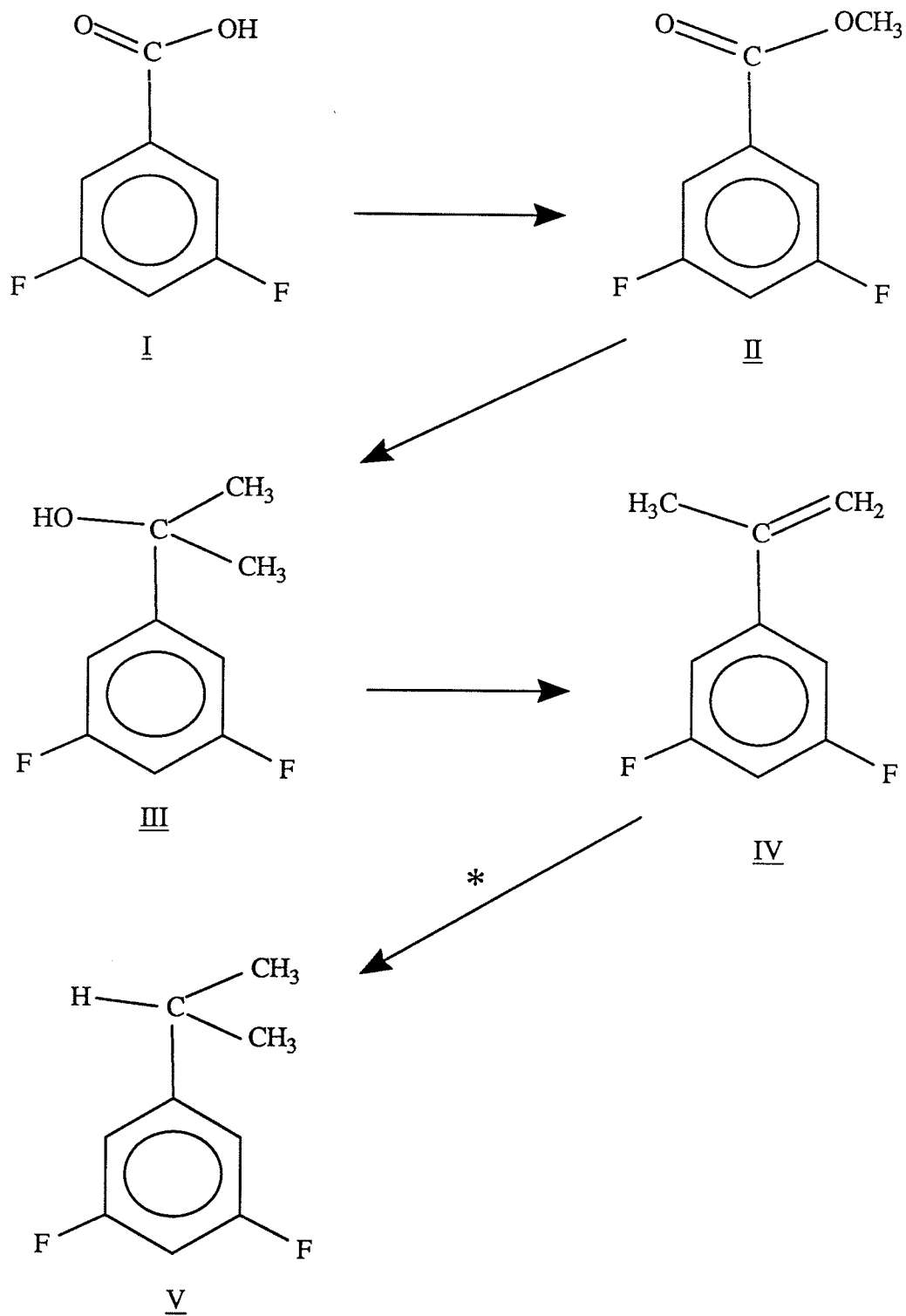
6.0 g of 3,5-difluorobenzoic acid (I) obtained from Fluorochem, was dissolved in a solution of 10 ml of acetyl chloride and 110 ml of methanol. This mixture was stirred at room temperature overnight, then refluxed for 8 hours. After evaporation of the solvent, the remaining residue was dissolved in ether, washed with sodium bicarbonate, and dried with magnesium sulfate. The solvent was removed under vacuum to give about 2.1 g of a slightly yellow oil. The proton nmr spectrum (60 MHz) was consistent with that expected for the methyl benzoate (II) while no acid (I) was detected.

A methyl magnesium iodide Grignard reagent was prepared by addition of 12 g of methyl iodide to 2 g of crushed magnesium turnings in ether (previously dried with sodium). This mixture was heated until a majority of the magnesium had reacted. A solution of the resulting ester (II) in 20 ml of ether was added slowly to the Grignard reagent. The mixture was refluxed for 30 minutes, poured into a mixture of ice and dilute hydrochloric acid, extracted with ether and dried with magnesium sulfate. The solvent was removed under reduced pressure to yield 1.8 g of a clear, slightly yellow oil. The proton nmr spectrum (60 MHz) was consistent with that expected for the alcohol (III) with a slight amount of ester (II) as an impurity.

A few crystals of toluene-p-sulfonic acid and 1.8 g of the alcohol (III) were added to 15 ml of benzene. The solution was stirred at room temperature overnight, then washed with dilute hydrochloric acid and dried over magnesium sulfate. The solvent was removed under vacuum until the volume of solvent remaining was approximately 5 ml. The remaining solvent was removed using a hot water bath and a Vigreux column. The proton nmr spectrum (300 MHz) was that expected for the alkene (IV) with no alcohol detected (III) and the ester impurity was also found.

Approximately 1 g of alkene (IV) was dissolved in methanol (previously distilled over magnesium) and approximately 200 mg of Pd/C catalyst was added and the mixture was hydrogenated with a low-pressure hydrogenator for approximately 3 days. This step as indicated by

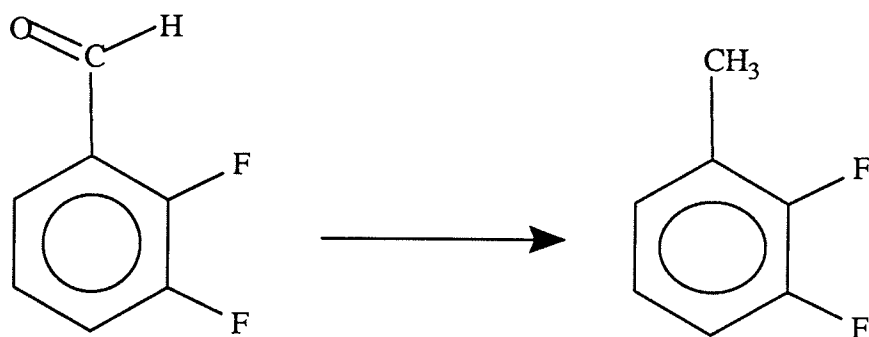
the asterisk in Scheme 1 was performed in Dr. Charlton's laboratory. The solution was then extracted with cyclopropane and dried over magnesium sulfate. The cyclopropane solvent was removed under reduced pressure and a small amount of the isopropylbenzene (V) was obtained ( $^1\text{H}$  nmr at 300 MHz).



Scheme 1

#### D. Preparation of 2,3-difluorotoluene

The 2,3-difluorotoluene was prepared using the scheme shown below

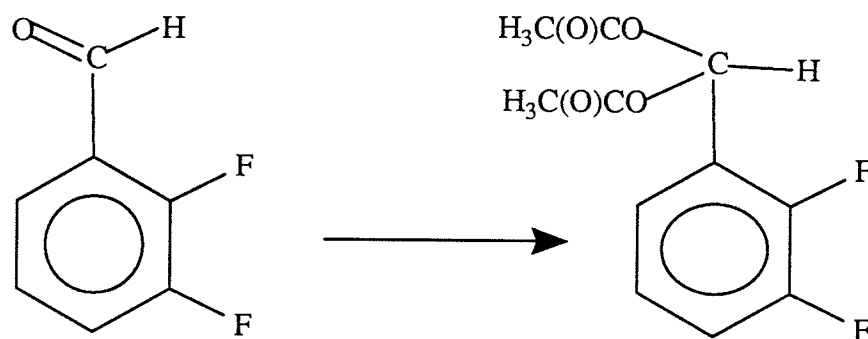


The corresponding 2,3-difluorobenzaldehyde was reduced using the Huang-Minlon method<sup>37</sup> without modification as described previously for the synthesis of 3,5-difluoroethylbenzene.

The resulting toluene gave an unmistakable <sup>1</sup>H nmr spectrum (300MHz).

E. Preparation of 2,3-difluoro- $\alpha,\alpha$ -diacetoxytoluene

The 2,3-difluoro- $\alpha,\alpha$ -diacetoxytoluene was prepared using a standard method as described below.

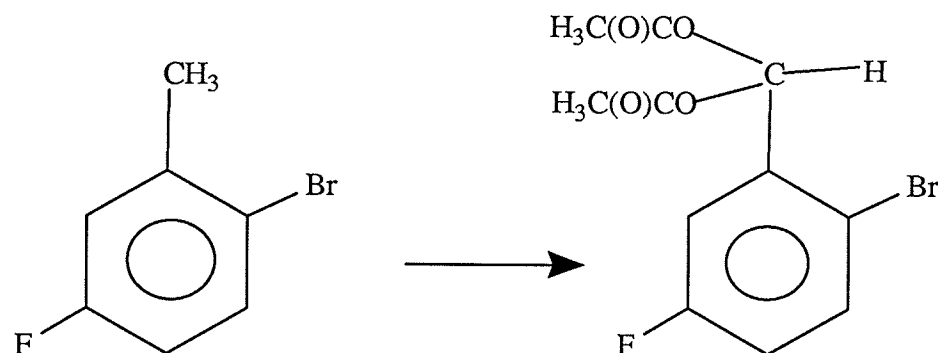


The 2,3-difluorobenzaldehyde (2.00g) obtained from Aldrich, p-toluenesulfonic acid (0.044g) and 10 ml of acetic anhydride were placed in a 100 ml round bottomed flask and stirred overnight. The resulting solid was washed twice with water to remove excess acetic anhydride and then air dried to give a white crystalline product (3.14g). The product was identified and confirmed by NMR (300MHz).



F. Preparation of 2-bromo-5-fluoro- $\alpha,\alpha$ -diacetoxytoluene

The 2-bromo-5-fluoro- $\alpha,\alpha$ -diacetoxytoluene was prepared using the method as shown below.



The corresponding 2-bromo-5-fluorotoluene (1.01g), obtained from Aldrich, was dissolved in a mixture of 10 ml acetic anhydride, 10 ml glacial acetic acid and 3 ml concentrated sulfuric acid which had been previously well cooled. When the temperature had fallen to  $5^\circ\text{C}$ , 1.7g of chromium trioxide was added in small portions at such a rate that the temperature did not rise above  $10^\circ\text{C}$ . The stirring was then continued for 30 min after the addition of chromium trioxide was completed. The contents of the flask were then poured into a 400 ml beaker 1/3-filled with crushed ice and then the beaker was filled to 200 ml with cold water. The resulting solid was then filtered using a Buchner funnel and the product was washed with cold water until the washings were colorless. The solid was then washed with two 20 ml portions of cold 2% sodium bicarbonate solution and finally with 10 ml of cold ethanol. The total yield of product was 0.432g and was identified and confirmed by NMR (300MHz).

## 2. Sample Preparation

NMR samples of the difluoro derivatives of toluene, ethylbenzene and isopropylbenzene and fluoro- $\alpha,\alpha$ -diacetoxytoluenes were prepared by weighing the appropriate amounts of the compound and the solvent of choice. 5 mole% solutions were prepared in a solvent mixture consisting of carbon disulfide (Fisher Scientific), 10 mole% cyclohexane- $d_{12}$  (99.5 atom% D from Aldrich Chemical) as an internal locking material, 0.25 mole% tetramethylsilane (Sigma Chemical) as an internal reference for  $^1\text{H}$  nmr spectra and 0.25 mole% hexafluorobenzene (Pierce Chemical) as an internal reference for  $^{19}\text{F}$  nmr spectra. The solutions were then transferred to precision-bore 5 mm sample tubes, fitted with ground glass joints and filtered through a small wad of cotton wool in a Pasteur pipette. The samples were then degassed using the freeze-pump-thaw technique four times. The nmr tubes were then flame-sealed.

### 3. Spectroscopic Method

Proton ( $^1\text{H}$ ) and fluorine ( $^{19}\text{F}$ ) nmr spectra were acquired on a Bruker AM 300 nmr spectrometer at a probe temperature of 300 K. Survey spectra with a sweep width of 6000 Hz were used to reference the compounds with respect to tetramethylsilane (TMS) and hexafluorobenzene ( $\text{C}_6\text{F}_6$ ). Each spectral region was then examined in detail, with sweep width and data region adjusted to give acquisition times of approximately 41 seconds. Proton sweep widths ranged from 50-200 Hz, while fluorine sweep widths were 100-200 Hz. As many as 128 scans were acquired. Zero-filling from 2-4 times the original data region was done before transforming the free induction decay curves (FIDs) using small amounts of gaussian and lorentzian multiplication in order to decrease the linewidth and increase resolution. Intrinsic linewidths at half-height were as small as 0.05 Hz (including spectra where the methyl groups in the sidechain were decoupled) after resolution enhancement, but more often were 0.05 to 0.10 Hz. Partial decoupling experiments were used to determine the signs of  $^5J_{\text{m}}(\text{F},\text{CH}_3)$  in 3,5-difluorotoluene,  $^5J_{\text{m}}(\text{F},\text{CH}_2)$  in 3,5-difluoroethylbenzene and  $^5J_{\text{m}}(\text{F},\text{CH})$  in 3,5-difluoroisopropylbenzene.

#### 4. Computations

Spectral analyses and simulations were performed using the program NUMARIT<sup>39</sup> in both the iterative and non-iterative modes; the program was coupled to a plotting routine.

Computer simulations using NUMARIT in the iterative mode were used to determine the sign of  $^5J_m(\text{F,CH})$  in 2,3-difluoro- $\alpha,\alpha$ -diacetoxytoluene.

Ab initio molecular orbital calculations were performed at the STO-3G level<sup>39a</sup> with the program MONSTERGAUSS<sup>40</sup>. CNDO/2 and INDO MO FPT<sup>41</sup> calculations of coupling constants were performed using the optimized geometries from the ab initio calculations.

All curves were statistically fitted to  $\sin^2\Theta$  and  $\sin^2(\Theta/2)$  functions using the SAS nonlinear regression program NLIN<sup>42</sup>. SAS/GRAPH<sup>43</sup> programs were written to plot curves on the computer system plotter. Smooth curves through data points were obtained by using a spline interpolation which is part of the SAS/GRAPH library.

Computations were performed on Amdahl 470/V8 or Amdahl 580/5850 systems.

## C. EXPERIMENTAL RESULTS

### 1) 3,5-difluorotoluene

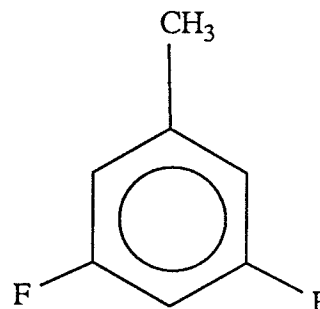
Results of the analyses of proton and fluorine spectra of a 2.5 mole% solution of 3,5-difluorotoluene in  $\text{CS}_2/\text{C}_6\text{D}_{12}$  appear in Table 1. The analysis of the  $\text{A}_3\text{BB}'\text{XX}'\text{C}$  spin system was straightforward. The sign of  $^5\text{J}_m(\text{CH}_3, \text{F})$  was determined using a double resonance experiment as shown in figure 7. All other signs and couplings between ring nuclei were taken from an earlier analysis of 3-fluorotoluene<sup>44</sup>.

A first-order representation of the line spectrum of the methyl protons and the *para* proton  $\text{H}_4$  appear in figure 6. Figures 8,9,10 show the methyl protons, *para* proton  $\text{H}_4$  and *meta* fluorine regions respectively.

TABLE 1

Proton and fluorine spectral parameters<sup>a</sup> for a 2.5 mole% solution of 3,5-difluorotoluene<sup>b</sup> in CS<sub>2</sub>/C<sub>6</sub>D<sub>12</sub> at 300K

$\nu(\text{CH}_3)$	698.788(0) <sup>c</sup>
$\nu(\text{H}_2=\text{H}_6)$	1974.780(0)
$\nu(\text{H}_4)$	1943.119(0)
$\nu(\text{F}_3=\text{F}_5)$	14675.910(0)



$^3J_o(\text{H}_2, \text{F}_3)$	9.028(0)
$^3J_o(\text{H}_4, \text{F}_5)$	8.894(0)
$^4J(\text{CH}_3, \text{H}_2)$	-0.694(0)
$^4J(\text{H}_2, \text{H}_4)$	2.335(0)
$^4J(\text{F}_3, \text{F}_5)$	6.644(1) <sup>d</sup>
$^4J(\text{H}_2, \text{H}_6)$	1.416(1)
$^5J(\text{H}_2, \text{F}_5)$	-0.916(0) <sup>d</sup>
$^5J(\text{CH}_3, \text{F}_3)$	-0.294(0) <sup>e</sup>
$^6J(\text{CH}_3, \text{H}_4)$	-0.588(0)

Transitions Calculated	512
Transitions Assigned	472
Peaks Observed	213
Largest Difference	0.021
RMS Deviation	0.004

## NOTES

- a In Hertz.  $^1\text{H}$  nmr at 300.135 MHz to high frequency of TMS.  $^{19}\text{F}$  nmr at 282.365 MHz to high frequency of  $\text{C}_6\text{F}_6$ . The *meta* fluorine was treated in the X approximation.
- b 2.5 mole% in solution mixture consisting of  $\text{CS}_2$ , 10 mole%  $\text{C}_6\text{D}_{12}$ , 0.25 mole% TMS and 0.25 mole%  $\text{C}_6\text{F}_6$ .
- c Numbers in parentheses are standard deviations in the last significant digit, as given by the NUMARIT analysis.
- d  $^4\text{J}(\text{F},\text{F})$  correlates with  $^5\text{J}(\text{H}_2,\text{F})$  by 0.511.
- e Sign is determined by double resonance experiments.



a) Determination of the relative sign of  $^5J_m(\text{F}, \text{CH}_3)$  by double resonance experiments

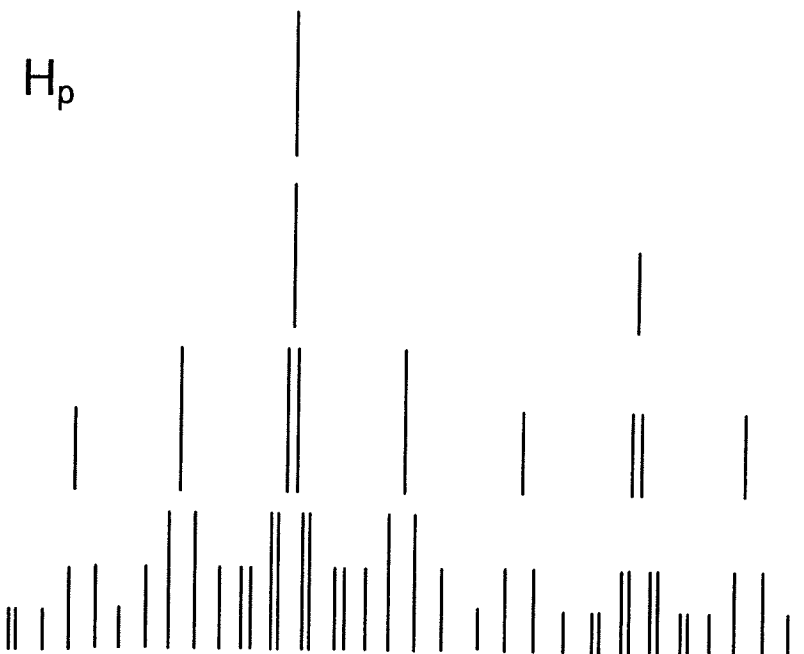
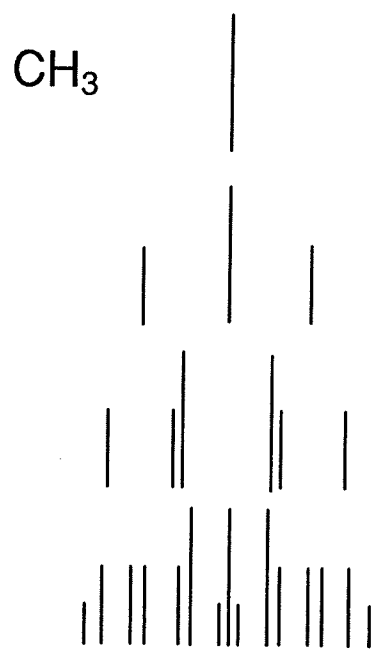
The position of a transition within a multiplet depends on the magnetic environment of the nucleus undergoing that transition. Consequently each transition for a nucleus corresponds to a specific orientation of the other coupled nuclei in the molecule. If the spin states of a nucleus are designated by + and -, and the high frequency (low field) transition is assumed + when the coupling constant is positive, the relative signs of the nuclear spin-spin coupling may be determined by double resonance experiments. Irradiation of a transition in the multiplet of a nucleus will perturb only transitions, in the multiplets of other nuclei, that share a common energy level. Since the high resolution nmr Hamiltonian is symmetric with respect to reversal of all signs, only the relative sign of coupling constants can be determined. Signs of coupling constants are taken relative to the one bond carbon-proton coupling which is known to be positive.

With reference to figure 6, irradiation of line 1 of the methyl protons perturbs lines 1, 2, 3 and 4 of the *para* proton resonance (see figure 7b). The irradiation causes the intensity of these four lines to decrease. These lines are associated with the + spin state of fluorine since the sign of  $^3J(\text{H}_4, \text{F})$  is positive. Therefore line 1 of the methyl group is designated as -, ie,  $^5J_m(\text{CH}_3, \text{F})$  is negative.

Irradiation of line 15 of the methyl protons perturbs lines 21, 22, 23 and 24 of the *para* proton resonance (see figure 7c). These lines are associated with the - spin state of fluorine, thus confirming the negative sign of  $^5J_m(\text{CH}_3, \text{F})$ .

FIGURE 6

A first order representation of the line spectrum of the methyl protons and the *para* proton H<sub>4</sub> of 3,5-difluorotoluene



CH<sub>3</sub>  
F  
H<sub>p</sub>

- 0 0- 00 +0- 00 +0 0+  
-- 0- +- +0- +- +0 0+  
12 34 56 78 910111213 1415

- - ++ - - ++ - - ++  
+ + + + + + + + 0 0 0 0  
1 2 3 4 5 6 7 8 9101112

- - ++ - - ++ - - ++  
0 0 0 0 - - - - - -  
13 14 15 16 1718 1920 2122 23 24

# FIGURE 7

Sign determination of  $^5J_m(\text{CH}_3, \text{F})$  in 3,5-difluorotoluene

- A) the spectral region of the *para* proton  $\text{H}_4$  of 3,5-difluorotoluene
- B) with irradiation of line 15 of the methyl group (low frequency methyl peak)
- C) with irradiation of line 1 of the methyl group (high frequency methyl peak)

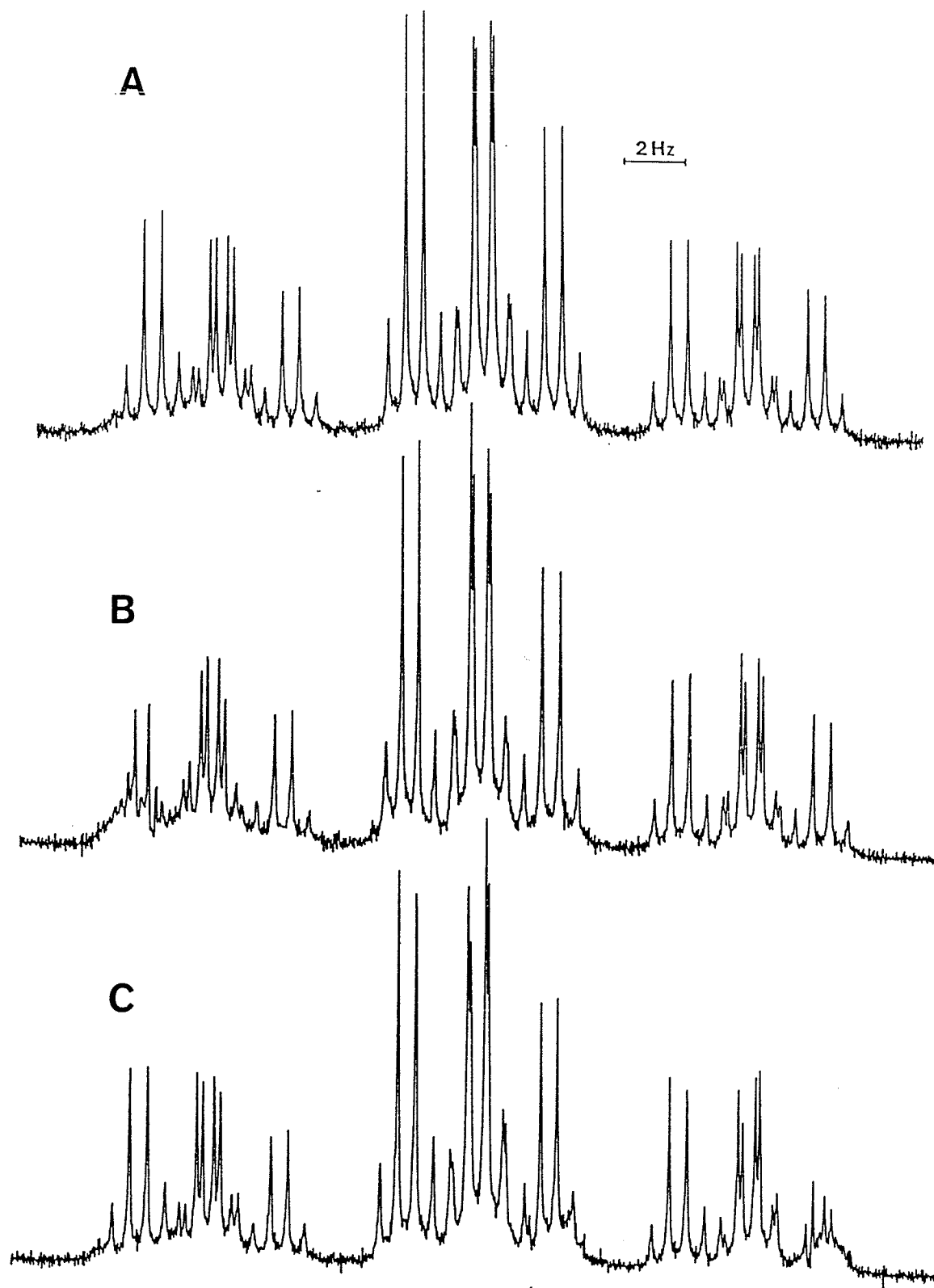


FIGURE 8

- A) the methyl proton region of 3,5-difluorotoluene
- B) computer simulation of the methyl proton region using the parameters from Table 1 assuming a linewidth of 0.08 Hz.

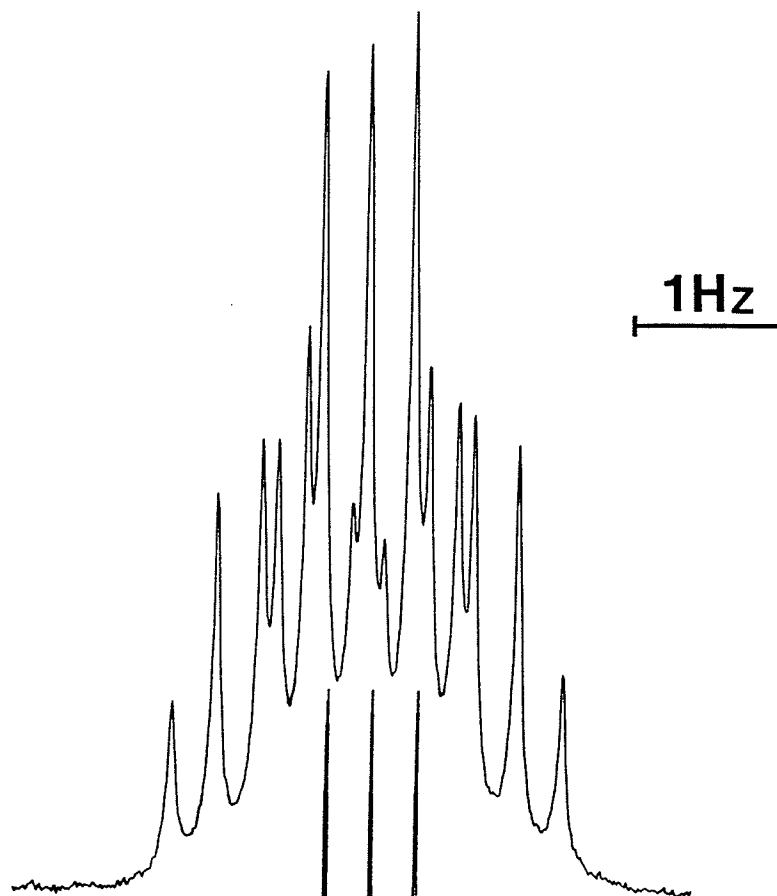
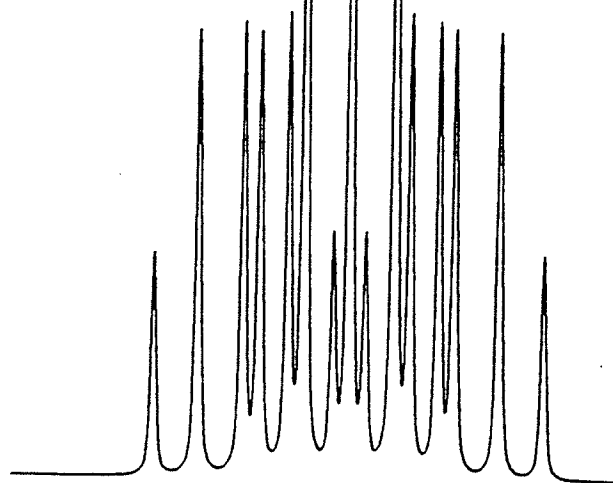
**A****B**

FIGURE 9

NMR spectrum of the *para* proton H<sub>4</sub> for 3,5-difluorotoluene

A) experimental

B) calculated



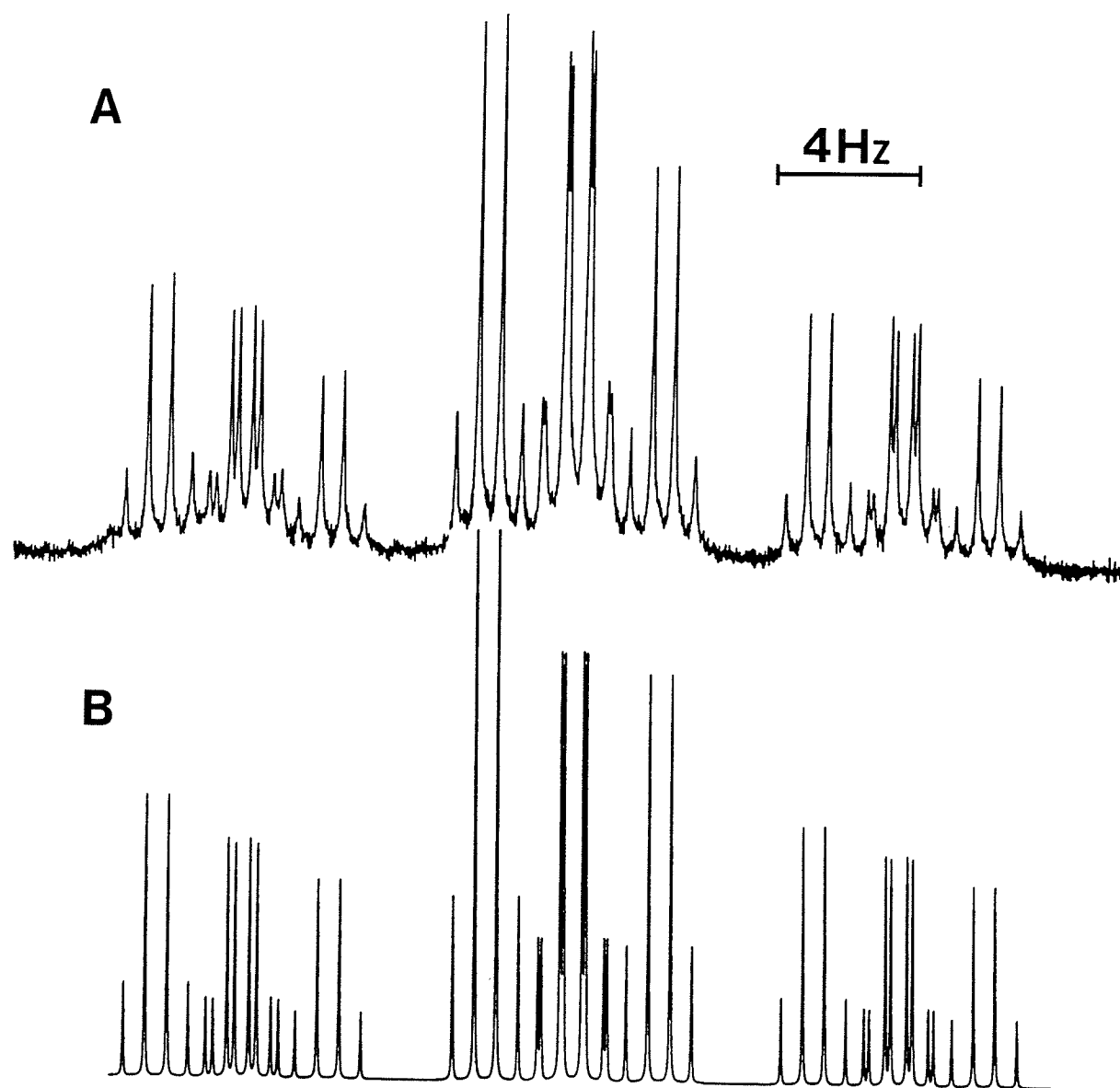
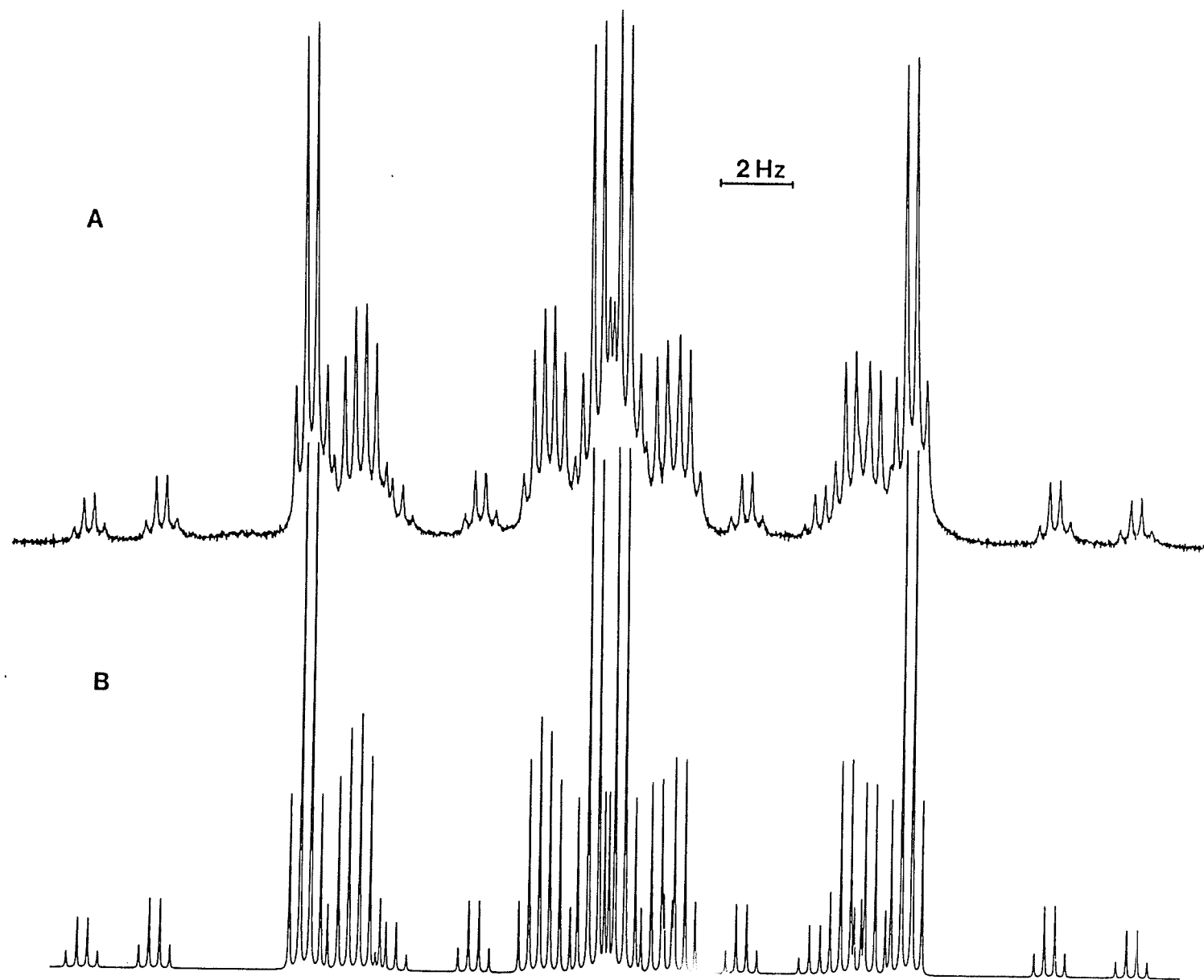


FIGURE 10

Fluorine-19 NMR spectrum for the *meta* fluorines for 3,5-difluorotoluene

A) experimental

B) calculated



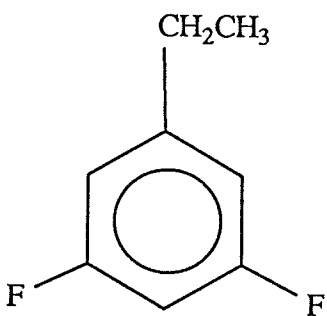
## 2) 3,5-difluoroethylbenzene

Results of the analyses of fluorine and proton nmr spectra for a 2.5 mole % solution of 3,5-difluoroethylbenzene in  $\text{CS}_2/\text{C}_6\text{D}_{12}$  appear in table 2. No problems were encountered in this rather complex 10 spin system. There was no observed coupling between the methyl protons and the *ortho* and *para* protons even though they were optimized in the NUMARIT analysis.

Figure 11 shows the determination of the relative sign of  $^5J_m(\text{CH}_2, \text{F})$  in 3,5-difluoroethylbenzene using a partial decoupling experiment. The methyl and methylene proton region, *meta* fluorine region and *para* proton region are also shown in figures 12, 13 and 14 respectively.

TABLE 2

Proton and fluorine spectral parameters<sup>a</sup> for a 2.5 mole% solution of  
3,5-difluoroethylbenzene<sup>b</sup> in CS<sub>2</sub>/C<sub>6</sub>D<sub>12</sub> at 300K

$\nu(\text{CH}_3)$	368.801(1) <sup>c</sup>		
$\nu(\text{CH}_2)$	784.110(1)		
$\nu(\text{H}_2=\text{H}_6)$	1982.139(0)		
$\nu(\text{H}_4)$	1943.709(0)		
$\nu(\text{F}_3=\text{F}_5)$	14743.371(0)		
$^3\text{J}(\text{CH}_3, \text{CH}_2)$	7.600(1)	$^5\text{J}(\text{CH}_3, \text{H}_2)$	0.003(1) <sup>e</sup>
$^3\text{J}(\text{H}_2, \text{F}_3)$	9.162(1)	$^5\text{J}(\text{CH}_2, \text{F}_3)$	-0.067(1) <sup>f</sup>
$^3\text{J}(\text{H}_4, \text{F}_5)$	8.843(0)	$^5\text{J}(\text{H}_2, \text{F}_5)$	-0.905(0) <sup>d</sup>
$^4\text{J}(\text{H}_2, \text{H}_4)$	2.337(1)	$^6\text{J}(\text{CH}_2, \text{H}_4)$	-0.463(1)
$^4\text{J}(\text{CH}_2, \text{H}_2)$	-0.651(1)	$^6\text{J}(\text{CH}_3, \text{F}_3)$	0.137(0)
$^4\text{J}(\text{H}_2, \text{H}_6)$	1.433(1)	$^7\text{J}(\text{CH}_3, \text{H}_4)$	0.000(0) <sup>e</sup>
$^4\text{J}(\text{F}_3, \text{F}_5)$	6.577(1) <sup>d</sup>		

Transitions Calculated	2432
Transitions Assigned	1438
Peaks Observed	306
Largest Difference	0.025
RMS Deviation	0.008

## NOTES

- a In Hertz.  $^1\text{H}$  nmr at 300.135 MHz to high frequency of TMS.  $^{19}\text{F}$  nmr at 282.365 MHz to high frequency of  $\text{C}_6\text{F}_6$ .
- b 2.5 mole% in solution mixture consisting of  $\text{CS}_2$ , 10 mole%  $\text{C}_6\text{D}_{12}$ , 0.25 mole% TMS and 0.25 mole%  $\text{C}_6\text{F}_6$ .
- c Numbers in parentheses are standard deviations in the last significant digit, as given by the NUMARIT analysis.
- d  $^4J(\text{F}_3, \text{F}_5)$  correlates with  $^5J(\text{H}_2, \text{F}_5)$  by 0.263.
- e These couplings were optimized even though they were not observed experimentally.
- f Sign is determined by partial decoupling experiments.

a) Determination of the sign of  $^5J_m(\text{CH}_2, \text{F})$  by double resonance experiments

A relatively small coupling exists between the methylene protons and the *meta* fluorine nucleus. For simplicity, a multiplet from the fluorine-19 nmr spectrum of 3,5-difluoroethylbenzene (figure 13) is shown in figure 11. Irradiation of the low frequency peak of the methyl proton region results in a decrease in linewidth and an increase in intensity of the high frequency peaks of the multiplets associated with coupling to the methylene protons (see figure 11b). A first-order reconstruction of the multiplet in B is shown where  $^5J(\text{F}, \text{CH}_2)/^3J(\text{CH}_2, \text{CH}_3)$  is negative. If this coupling ratio were positive then the observed spectrum would appear as the mirror image of B. Because  $^3J(\text{CH}_2, \text{CH}_3)$  is positive, this experiment implies a negative value for  $^5J_m(\text{F}, \text{CH}_2)$ .

FIGURE 11

Sign determination of  $^5J_m(\text{CH}_2, \text{F})$  in 3,5-difluoroethylbenzene

A) a low frequency multiplet with no irradiation

B) a low frequency multiplet with irradiation of the low frequency peak in the methyl proton region

C) predicted low frequency multiplet with irradiation of the low frequency peak in the methyl proton region



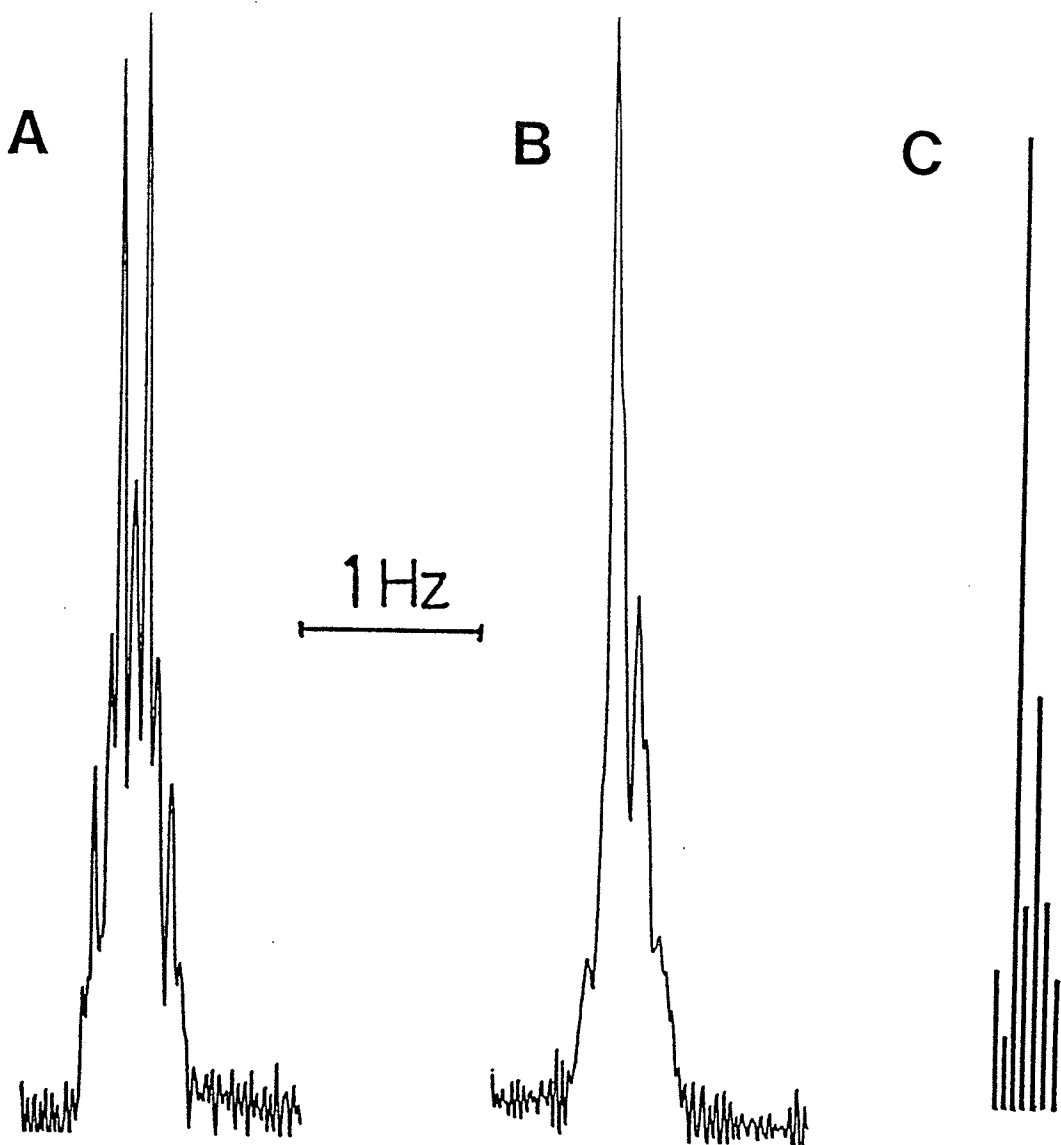


**FIGURE 12**

The proton nmr regions for the ethyl sidechain in 3,5-difluoroethylbenzene

A) methyl proton region

B) methylene proton region

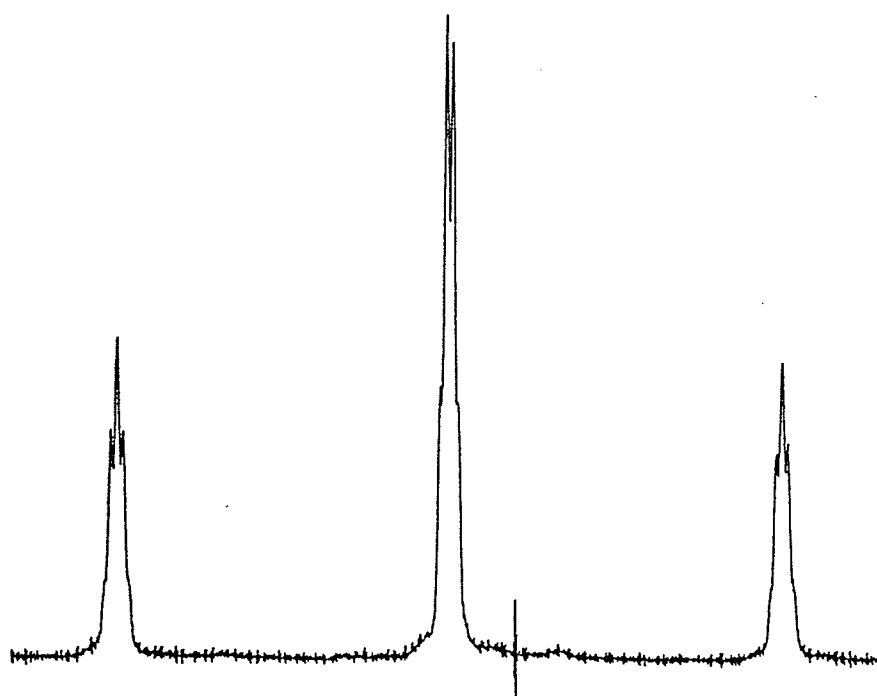
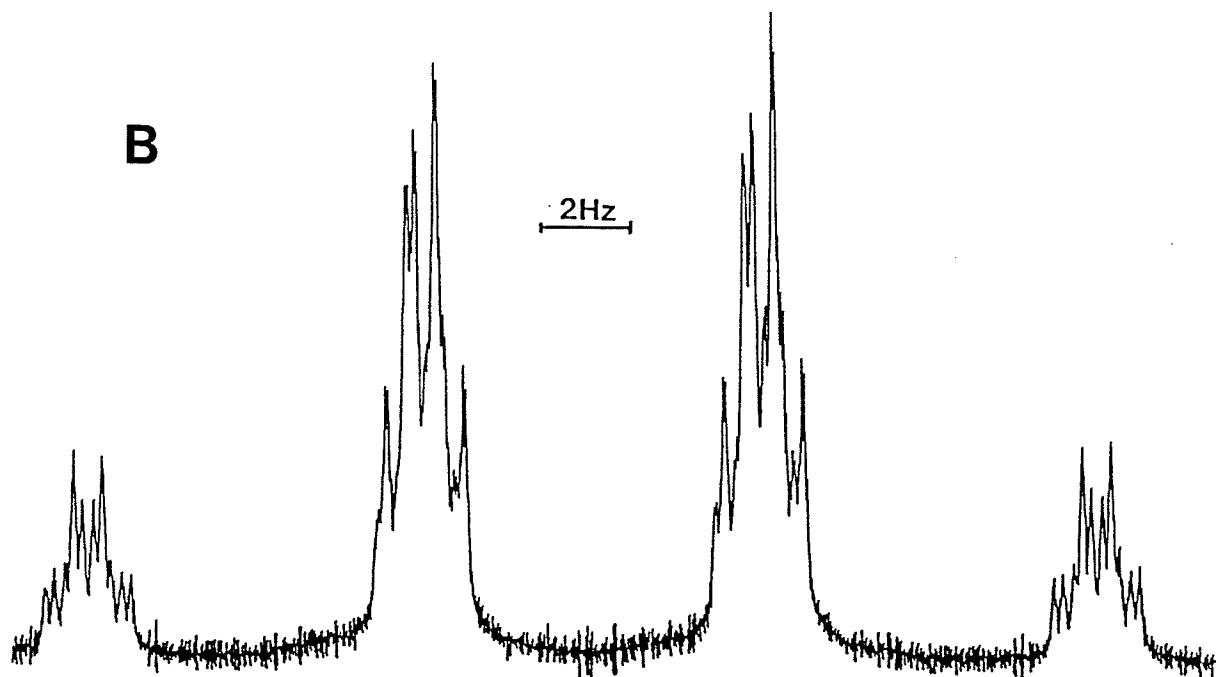
**A****B**

FIGURE 13

Fluorine-19 nmr spectrum for the *meta* fluorines in 3,5-difluoroethylbenzene

A) experimental

B) calculated

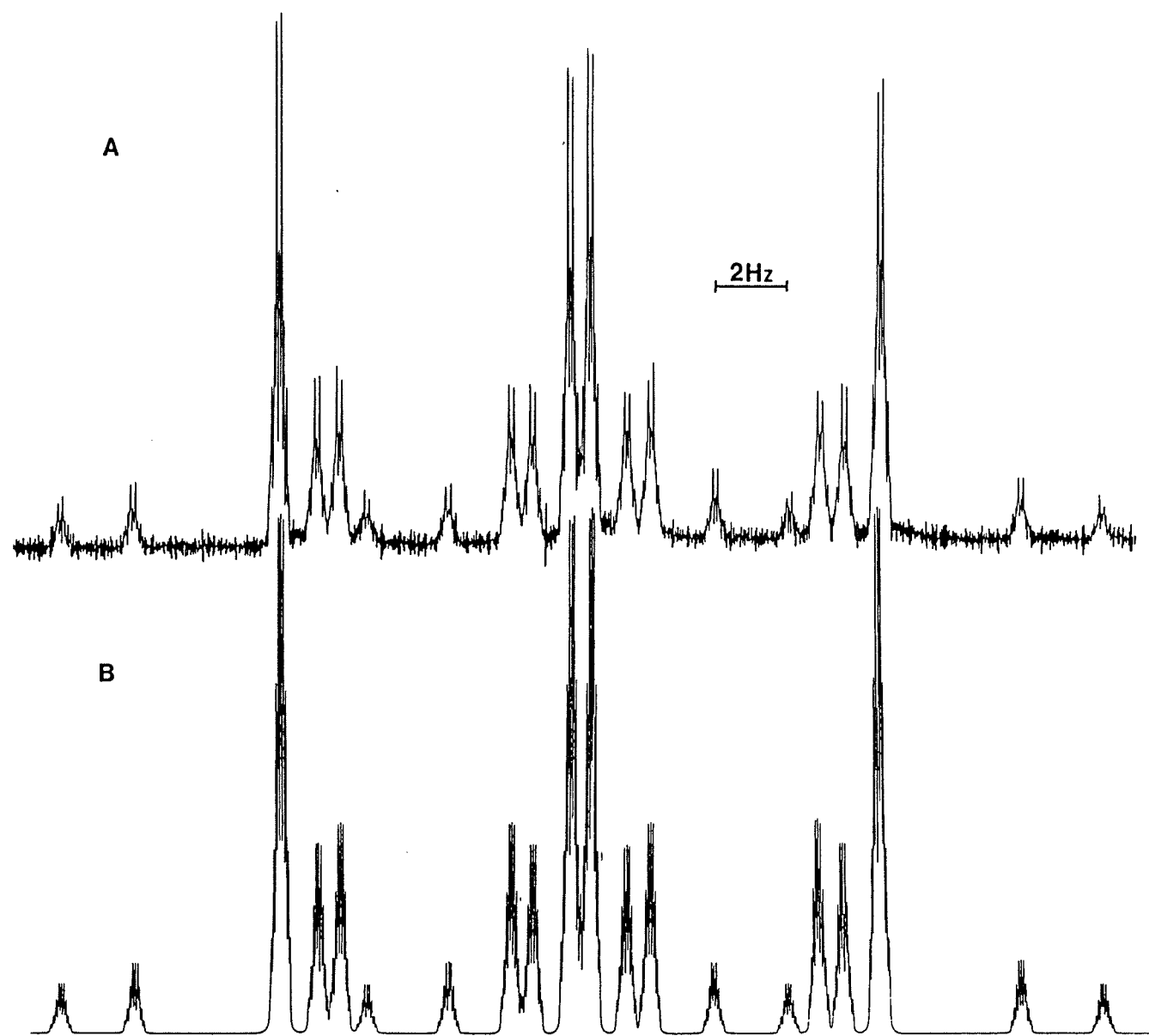
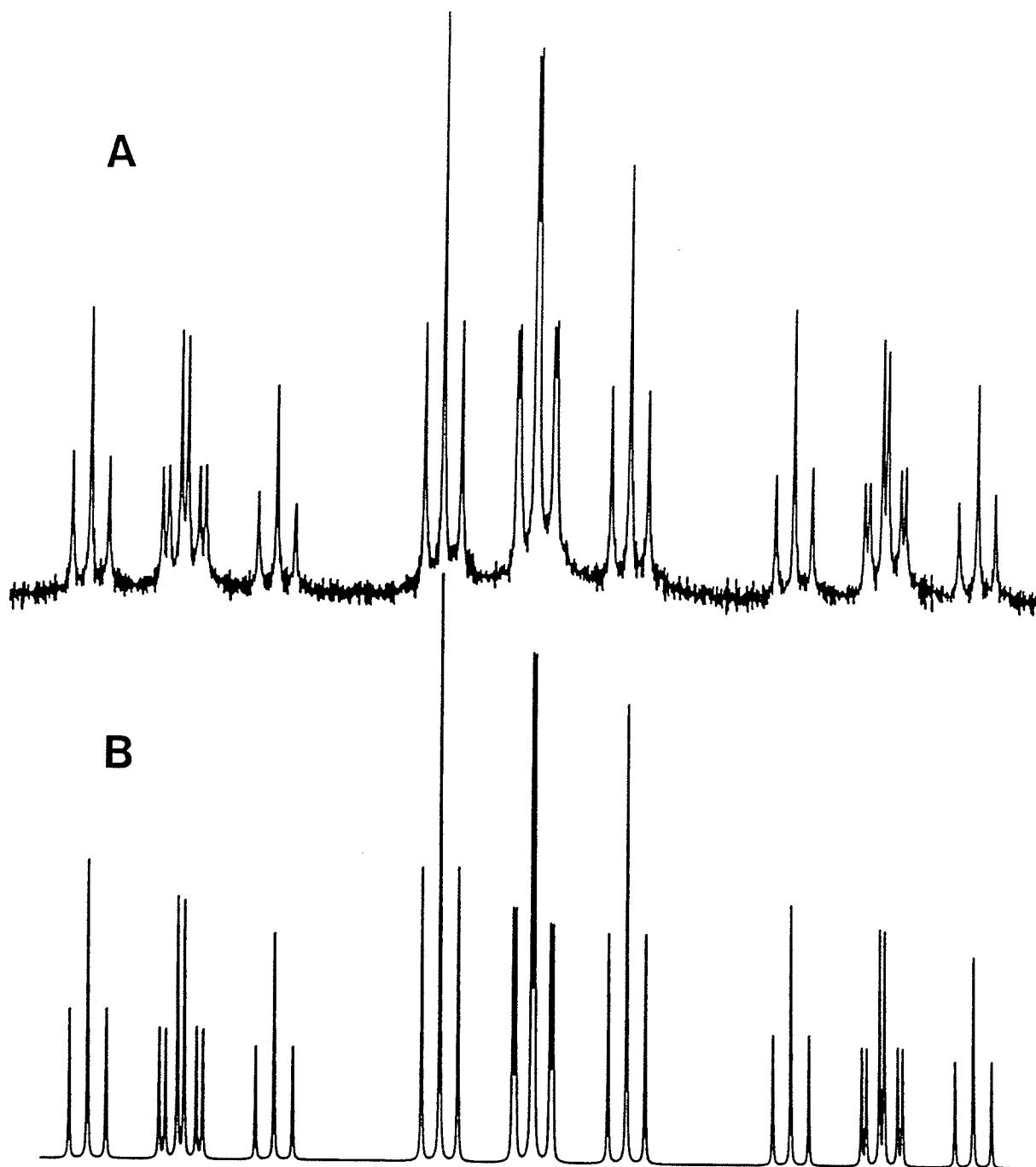


FIGURE 14

NMR spectrum for the *para* proton  $H_4$  in 3,5-difluoroethylbenzene

A) experimental

B) calculated



### 3) 3,5-difluoroisopropylbenzene

In Table 3, the results for the analyses of proton and fluorine nmr spectra of a 1.0 mole % solution of 3,5-difluoroisopropylbenzene in  $\text{CS}_2/\text{C}_6\text{D}_{12}$  are shown. Some difficulties were encountered in this analysis. Because there are small couplings from the *meta* fluorines to the methylene and methyl protons of the sidechain, a rather complex fluorine nmr spectrum occurs as shown in figure 15a. Due to experimental difficulties, a very small amount of compound was prepared which led to a low signal/noise ratio in the fluorine region causing a more difficult analysis. There are no observed couplings from the methyl protons to the *ortho* or *para* protons even though they are optimized in the NUMARIT analyses.

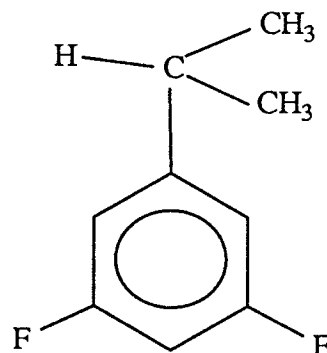
A determination of the relative sign of  $^5J_m(\text{F},\text{CH})$  in 3,5-difluoroisopropylbenzene using a partial decoupling experiment is shown in figure 15. The *para* proton region is also shown in figure 16.



TABLE 3

Proton and fluorine spectral parameters<sup>a</sup> for a 1.0 mole%<sup>b</sup> solution of  
3,5-difluoroisopropylbenzene in CS<sub>2</sub>/C<sub>6</sub>D<sub>12</sub> at 300K

$\nu(\text{CH}_3)$	370.610(3) <sup>c</sup>
$\nu(\text{CH})$	853.592(2)
$\nu(\text{H}_2=\text{H}_6)$	1992.763(1)
$\nu(\text{H}_4)$	1943.830(1)
$\nu(\text{F}_3=\text{F}_5)$	14799.668(1)



$^3\text{J}(\text{CH}_3, \text{CH})$	6.896(1)	$^5\text{J}(\text{CH}_3, \text{H}_2)$	-0.001(1) <sup>e</sup>
$^3\text{J}(\text{H}_2, \text{F}_3)$	9.412(1)	$^5\text{J}(\text{CH}, \text{F}_3)$	+0.362(2) <sup>f</sup>
$^3\text{J}(\text{H}_4, \text{F}_5)$	8.763(1)	$^5\text{J}(\text{H}_2, \text{F}_5)$	-0.909(1) <sup>d</sup>
$^4\text{J}(\text{CH}, \text{H}_2)$	-0.590(2)	$^6\text{J}(\text{CH}_3, \text{F}_3)$	0.123(1)
$^4\text{J}(\text{H}_2, \text{H}_6)$	1.482(2)	$^6(\text{CH}, \text{H}_4)$	-0.245(2)
$^4\text{J}(\text{H}_2, \text{H}_4)$	2.336(1)	$^7\text{J}(\text{CH}_3, \text{H}_4)$	-0.000(1) <sup>e</sup>
$^4\text{J}(\text{F}_3, \text{F}_5)$	6.523(2) <sup>d</sup>		

Transitions Calculated	2936
Transitions Assigned	1008
Peaks Observed	188
Largest Difference	-0.047
RMS Deviation	0.018

## NOTES

- a In Hertz.  $^1\text{H}$  nmr at 300.135 MHz to high frequency of TMS.  $^{19}\text{F}$  nmr at 282.365 MHz to high frequency of  $\text{C}_6\text{F}_6$ . Unless otherwise stated signs of couplings assumed to be as they appear in the table.
- b Approximately 1.0 mole% in solution mixture consisting of  $\text{CS}_2$ , 10 mole%  $\text{C}_6\text{D}_{12}$ , 0.25 mole% TMS and 0.25 mole%  $\text{C}_6\text{F}_6$ .
- c Numbers in parentheses are standard deviations in the last significant digit, as given by the NUMARIT analysis.
- d  $^4\text{J}(\text{F}_3, \text{F}_5)$  correlates with  $^5\text{J}(\text{H}_2, \text{F}_5)$  by 0.340.
- e These couplings were optimized even though they were not observed experimentally.
- f Sign is determined by partial decoupling experiments.

a) Determination of the relative sign of  $^5J_m(\text{CH},\text{F})$  by double resonance experiments

A relatively small coupling exists between the methine proton and the *meta* fluorine-19 nucleus. Partial decoupling of the low frequency peak of the methyl doublet results in a decrease in linewidth and an increase in intensity of the low frequency peaks of the doublets associated with coupling to the methine proton (see figure 15b). Partial decoupling of the high frequency methyl peak perturbed the high frequency peaks of the *meta* fluorine-19 doublets (see figure 15c). These experiments imply a positive value for  $^5J_m(\text{CH},\text{F})$ .

FIGURE 15

Sign determination of  $^5J_m(\text{CH},\text{F})$  in 3,5-difluoroisopropylbenzene

- A) *meta* fluorine region with no irradiation of peaks in the methyl region
- B) with irradiation of the low frequency peak of the methyl doublet
- C) with irradiation of the high frequency peak of the methyl doublet

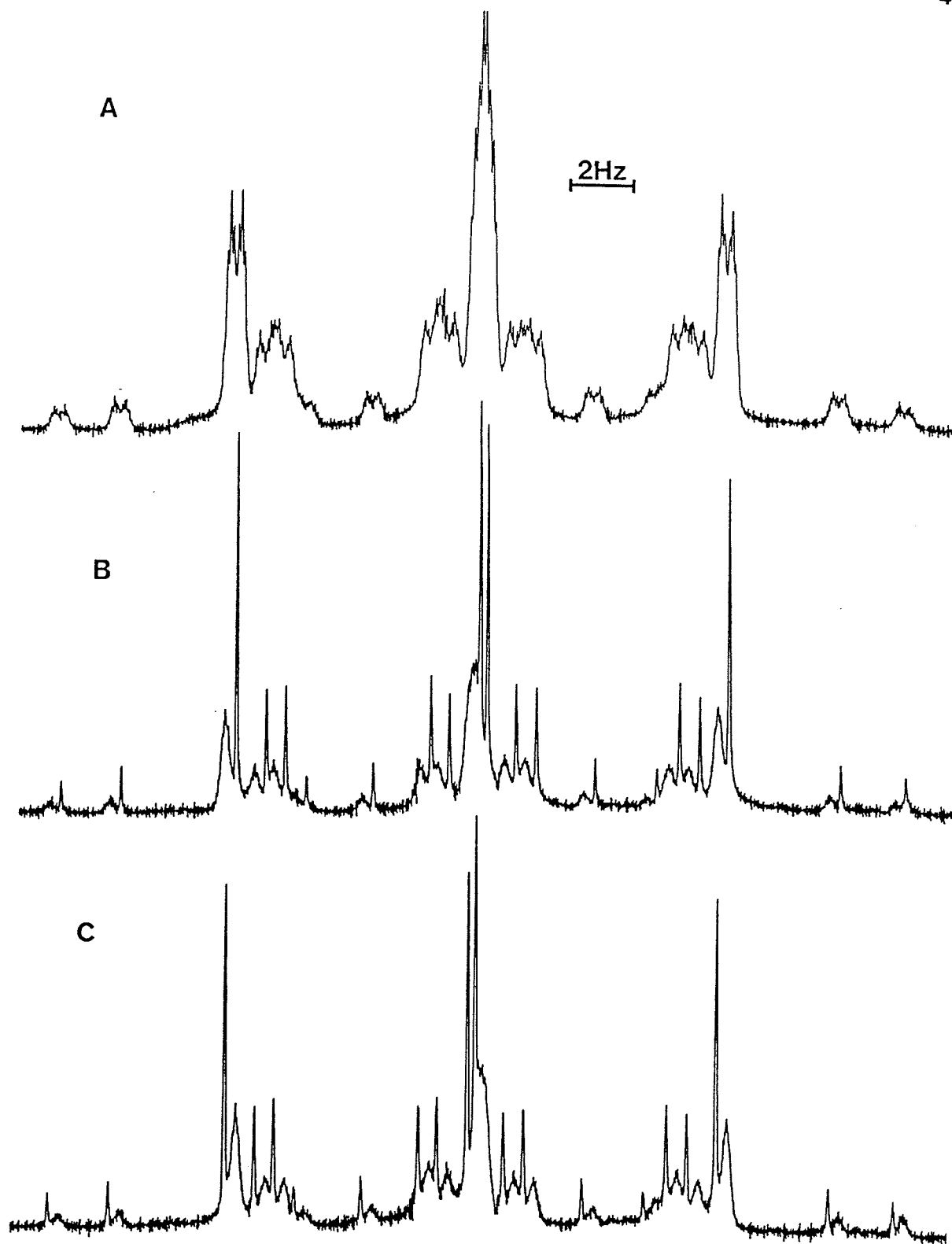
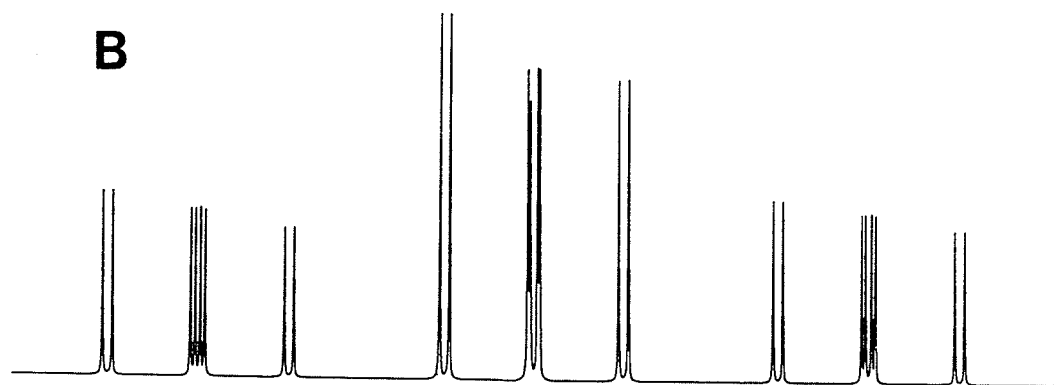
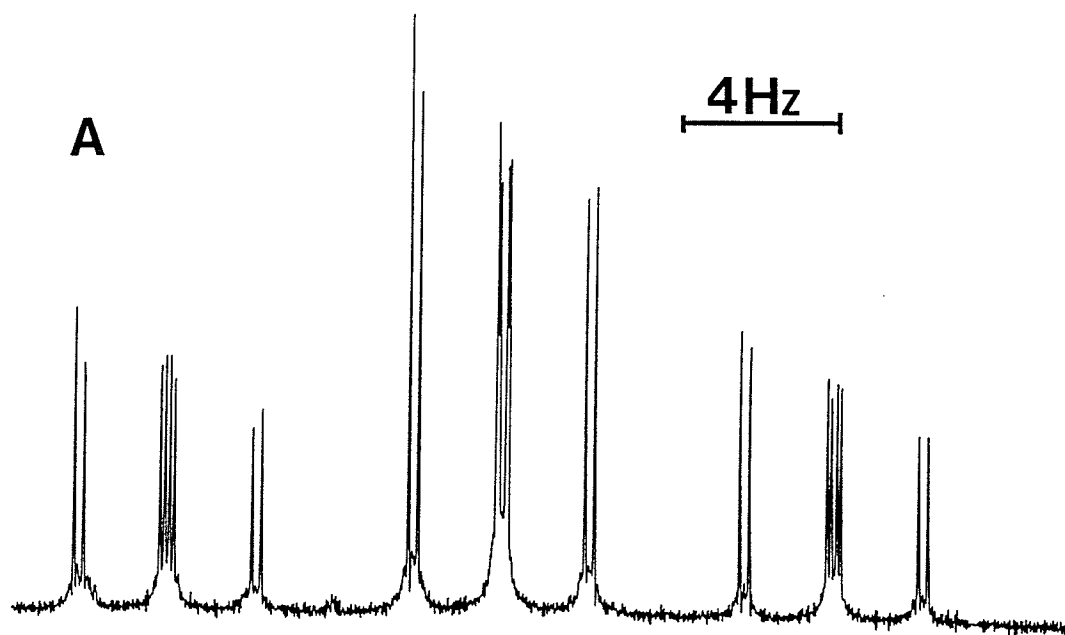


FIGURE 16

NMR spectrum for the *para* proton H<sub>4</sub> in 3,5-difluoroisopropylbenzene

A) experimental

B) calculated



## 4) 2,3-difluorotoluene

The spectral parameters for a 2.0 mole % solution of 2,3-difluorotoluene in  $\text{CS}_2/\text{C}_6\text{D}_{12}$  appear in Table 4. The major problem encountered in the analysis was the small shift differences between the ring protons. Here, reasonably high precision was attained, as indicated by the standard deviations of the parameters. The nature of the ring spin-system entailed relatively large correlations between shift values and coupling constants within the phenyl moiety. Otherwise, the analysis was straightforward. Signs and couplings were taken from previous analyses of 2-fluorotoluene<sup>45</sup> and 3-fluorotoluene.<sup>46a</sup>

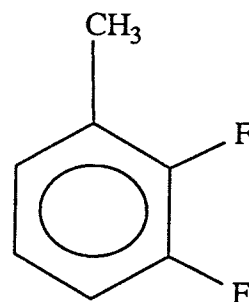
The methyl proton region, ring proton region and both *ortho* and *meta* fluorine regions are shown in figures 17, 18, 19 and 20, respectively.



TABLE 4

Proton and fluorine spectral parameters<sup>a</sup> for a 3.9 mole% solution of 2,3-difluorotoluene<sup>b</sup> in CS<sub>2</sub>/C<sub>6</sub>D<sub>12</sub> at 300K

$\nu(\text{CH}_3)$	673.877(1) <sup>c</sup>
$\nu(\text{H}_4)$	2055.610(2) <sup>d</sup>
$\nu(\text{H}_2)$	2049.887(2)
$\nu(\text{F}_5)$	6709.062(1) <sup>d</sup>
$\nu(\text{H}_3)$	2057.719(2)
$\nu(\text{F}_6)$	5652.258(1) <sup>d</sup>



$^3J_o(\text{H}_2, \text{H}_3)$	7.733(3)	$^5J_p(\text{H}_3, \text{F}_6)$	-1.744(3) <sup>d</sup>
$^3J_o(\text{H}_3, \text{H}_4)$	8.289(3)	$^4J_m(\text{H}_2, \text{F}_6)$	6.346(3) <sup>d</sup>
$^4J_m(\text{H}_2, \text{H}_4)$	1.644(3)	$^4J_o(\text{CH}_3, \text{F}_6)$	2.273(1)
$^3J_o(\text{H}_4, \text{F}_5)$	9.991(4) <sup>d</sup>	$^5J_m(\text{CH}_3, \text{F}_5)$	-0.170(1)
$^4J_m(\text{H}_3, \text{F}_5)$	4.912(3)	$^6J_p(\text{CH}_3, \text{H}_4)$	-0.575(2) <sup>e</sup>
$^5J_p(\text{H}_2, \text{F}_5)$	-1.561(3) <sup>d</sup>	$^5J_m(\text{CH}_3, \text{H}_3)$	0.328(2) <sup>e</sup>
$^3J_o(\text{F}_5, \text{F}_6)$	-20.869(2)	$^4J_o(\text{CH}_3, \text{H}_2)$	-0.774(2)
$^4J_m(\text{H}_4, \text{F}_6)$	7.439(3) <sup>d</sup>		

Transitions Calculated	745
Transitions Assigned	511
Peaks Observed	245
Largest Difference	0.031
RMS Deviation	0.013

## NOTES

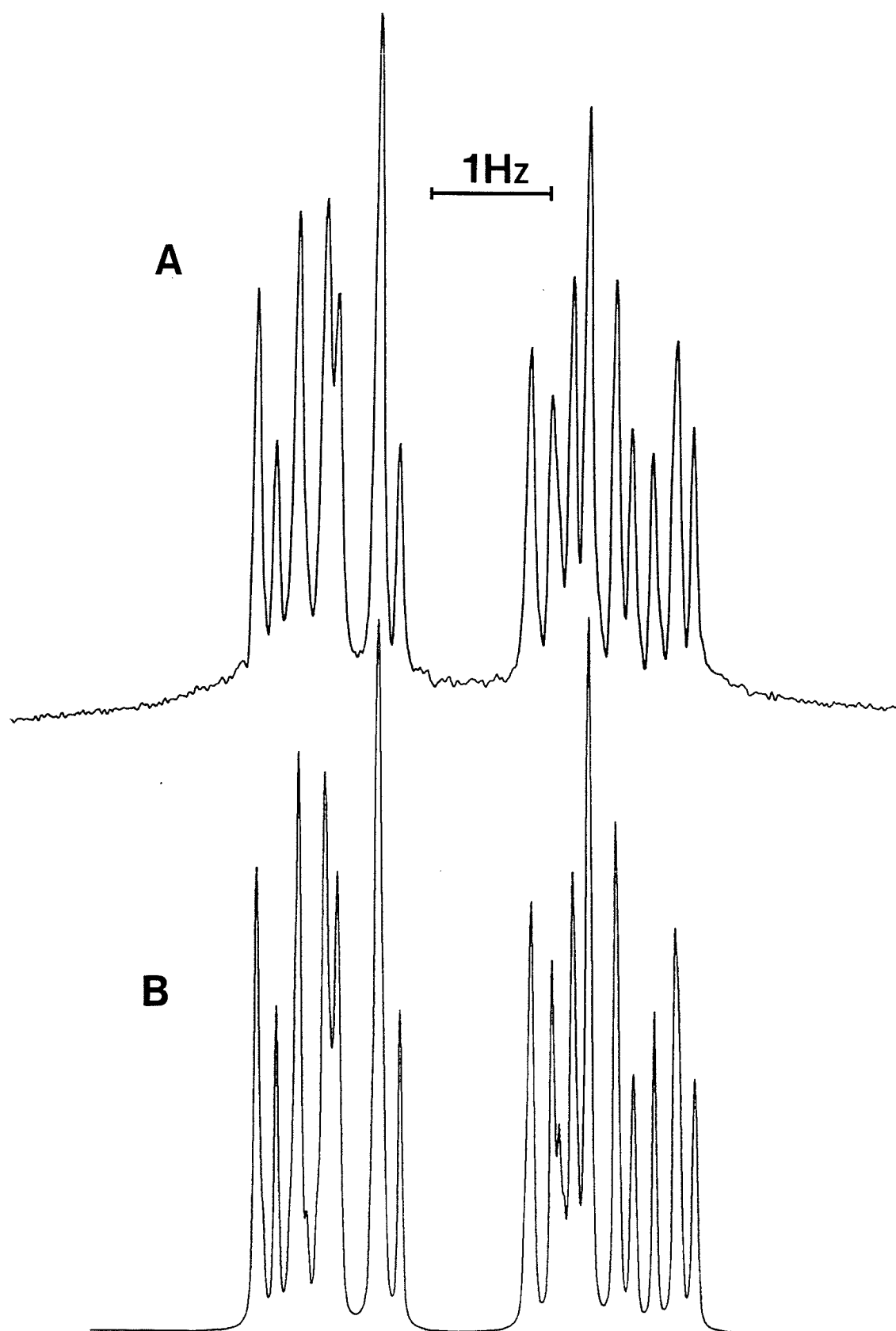
- a In Hertz.  $^1\text{H}$  nmr at 300.135 MHz to high frequency of TMS. Unless otherwise stated, signs of couplings assumed to be as they appear in the table.
- b Approximately 3.9 mole % in solution mixture consisting of  $\text{CS}_2$ , 10 mole %  $\text{C}_6\text{D}_{12}$ , 0.25 mole % TMS and 0.25 mole %  $\text{C}_6\text{F}_6$ .
- c Numbers in parentheses are standard deviations in the last significant digit, resulting from the NUMARIT analysis.
- d  $\nu_4$  correlates with  $\nu_5$  by -0.307.  $\nu_4$  correlates with  $^4J_m(\text{F}_6, \text{H}_4)$  by 0.344.  $\nu_4$  correlates with  $^3J_o(\text{F}_5, \text{H}_4)$  by -0.351.  $\nu_4$  correlates with  $^5J_p(\text{F}_5, \text{H}_2)$  by 0.397.  $\nu_5$  correlates with  $^5J_p(\text{F}_6, \text{H}_3)$  by 0.315.  $\nu_5$  correlates with  $^5J_p(\text{F}_5, \text{H}_2)$  by -0.274.  $\nu_6$  correlates with  $^4J_m(\text{F}_6, \text{H}_2)$  by 0.313.  $\nu_6$  correlates with  $^3J_o(\text{F}_5, \text{H}_4)$  by 0.320.  $\nu_6$  correlates with  $^5J_p(\text{F}_5, \text{H}_2)$  by -0.366.
- e  $^6J_p(\text{CH}_3, \text{H}_4)$  correlates with  $^5J_m(\text{CH}_3, \text{H}_3)$  by -0.300.

FIGURE 17

Methyl proton region of 2,3-difluorotoluene

A) experimental

B) calculated



**FIGURE 18**

**Ring proton region of 2,3-difluorotoluene**

**A) experimental**

**B) calculated**

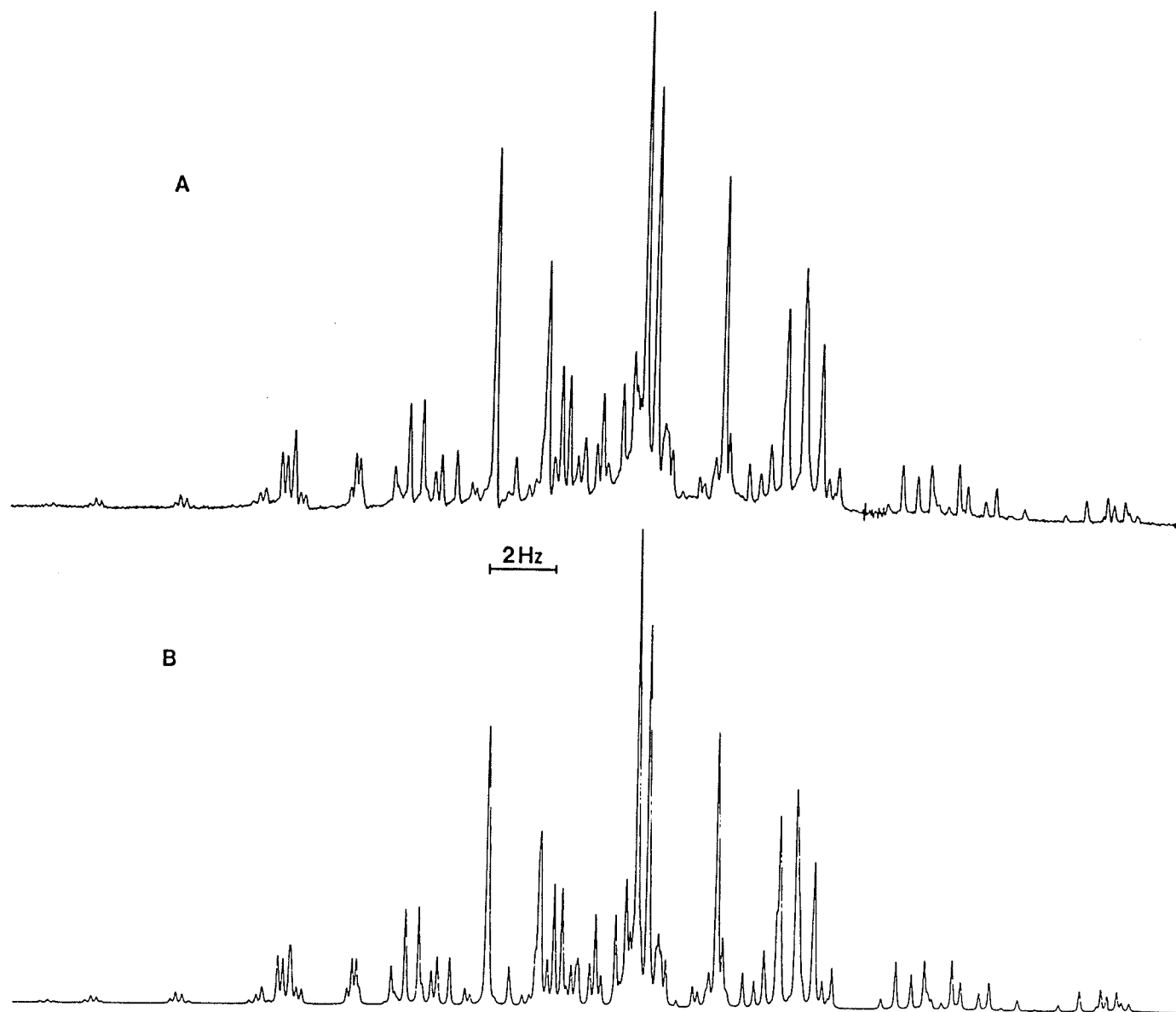


FIGURE 19

$^{19}\text{F}$  nmr spectrum for the *meta* fluorine  $\text{F}_5$  region in 2,3-difluorotoluene

A) experimental

B) calculated

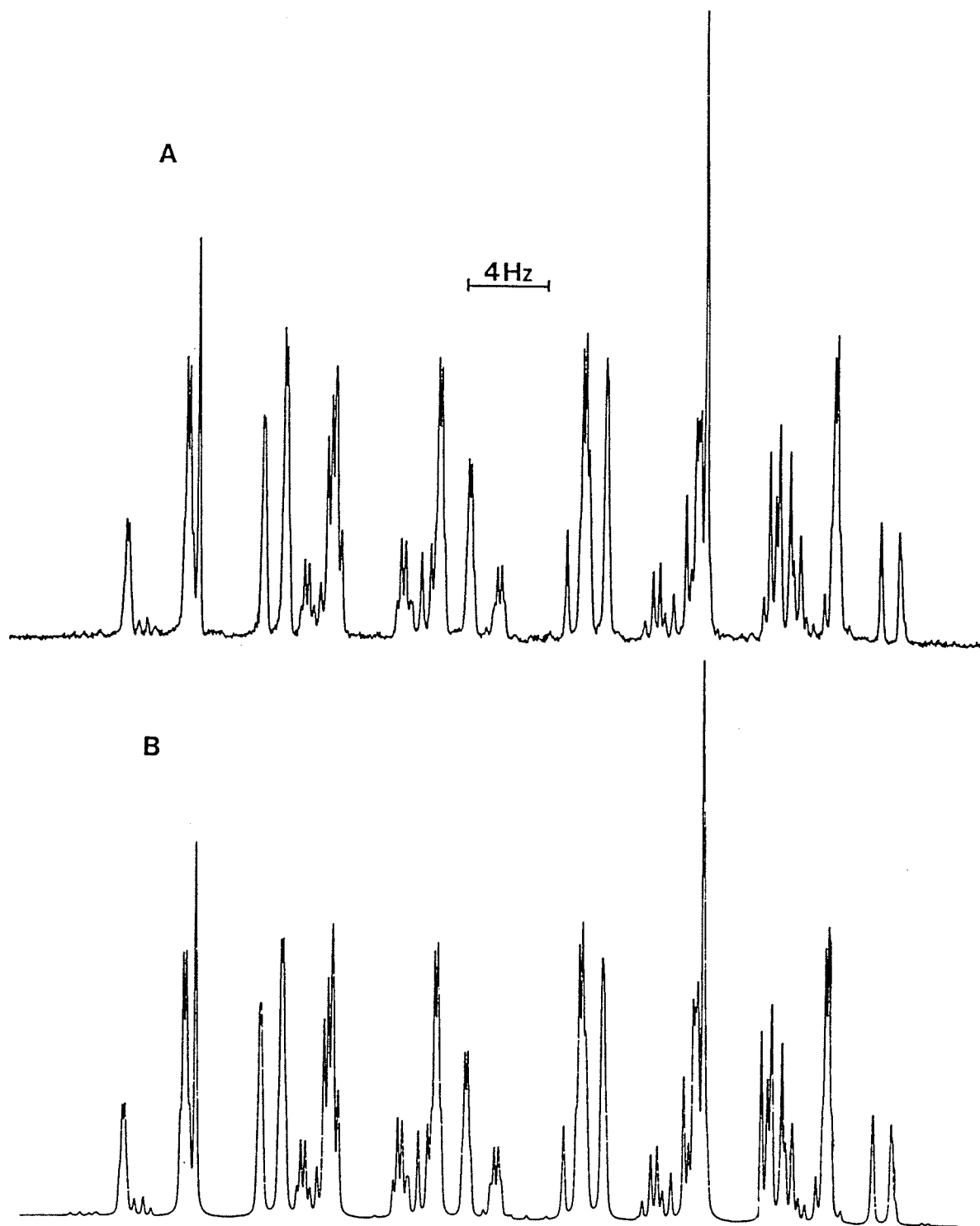


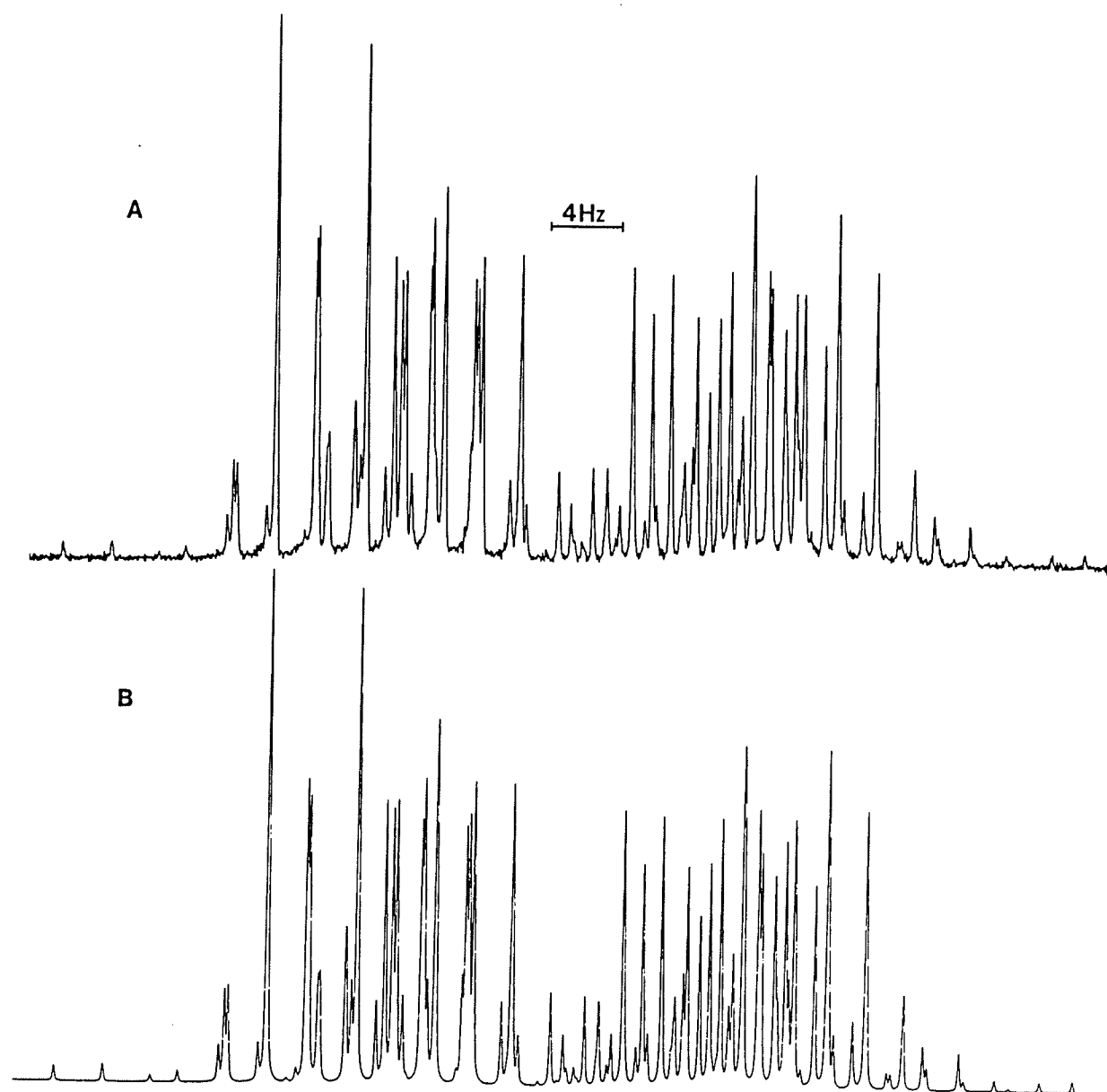


FIGURE 20

The *ortho* fluorine F<sub>6</sub> region of 2,3-difluorotoluene

A) experimental

B) calculated



### 5) 2,3-difluoro- $\alpha,\alpha$ -diacetoxytoluene

The results for the analyses of fluorine and proton nmr spectra of a 2.0 mole % solution of 2,3-difluoro- $\alpha,\alpha$ -diacetoxytoluene in  $\text{CS}_2/\text{C}_6\text{D}_{12}$  and a 2.1 mole % solution of 2,3-difluoro- $\alpha,\alpha$ -diacetoxytoluene in acetone- $\text{d}_6$  appear in Table 5.

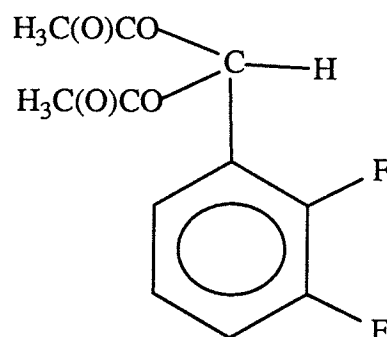
The analyses were straightforward. For each of the two solutions, the chemical shift values for both the methyl and methine protons were not optimized. The proton nmr spectrum for the methyl region is a sharp doublet with the methyl protons coupling to the methine proton only. Although the magnitude of this coupling is given in Table 5, its relative sign was not determined. In contrast to the methyl proton region, the methine proton is coupled not only to the methyl protons but also to the rest of the ring nuclei and gives rise to a very broad and unresolved proton nmr spectrum. The methyl and methine proton nmr spectra are compared in figure 22.

The relative sign of  $^5J_m(\text{F},\text{CH})$  was determined using the experimental nmr spectra of the *meta* fluorines and the program NUMARIT<sup>39</sup> in the iterative mode as shown in figure 21. All other signs and couplings between ring nuclei were taken from the analysis of 2,3-difluorotoluene.

The *meta* proton, *ortho* and *para* proton, *ortho* fluorine and *meta* fluorine nmr spectra are given in figures 23, 24, 25 and 26, respectively.

TABLE 5

Proton and fluorine spectral parameters<sup>a</sup> for a 2.0 mole% solution of  
 2,3-difluoro- $\alpha,\alpha$ -diacetoxytoluene in  $\text{CS}_2/\text{C}_6\text{D}_{12}$ <sup>b</sup> and a 2.1 mole% solution of  
 2,3-difluoro- $\alpha,\alpha$ -diacetoxytoluene in acetone- $\text{d}_6$ <sup>c</sup> at 300K



	$\text{CS}_2/\text{C}_6\text{D}_{12}$	Acetone- $\text{d}_6$
$\nu(\text{CH}_3)$	601.075 <sup>d</sup>	638.001 <sup>d</sup>
$\nu(\text{CH})$	2306.700 <sup>d</sup>	2366.200 <sup>d</sup>
$\nu(\text{H}_2)$	2155.597(2) <sup>e</sup>	2231.833(1) <sup>e</sup>
$\nu(\text{H}_3)$	2113.489(2)	2190.369(1)
$\nu(\text{H}_4)$	2131.816(2)	2227.521(1)
$\nu(\text{F}_5)$	7084.258(2) <sup>g</sup>	6940.652(1) <sup>h</sup>
$\nu(\text{F}_6)$	5780.187(2) <sup>g</sup>	5623.633(1)

TABLE 5 (cont'd)

	CS <sub>2</sub> /C <sub>6</sub> D <sub>12</sub>	Acetone-d <sub>6</sub>
<sup>5</sup> J(CH <sub>3</sub> ,CH)	(±)0.063 <sup>f</sup>	(±)0.059 <sup>f</sup>
<sup>3</sup> J <sub>o</sub> (H <sub>2</sub> ,H <sub>3</sub> )	7.913(2)	7.953(1)
<sup>4</sup> J <sub>m</sub> (H <sub>2</sub> ,H <sub>4</sub> )	1.646(2)	1.612(1)
<sup>3</sup> J <sub>o</sub> (H <sub>3</sub> ,H <sub>4</sub> )	8.306(2)	8.377(1)
<sup>5</sup> J <sub>p</sub> (H <sub>2</sub> ,F <sub>5</sub> )	- 1.632(2)	- 1.626(1)
<sup>4</sup> J <sub>m</sub> (H <sub>3</sub> ,F <sub>5</sub> )	4.667(3)	4.824(1)
<sup>3</sup> J <sub>o</sub> (H <sub>4</sub> ,F <sub>5</sub> )	9.880(2)	10.506(1) <sup>h</sup>
<sup>4</sup> J <sub>m</sub> (H <sub>2</sub> ,F <sub>6</sub> )	5.713(3)	5.938(1)
<sup>5</sup> J <sub>p</sub> (H <sub>3</sub> ,F <sub>6</sub> )	- 1.818(3) <sup>g</sup>	- 1.834(1) <sup>h</sup>
<sup>4</sup> J <sub>m</sub> (H <sub>4</sub> ,F <sub>6</sub> )	7.476(3)	7.754(1)
<sup>3</sup> J <sub>o</sub> (F <sub>5</sub> ,F <sub>6</sub> )	-20.940(3) <sup>g</sup>	-20.147(1)
<sup>4</sup> J <sub>o</sub> (CH,H <sub>2</sub> )	- 0.506(3)	- 0.526(2)
<sup>5</sup> J <sub>m</sub> (CH,H <sub>3</sub> )	0.338(3)	0.357(2)
<sup>6</sup> J <sub>p</sub> (CH,H <sub>4</sub> )	- 0.185(3)	- 0.202(2)
<sup>5</sup> J <sub>m</sub> (CH,F <sub>5</sub> )	(±)0.043(4) <sup>g</sup>	- 0.147(2)
<sup>4</sup> J <sub>o</sub> (CH,F <sub>6</sub> )	0.204(5) <sup>g</sup>	0.289(2)
Transitions Calculated	218	227
Transitions Assigned	131	143
Peaks Observed	146 <sup>i</sup>	147 <sup>j</sup>
Largest Difference	0.024	0.012
RMS Deviation	0.008	0.005

## NOTES

- a In Hertz.  $^1\text{H}$  nmr at 300.135 MHz to high frequency of TMS.  $^{19}\text{F}$  nmr at 282.365 MHz to high frequency of  $\text{C}_6\text{F}_6$ . Both the *meta* and *ortho* fluorines are treated in the X approximation. Unless otherwise stated, the signs of the couplings are as they appear in the table.
- b 2.0 mole % in solution mixture consisting of  $\text{CS}_2$ , 10.0 mole %  $\text{C}_6\text{D}_{12}$ , 0.25 mole % TMS and 0.25 mole %  $\text{C}_6\text{F}_6$ .
- c 2.1 mole % in solution mixture consisting of acetone- $\text{d}_6$ , 1 drop of TMS and 1 drop of  $\text{C}_6\text{F}_6$ .
- d An approximate value for the chemical shift of this proton and this shift value was not optimized in the analysis.
- e Numbers in parentheses are standard deviations in the last significant digit as given by the NUMARIT analysis.
- f Sign was not determined.
- g  $\nu(\text{F}_6)$  correlates with  $^4\text{J}_\text{o}(\text{CH}, \text{F}_6)$  by -0.456 and with  $^5\text{J}_\text{p}(\text{H}_3, \text{F}_6)$  by -0.266.  $\nu(\text{F}_5)$  correlates with  $^5\text{J}_\text{m}(\text{CH}, \text{F}_5)$  by -0.231 and with  $^3\text{J}_\text{o}(\text{F}_5, \text{F}_6)$  by -0.240.  $^4\text{J}_\text{o}(\text{CH}, \text{F}_6)$  correlates with  $^5\text{J}_\text{p}(\text{H}_3, \text{F}_6)$  by 0.271.
- h  $\nu(\text{F}_5)$  correlates with  $^3\text{J}_\text{o}(\text{H}_4, \text{F}_5)$  by 0.296.  $^3\text{J}_\text{o}(\text{H}_4, \text{F}_5)$  correlates with  $^5\text{J}_\text{p}(\text{H}_3, \text{F}_6)$  by -0.225.
- i Only an estimated value for the number of peaks : methyl(2), methine(many), ring(90) and fluorine(54).
- j Only an estimated value for the number of peaks : methyl(2), methine(many), ring(81) and fluorine(64).

a) Determination of the relative sign of  $^5J_m(\text{F},\text{CH})$  in  
2,3-difluoro- $\alpha,\alpha$ -diacetoxytoluene

Figure 21 shows the determination of the relative sign for 2,3-difluoro- $\alpha,\alpha$ -diacetoxytoluene in  $\text{CS}_2/\text{C}_6\text{D}_{12}$ . The correct sign for the long-range coupling,  $^5J_m(\text{F},\text{CH})$ , is found in the absence of double resonance experiments. The sign of this coupling was not determined for the acetone- $\text{d}_6$  solution, but, from the iterative NUMARIT analysis,  $^5J_m(\text{F},\text{CH})$  appears to be positive.

After assignment of all the transitions in the *meta* fluorine  $\text{F}_5$  region, a negative value for  $^5J_m(\text{F},\text{CH})$  was obtained via NUMARIT in the iterative mode. The negative sign was clearly confirmed by comparison of the observed fluorine nmr spectrum with calculated spectra using both signs for  $^5J_m(\text{F},\text{CH})$  as shown in figure 21.

FIGURE 21

Sign determination of  $^5J_m(\text{F,CH})$  in 2,3-difluoro- $\alpha,\alpha$ -diacetoxytoluene

A) experimental *meta* fluorine-19 region

B) simulated *meta* fluorine-19 region with  $^5J_m(\text{F,CH}) < 0$

C) simulated *meta* fluorine-19 region with  $^5J_m(\text{F,CH}) > 0$



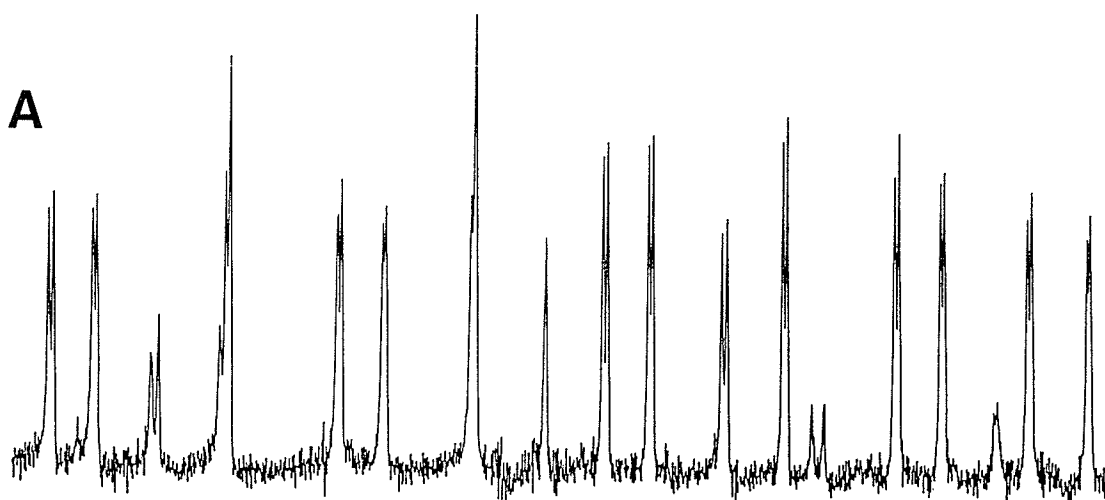
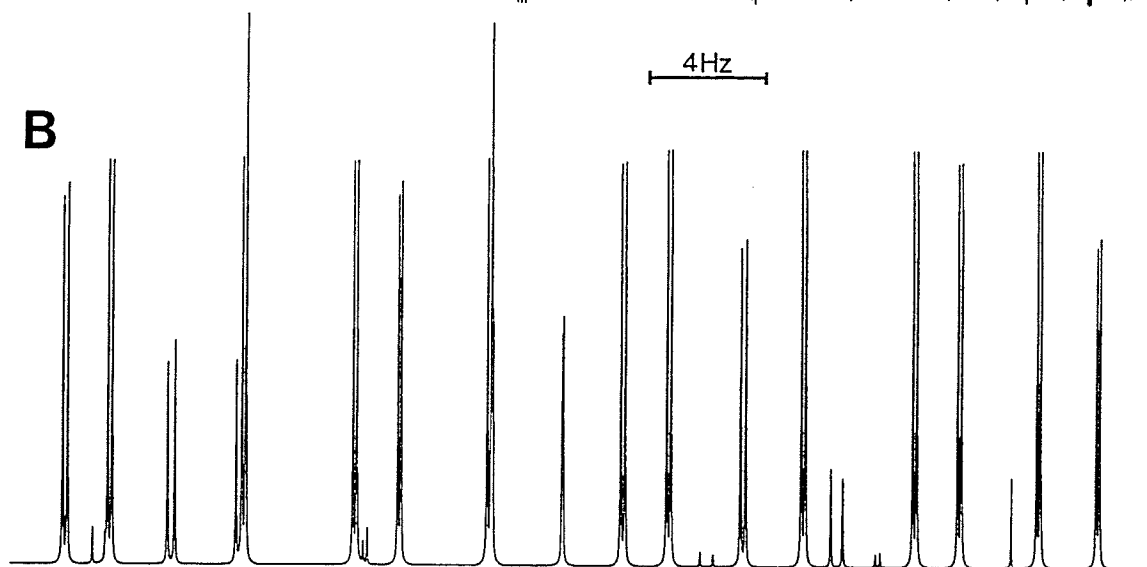
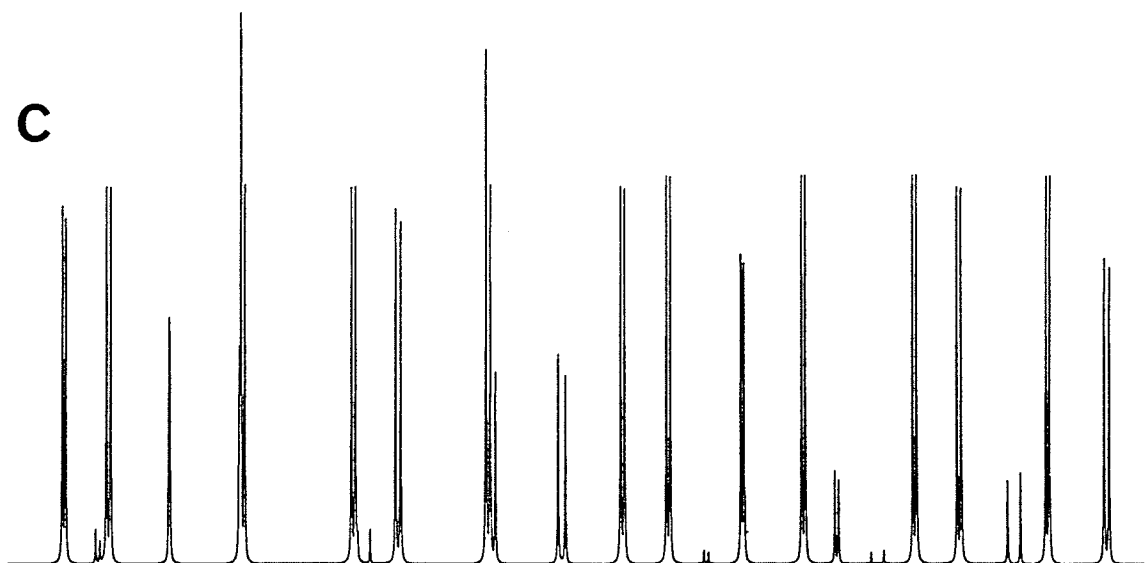
**A****B****C**

FIGURE 22

The methyl and methine regions of 2,3-difluoro- $\alpha,\alpha$ -diacetoxytoluene

A) methyl proton region

B) methine proton region

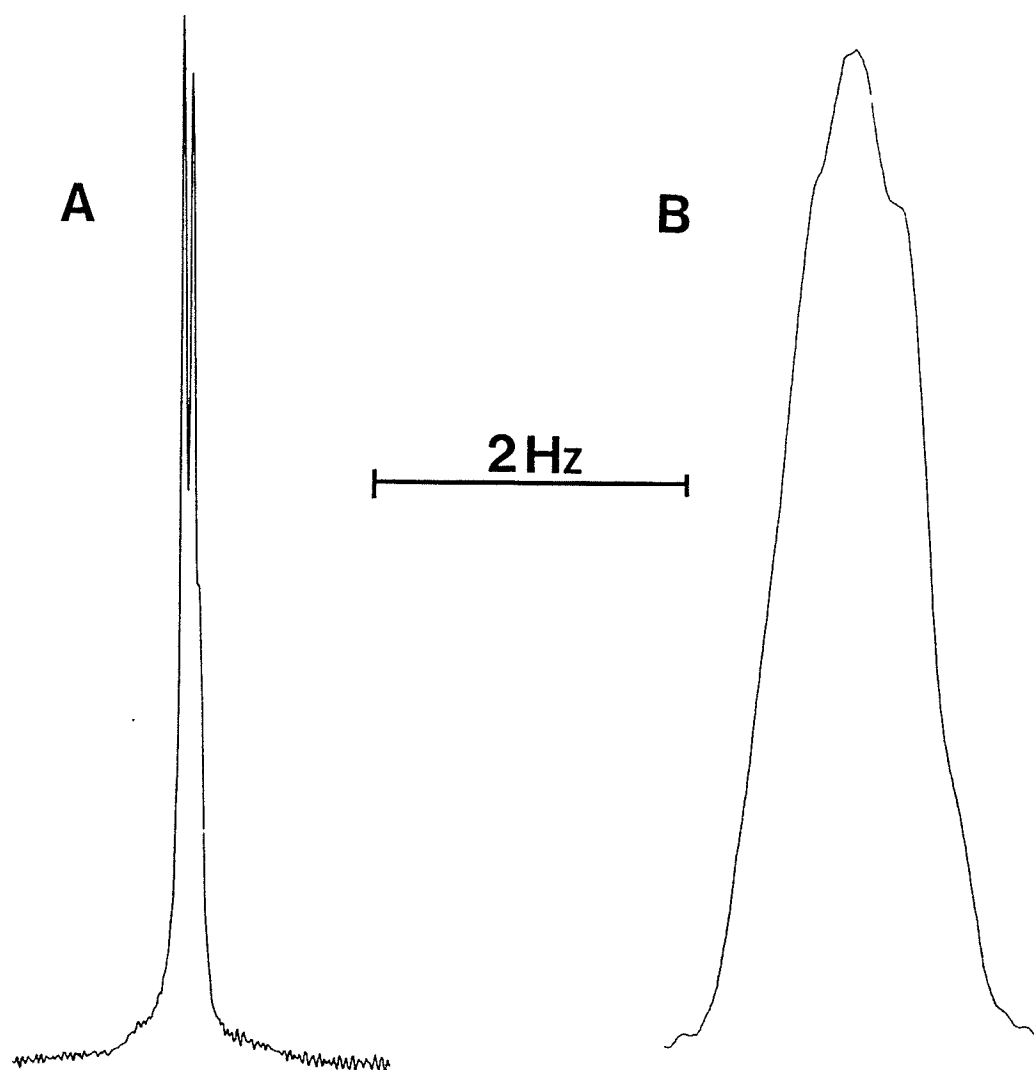


FIGURE 23

The *meta* ring proton region of 2,3-difluoro- $\alpha,\alpha$ -diacetoxytoluene

A) experimental

B) calculated

Note that some impurity peaks are present in the experimental spectrum.

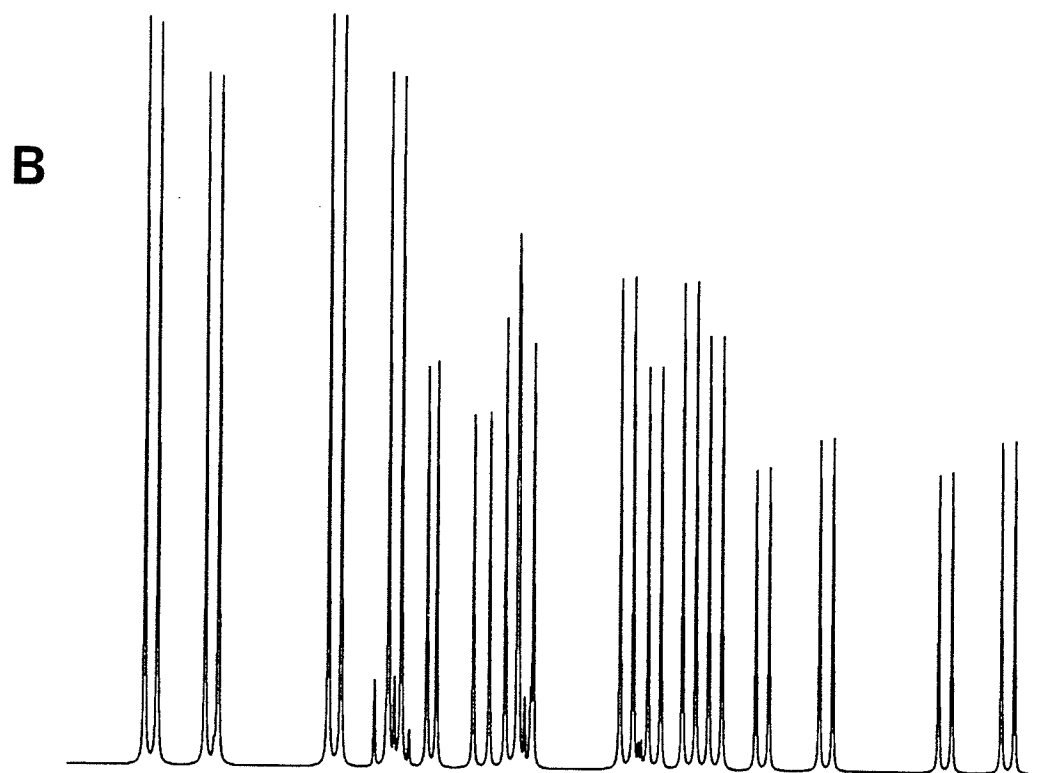
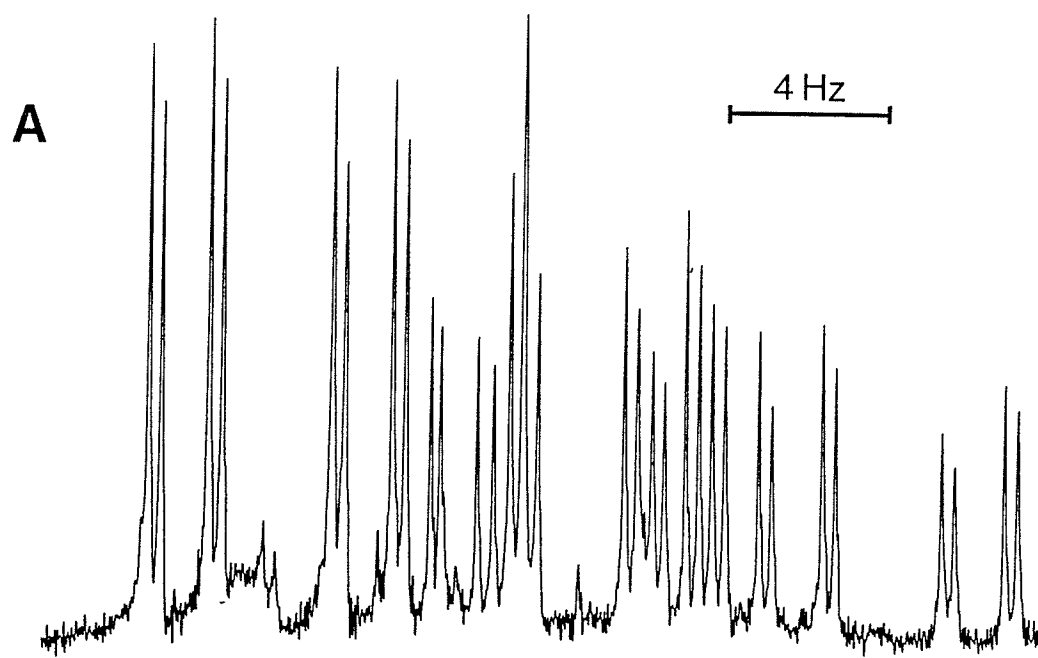


FIGURE 24

The *ortho* and *para* proton regions of 2,3-difluoro- $\alpha,\alpha$ -diacetoxytoluene

A) experimental

B) calculated

Note that some impurity peaks are present in the experimental spectrum.

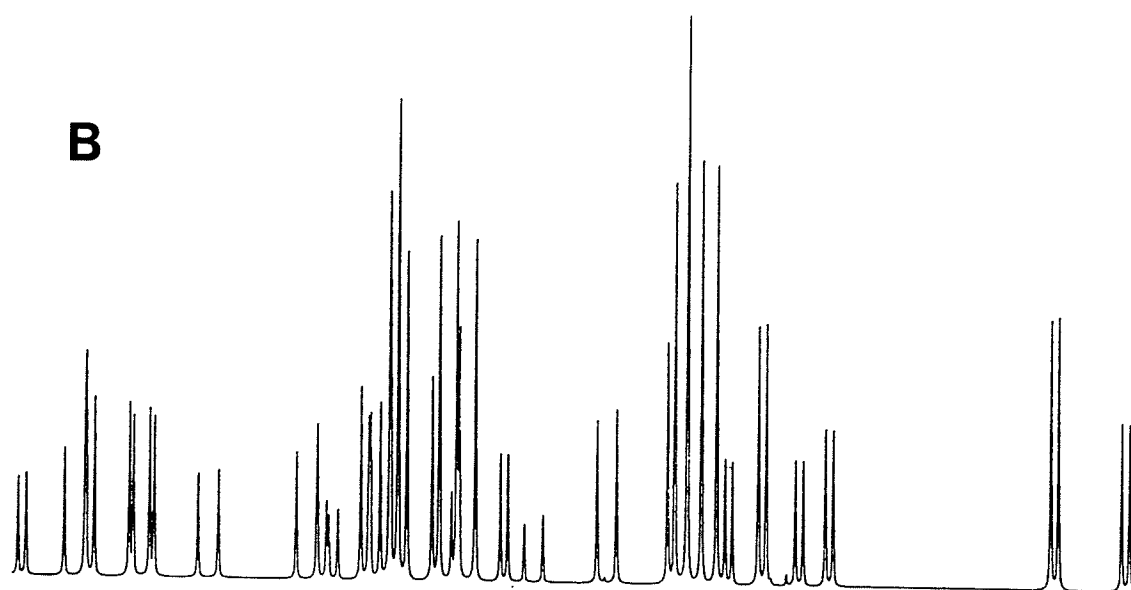
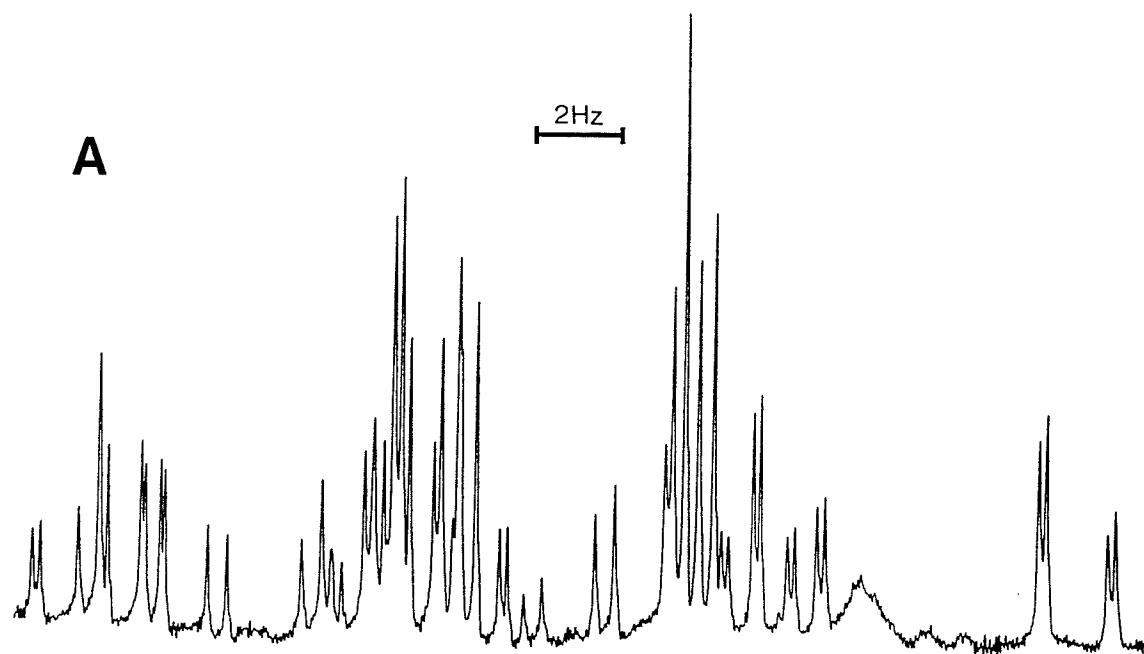


FIGURE 25

The *ortho* fluorine region of 2,3-difluoro- $\alpha,\alpha$ -diacetoxytoluene

A) experimental

B) calculated



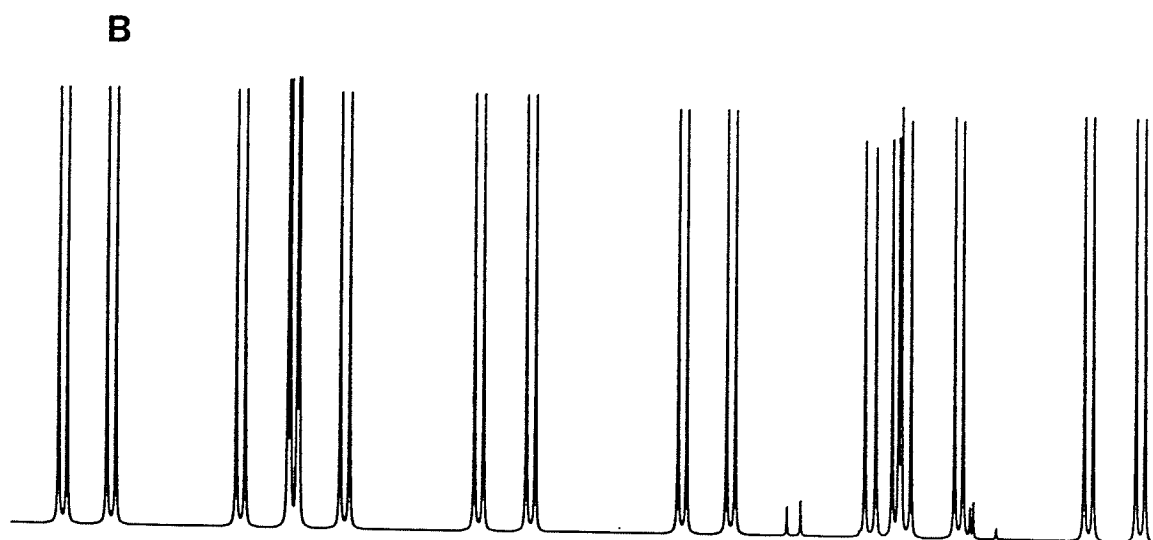
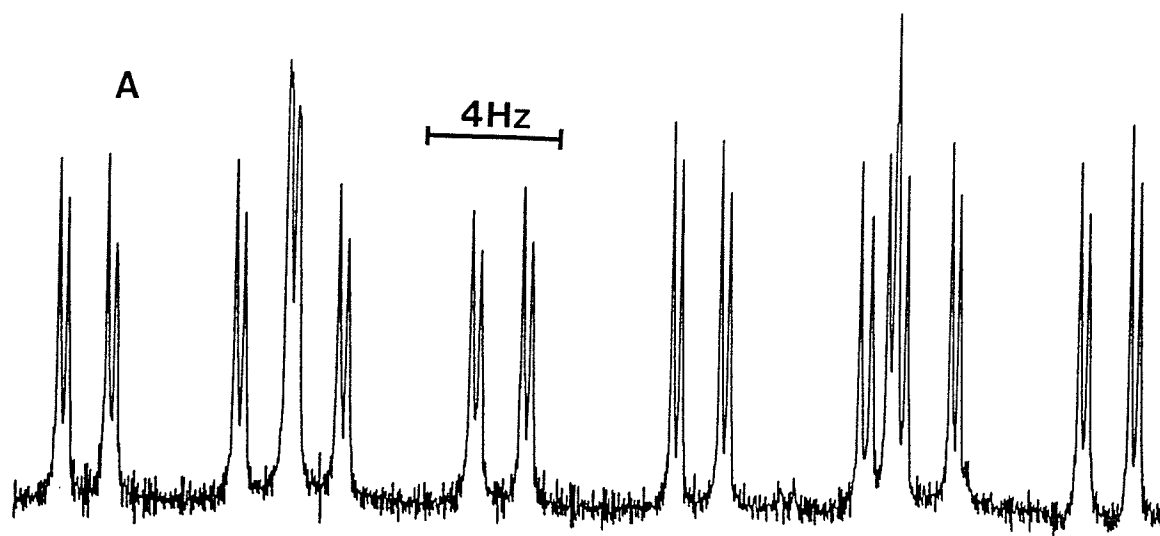
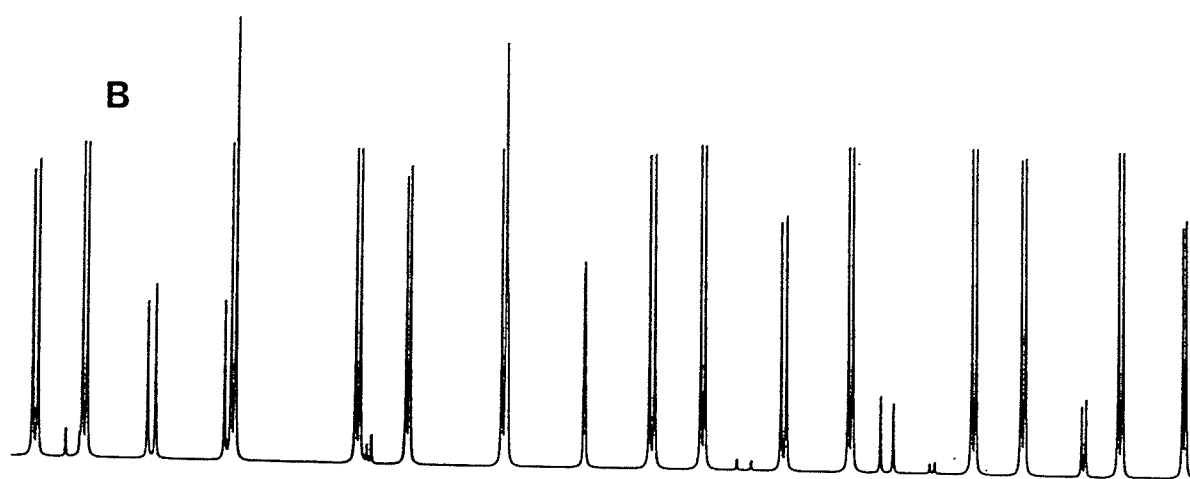
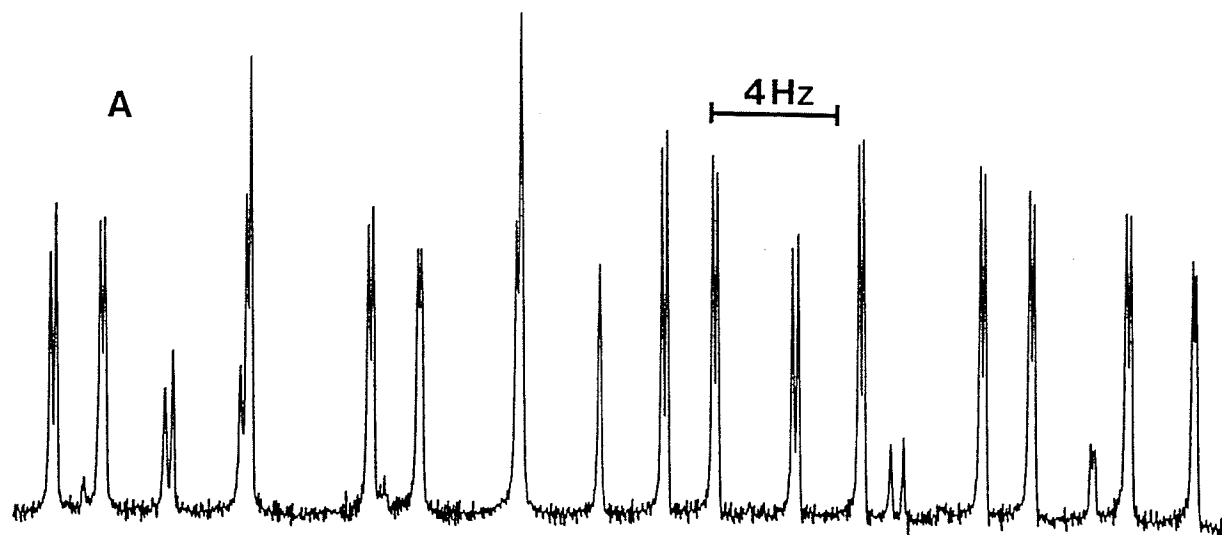


FIGURE 26

The *meta* fluorine region of 2,3-difluoro- $\alpha,\alpha$ -diacetoxytoluene

A) experimental

B) calculated



6) 2-bromo-5-fluoro- $\alpha,\alpha$ -diacetoxytoluene

Results for the analysis of the proton and fluorine spectra for a 3.2 mole % solution of 2-bromo-5-fluoro- $\alpha,\alpha$ -diacetoxytoluene in  $\text{CS}_2/\text{C}_6\text{D}_{12}$  are shown in Table 6. Here the chemical shift value for the methine proton was not optimized. Again the methyl proton region shows a sharp doublet indicating that there is coupling only to the methine proton. The magnitude of this coupling is given in Table 6, but its relative sign was not determined. Also, the methine proton, coupled both to the methyl substituents and ring nuclei, is broad and unresolved. The methyl and methine proton regions appear in figure 27.

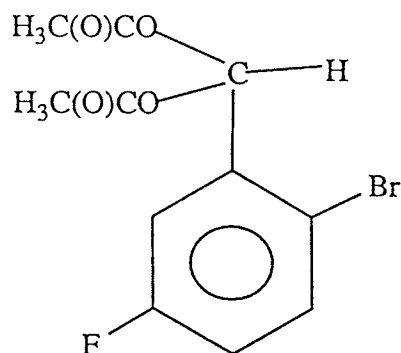
For the *meta* proton region shown in figure 28, the correct magnitude for the  $^5J_{\text{m}}(\text{CH}, \text{H}_3)$  coupling is uncertain as it is poorly resolved. All of the signs of the couplings between ring nuclei were taken from a previous analysis of 2-chloro-5-fluorotoluene.

The *meta* proton, *ortho* proton, *para* proton and *meta* fluorine regions are shown in figures 28, 29, 30 and 31, respectively.

TABLE 6

Proton and fluorine spectral parameters<sup>a</sup> for a 3.2 mole% solution of  
2-bromo-5-fluoro- $\alpha,\alpha$ -diacetoxytoluene<sup>b</sup> in CS<sub>2</sub>/C<sub>6</sub>D<sub>12</sub> at 300K

$\nu(\text{CH}_3)$	608.555(0) <sup>c</sup>
$\nu(\text{CH})$	2295.713 <sup>d</sup>
$\nu(\text{H}_3)$	2238.675(0)
$\nu(\text{H}_4)$	2072.374(0)
$\nu(\text{F})$	13893.908(0)
$\nu(\text{H}_6)$	2149.722(0) <sup>e</sup>



$^3J_o(\text{F}, \text{H}_4)$	7.582(0)	$^5J_m(\text{CH}, \text{H}_3)$	0.044(1) <sup>e</sup>
$^4J_m(\text{F}, \text{H}_3)$	5.100(0)	$^4J_o(\text{CH}, \text{H}_6)$	- 0.459(0)
$^3J_o(\text{F}, \text{H}_5)$	8.911(0)	$^3J_o(\text{H}_3, \text{H}_4)$	8.770(0) <sup>e</sup>
$^5J(\text{CH}_3, \text{CH})$	( $\pm$ )0.065(0) <sup>f</sup>	$^4J_m(\text{H}_4, \text{H}_6)$	3.087(0)
$^6J_p(\text{CH}, \text{H}_4)$	- 0.231(0)	$^5J_p(\text{H}_3, \text{H}_6)$	0.319(0)
$^5J_m(\text{CH}, \text{F})$	1.037(0)		

Transitions Calculated	1664
Transitions Assigned	1327
Peaks Observed	69
Largest Difference	-0.011
RMS Deviation	0.003

## NOTES

- a In Hertz.  $^1\text{H}$  nmr at 300.135 MHz to high frequency of TMS.  $^{19}\text{F}$  nmr at 282.365 MHz to high frequency of  $\text{C}_6\text{F}_6$ .
- b 3.2 mole% in solution mixture consisting of  $\text{CS}_2$ , 10 mole%  $\text{C}_6\text{D}_{12}$ , 0.25 mole% TMS and 0.25 mole%  $\text{C}_6\text{F}_6$ .
- c Numbers in parentheses are standard deviations in the last significant digit, as given by the NUMARIT analysis.
- d An approximate value for the shift of the methine proton and this shift value was not optimized in the analysis.
- e  $\nu(\text{H}_3)$  correlates with  $^5J_{\text{m}}(\text{CH}, \text{H}_3)$  by 0.509.  $\nu(\text{H}_3)$  correlates with  $^3J_{\text{o}}(\text{H}_3, \text{H}_4)$  by 0.287.  $^5J_{\text{m}}(\text{CH}, \text{H}_3)$  correlates with  $^3J_{\text{o}}(\text{H}_3, \text{H}_4)$  by -0.287.
- f Sign was not determined.

**FIGURE 27**

**The methyl and methine proton regions of 2-bromo-5-fluoro- $\alpha,\alpha$ -diacetoxytoluene**

**A) methyl proton region**

**B) methine proton region**

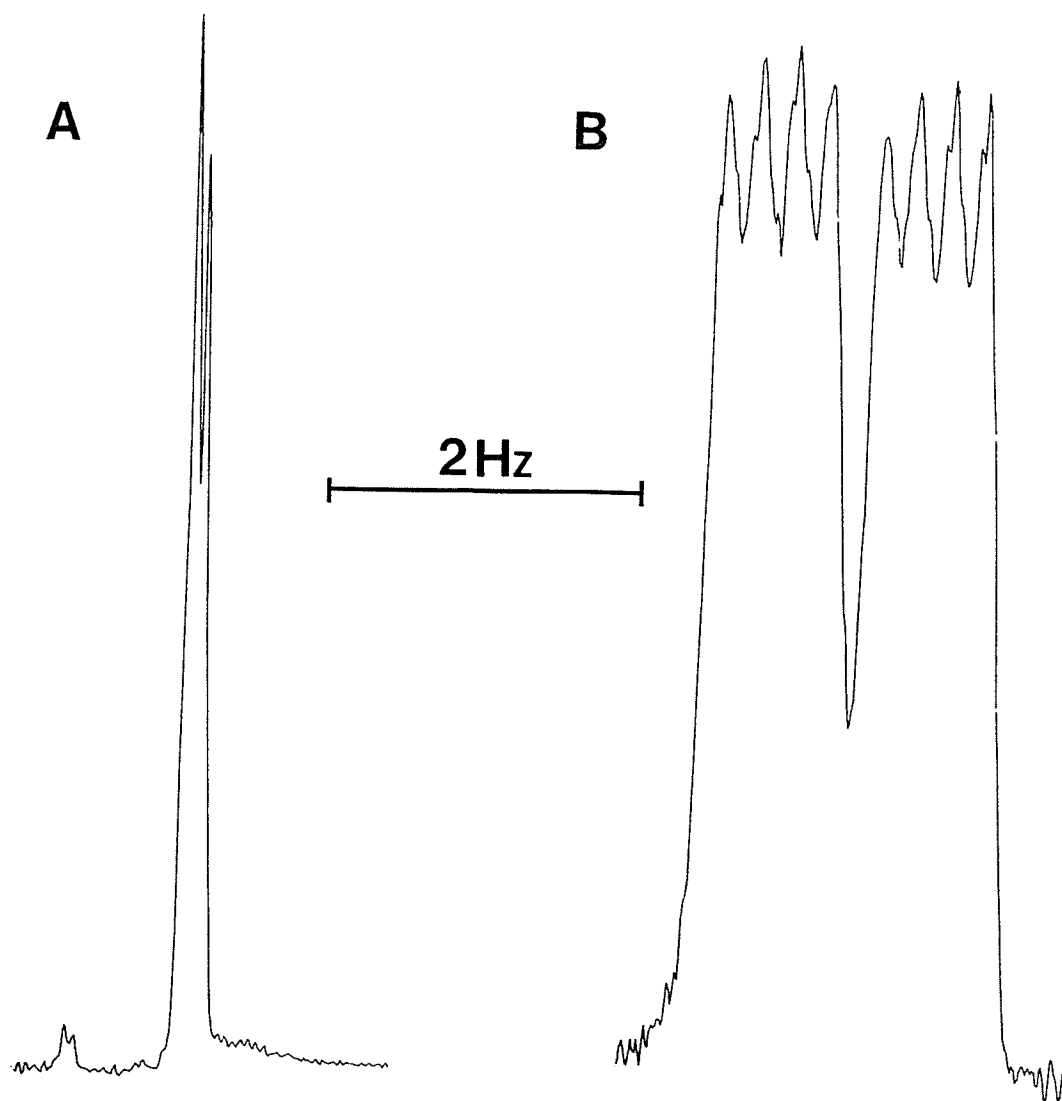




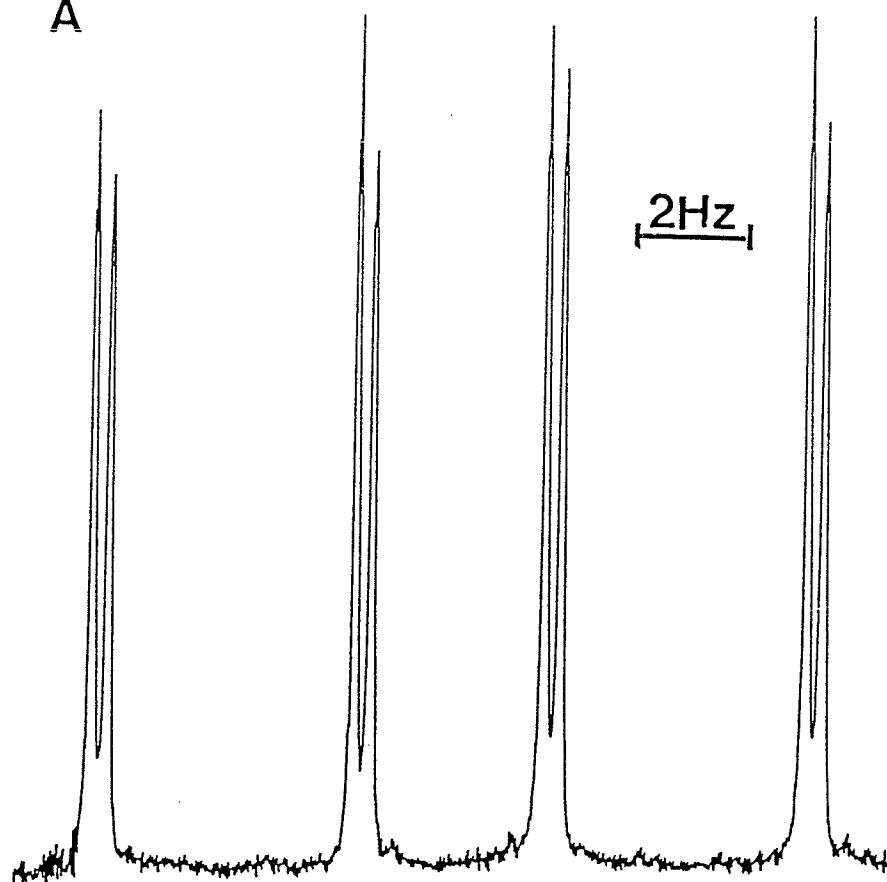
FIGURE 28

The *meta* proton ring region of 2-bromo-5-fluoro- $\alpha,\alpha$ -diacetyltoluene

A) observed

B) calculated

A



B

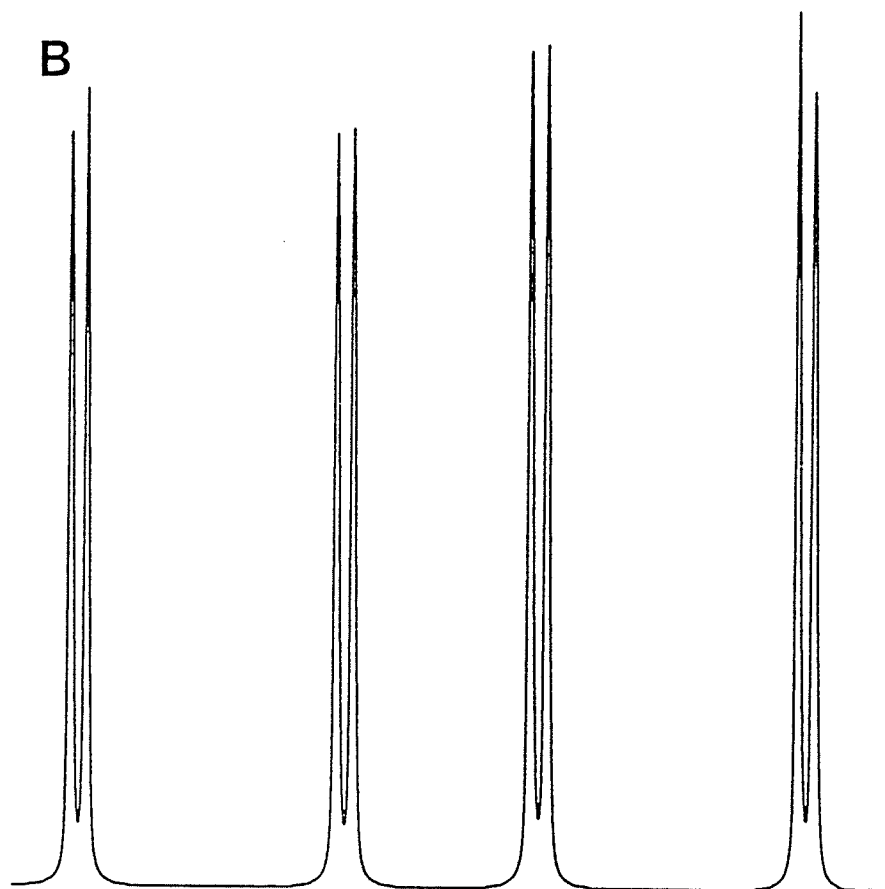


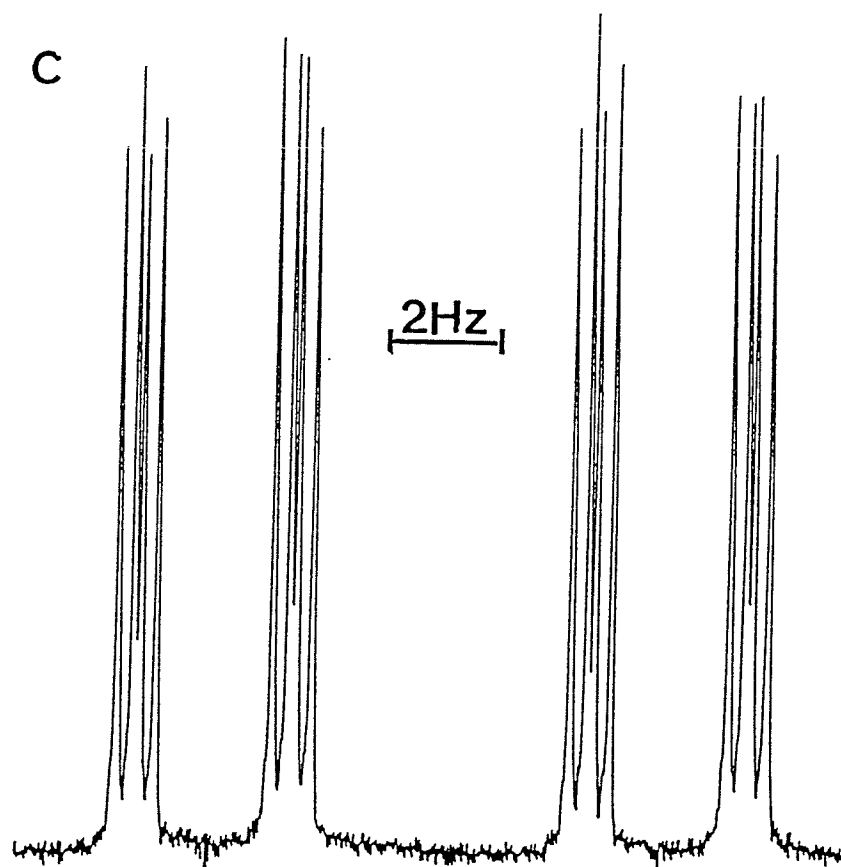
FIGURE 29

The *ortho* proton ring region of 2-bromo-5-fluoro- $\alpha,\alpha$ -diacetoxytoluene

A) observed

B) calculated

C



D

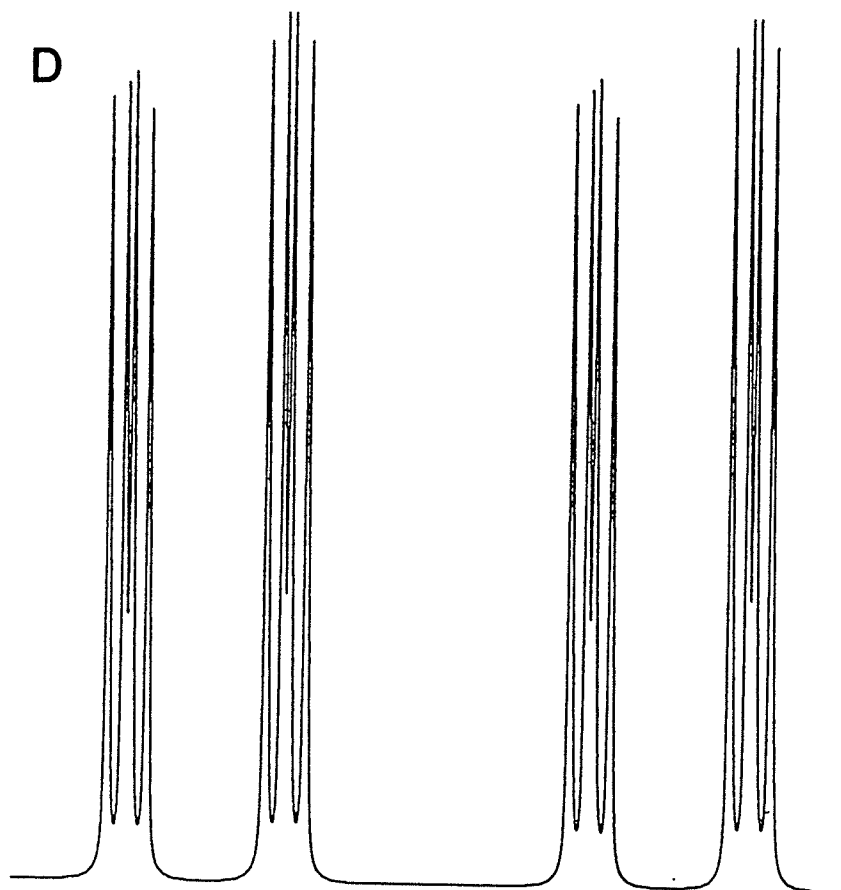


FIGURE 30

The *para* proton region of 2-bromo-5-fluoro- $\alpha,\alpha$ -diacetyltoluene

A) observed

B) calculated

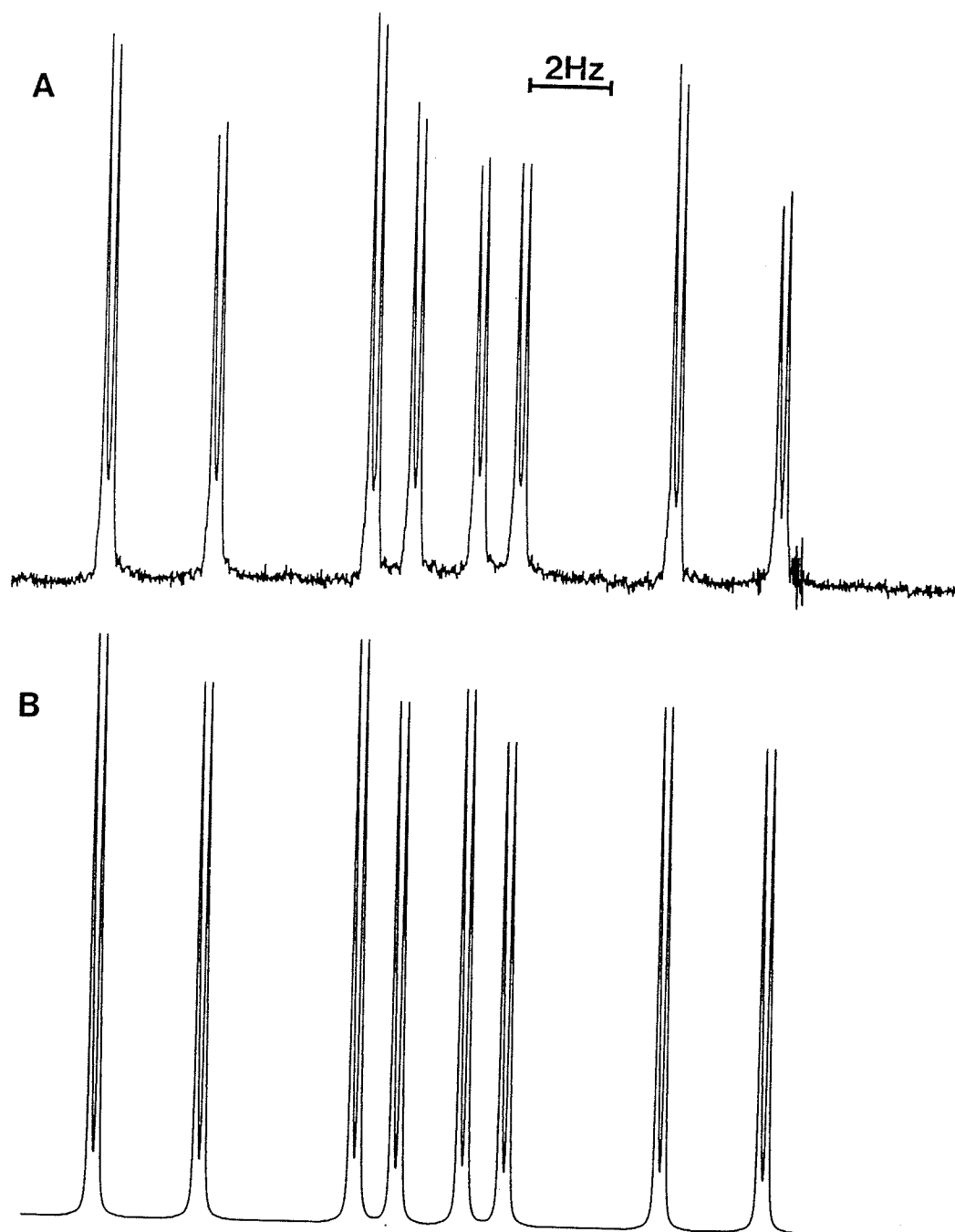
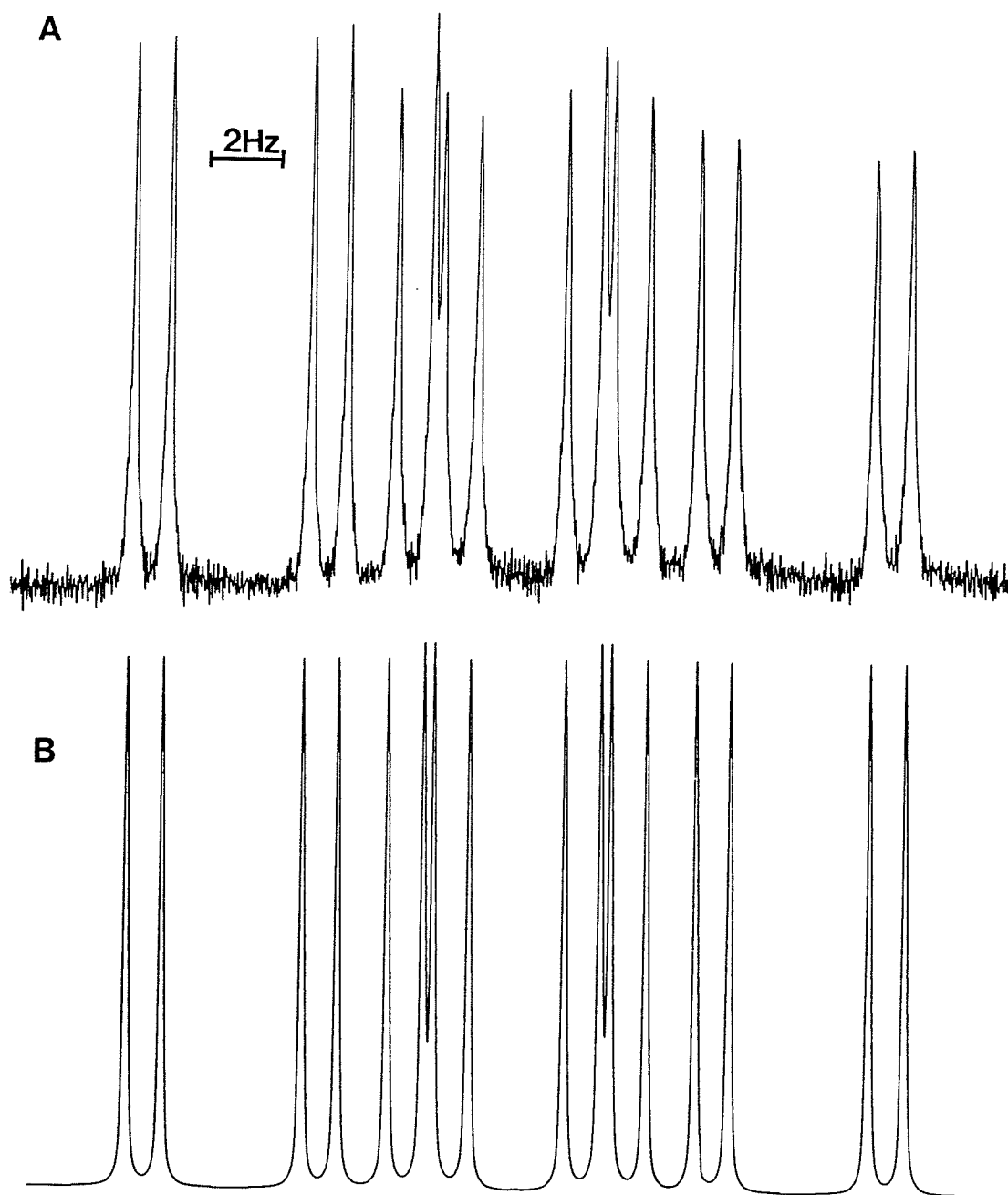


FIGURE 31

$^{19}\text{F}$  nmr spectrum of the *meta* fluorine in 2-bromo-5-fluoro- $\alpha,\alpha$ -diacetoxytoluene

A) observed

B) calculated





## D. DISCUSSION

Table 7 gives INDO MO FPT values for  ${}^5J_m(\text{F},\text{CH}_3)$  for different angles,  $\Theta$ , in 3,5-difluorotoluene. The data are then fitted precisely to a curve of the type  $A + B\sin^2\Theta + C\sin^2(\Theta/2)$  resulting in equation 11 with a maximum deviation of 0.02 Hz and an

$${}^5J_m(\text{F},\text{CH}_3) / \text{Hz} = 0.388 - 2.433\sin^2\Theta + 1.685\sin^2(\Theta/2) \quad (11)$$

average deviation of 0.007 Hz.

Dividing equation 11 into components, it is found that these calculations indicate  ${}^5J_m(\text{F},\text{CH}_3)$  arises from two positive  $\sigma$ -contributions, one with a  $\cos^2\Theta$  dependence and the other with a  $\sin^2(\Theta/2)$  dependence and a negative  $\sigma$ - $\pi$  contribution, with a  $\sin^2\Theta$  dependence. This decomposition is given in equation 12 where  ${}^5J_0^\sigma$  is 0.388

$${}^5J_m(\text{F},\text{CH}_3) / \text{Hz} = {}^5J_0^\sigma \cos^2\Theta + {}^5J_{90}^\pi \sin^2\Theta + {}^5J_{180}^\sigma \sin^2(\Theta/2) \quad (12)$$

$$= {}^5J_0^\sigma + ({}^5J_{90}^\pi - {}^5J_0^\sigma) \sin^2\Theta + {}^5J_{180}^\sigma \sin^2(\Theta/2)$$

Hz,  ${}^5J_{90}^\pi$  is -2.045 Hz and  ${}^5J_{180}^\sigma$  is 1.685 Hz. Since the six-fold internal barrier to rotation in 3,5-difluorotoluene is negligible, both  $\langle \sin^2\Theta \rangle$  and  $\langle \sin^2(\Theta/2) \rangle$  are 0.5. Then, using equation 11, the value for  ${}^5J_m(\text{F},\text{CH}_3)$  is 0.014 Hz. The observed value is -0.294 Hz. Therefore, if each of the computed values in Table 7 is decreased by 0.308 Hz, then equation 11 reproduces the observed coupling. This procedure leads to equation 13. This

$${}^5J_m(\text{F},\text{CH}_3) / \text{Hz} = 0.080 - 2.433\sin^2\Theta + 1.685\sin^2(\Theta/2) \quad (13)$$

equation suggests that the value of  ${}^5J_m(\text{F},\text{CH}_3)$  approaches zero at  $\Theta = 0^\circ$ . Both equation 13 and the adjusted values from Table 7 are plotted in figure 32.

From CNDO/2 MO FPT calculations for 3,5-difluorotoluene, the results shown in Table 7 are reproduced by equation 14 which is similar in form to equation 11.

$${}^5J_m(\text{F},\text{CH}_3) / \text{Hz} = 0.597 - 1.021\sin^2\Theta + 0.940\sin^2(\Theta/2) \quad (14)$$

CNDO/2 calculations generally give  $\sigma$ -electron contributions to coupling constants, while INDO calculations include the  $\pi$ -electron contributions. Equations 11 and 14 differ by a coefficient of -1.4 Hz in the  $\sin^2\Theta$  term. Assuming fast internal rotation, the  $\sigma$ - $\pi$  contribution would be rotationally averaged to -0.7 Hz, in qualitative agreement with

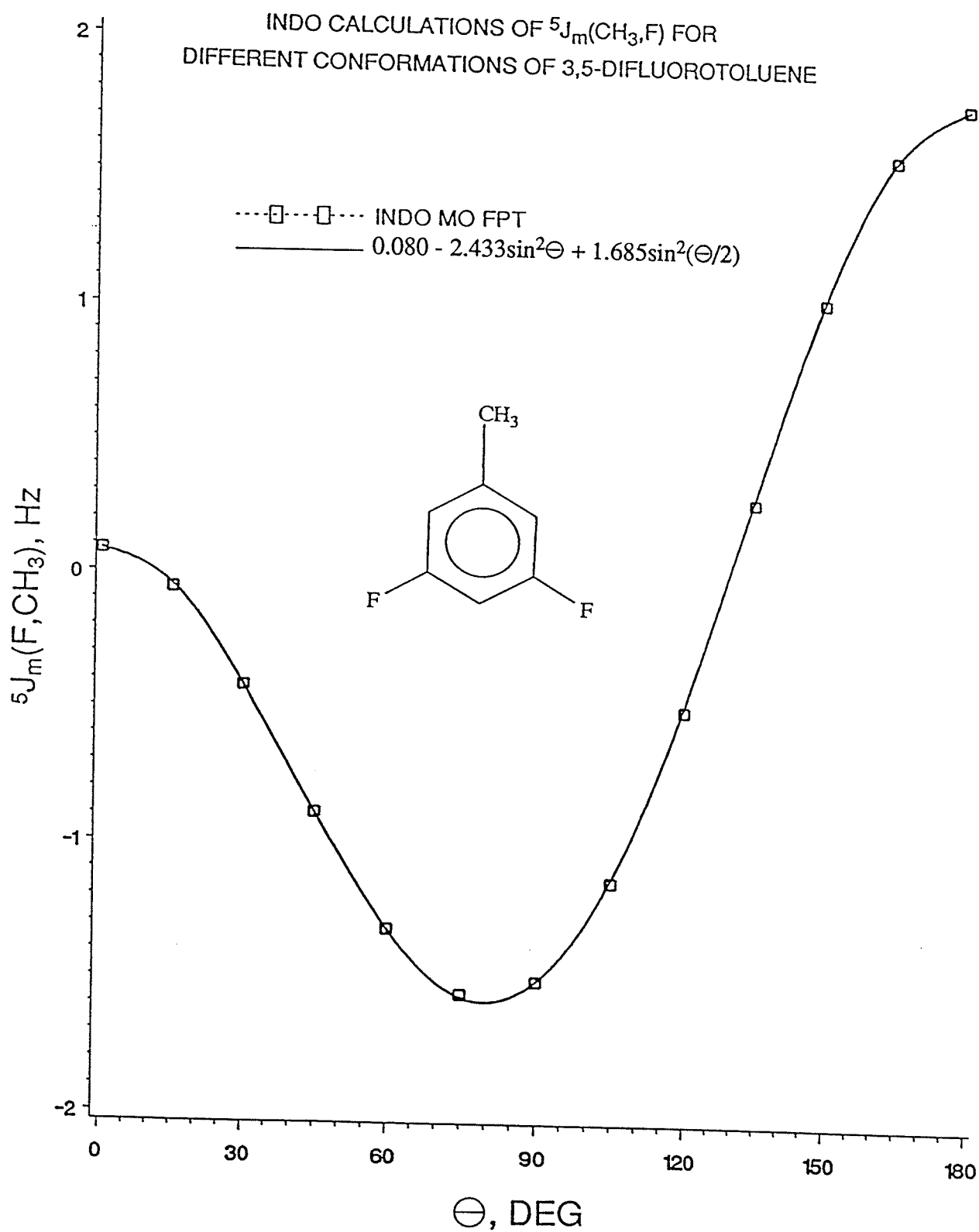
TABLE 7

INDO and CNDO/2 MO FPT values in Hz for  $^5J_m(\text{F,CH})$  in 3,5-difluorotoluene for a standard geometry

$\ominus$	INDO	$\ominus$	CNDO/2
0	0.388	0	0.597
15	0.253	15	0.543
30	-0.109	30	0.400
45	-0.580	45	0.219
60	-1.010	60	0.064
75	-1.251	75	-0.006
90	-1.203	90	0.046
105	-0.833	105	0.229
120	-0.193	120	0.522
135	0.589	135	0.872
150	1.339	150	1.207
165	1.878	165	1.449
180	2.073	180	1.537

FIGURE 32

A plot of the angular dependence of  $^5J_m(\text{F}, \text{CH}_3)$  for 3,5-difluorotoluene from INDO MO  
FPT calculations



the PRMO approach.<sup>46</sup> A value for  ${}^5J_{90}{}^\pi$  of -2.3 Hz (see equation 13 and 14) seems to be an overestimate, therefore the coefficients in equation 13 can only be treated as empirical.

The validity of equation 13 is now tested as follows. The coefficients A, B and C have been adjusted to fit the observed value for  ${}^5J(\text{F},\text{CH}_3)$  of -0.294 Hz in 3,5-difluorotoluene. For 3,5-difluoroethylbenzene and 3,5-difluoroisopropylbenzene, the expectation values of  $\langle \sin^2(\Theta/2) \rangle$  are both 0.5, since the geometry-optimized STO-3G MO computations (unpublished results from this laboratory) yield evenfold internal rotational barriers<sup>47</sup>. Using equation 5, the expectation values of  $\langle \sin^2\Theta \rangle$  can be derived from  ${}^6J_p(\text{H},\text{CH}_3)$ . For 3,5-difluorotoluene,  ${}^6J_p(\text{H},\text{CH}_3)$  is -0.588(0) Hz, implying  ${}^6J_{90}{}^\pi$  as -1.176 Hz. Recently a discussion involving the  ${}^6J_{90}{}^\pi$  in ethylbenzene<sup>47</sup> shows there is a small reduction in  ${}^6J_{90}{}^\pi$  when a methyl substituent on the  $\alpha$ -carbon atom is present, suggesting that  ${}^6J_{90}{}^\pi$  is -1.137 Hz in 3,5-difluoroethylbenzene. Then  $\langle \sin^2\Theta \rangle$  in 3,5-difluoroethylbenzene is -0.463/-1.137 or 0.407. The presence of a second methyl substituent results in a further reduction of  ${}^6J_{90}{}^\pi$ , giving  $\langle \sin^2\Theta \rangle$  in 3,5-difluoroisopropylbenzene as -0.245/-1.098 or 0.223. Substitution of these estimates of  $\langle \sin^2\Theta \rangle$  into equation 13 gives -0.068 Hz for  ${}^5J_m(\text{F},\text{CH}_2)$  in 3,5-difluoroethylbenzene and 0.380 Hz for  ${}^5J_m(\text{F},\text{CH})$  in 3,5-difluoroisopropylbenzene. Experimental measurements, shown in Tables 2 and 3, give -0.067(1) and 0.362(2) Hz, respectively. The model is therefore considered satisfactory.

Note, however, that if methyl substitution causes a reduction in the magnitude of  ${}^6J_{90}{}^\pi$  in 3,5-difluoroethylbenzene and 3,5-difluoroisopropylbenzene, then a similar reduction in the  ${}^5J_{90}{}^\pi$  component of  ${}^5J_m$  is inherent. But, the corresponding changes in the other components of  ${}^5J_m$  have not been studied. In ethylbenzene, equation 3 which describes  ${}^5J_m(\text{H},\text{CH}_2)$ , implies compensatory effects<sup>47</sup> on  ${}^5J_{90}{}^\pi$  and  ${}^5J_{180}{}^\sigma$  due to the presence of a methyl group. Therefore equation 13 is best treated as empirical.

Examination of the  ${}^1\text{H}$  nmr spectral analysis of rigid 2,7-difluorofluorene in  $\text{CS}_2/\text{C}_6\text{D}_{12}$  solution (an unpublished analysis from this laboratory) gives  ${}^5J_m(\text{F},\text{CH}_2)$  as

-1.06(1) Hz. A full geometry-optimized STO-3G MO structure of fluorene indicates the methylene H-C-H angle as  $107.3^\circ$  and the dihedral angle  $\Theta$  as very close to  $60^\circ$ . An INDO MO FPT calculation on 2-fluorofluorene, with the optimized STO-3G structure and a standard C-F bond length of 1.33 Å, gives  $^5J_m(\text{F},\text{CH}_2)$  as -0.76 Hz. A comparison of equations 11 and 13 shows that  $^5J_m(\text{F},\text{CH}_2)$  is again overestimated by 0.31 Hz and after the value is adjusted  $^5J_m(\text{F},\text{CH}_2)$  is -1.07 Hz, as observed.

It is worthwhile to note that for 2-fluorofluorene, while the measured value of  $^6J_p(\text{H},\text{CH}_2)$  is -0.72 Hz,  $^6J_{90}^\pi$  is -0.93 Hz as compared to -1.20 Hz in toluene<sup>48</sup>. Therefore equation 13 which is acceptable for toluene derivatives, does not apply quantitatively to  $^5J(\text{F},\text{CH}_2)$  in 2,7-difluorofluorene. Nevertheless, qualitatively, the large negative  $^5J(\text{F},\text{CH}_2)$  in this molecule is encouraging since the coupling constant ranges from -0.3 to 0.4 Hz in 3,5-difluorotoluene, 3,5-difluoroethylbenzene and 3,5-difluoroisopropylbenzene, while equation 13 predicts large negative values for a large values of  $\sin^2\Theta$ .

For  $^5J_m(\text{H},\text{CH}_3)$  in toluene all the experimental evidence is consistent with a zero value<sup>49,50</sup> at  $\Theta = 0^\circ$ . Yet, significant values for this coupling are computed using both INDO and CNDO/2 calculations at this angle. Since equation 13 reproduces  $^5J_m(\text{F},\text{CH}_3)$  in 3,5-difluorotoluene, and therefore predicts a very small coupling at  $\Theta = 0^\circ$ , it raises some doubt as to whether the substantial numbers computed for  $\Theta = 0^\circ$  exist or not.

A test for the existence of a significant  $^5J_m$  at  $\Theta = 0^\circ$  is now shown. Unfortunately, numerous attempts at the preparation of 2-chloro-3-fluoroisopropylbenzene were unsuccessful. However, 2,3-difluorobenzaldehyde was used to prepare 2,3-difluoro- $\alpha,\alpha$ -diacetoxytoluene by standard methods and 2,3-difluorotoluene<sup>36</sup> using a reduction method as described in the materials and syntheses section.

The results for the analyses of the  $^1\text{H}$  and  $^{19}\text{F}$  nmr spectra for 2,3-difluorotoluene in the  $\text{CS}_2/\text{C}_6\text{D}_{12}$  solution, shown in Table 4 give  $^5J_m(\text{H},\text{CH})$  and  $^6J_p(\text{H},\text{CH})$  as 0.328(2) and -0.575(2) Hz, respectively. The low barrier to internal rotation

and the threefold symmetry of the methyl group results in a  $\langle \sin^2 \Theta \rangle$  value of 0.5. Using equation 5,  ${}^6J_{90}^\pi$  is computed as -1.15 Hz in this molecule, as compared to -1.20 Hz in toluene. From equation 3,  ${}^5J_{90}^\pi$  is therefore 0.322 Hz while  ${}^5J_{180}^\sigma$  is 0.334 Hz. In 2,3-difluorotoluene  ${}^5J_m(\text{F}, \text{CH}_3)$  is -0.170(1) Hz, larger than in 3-fluorotoluene<sup>52</sup>. In a similar procedure used to deduce equation 13, the angle independent term is adjusted to 0.204 Hz which reproduces the coupling in 2,3-difluorotoluene. With these reference points,  ${}^5J_m(\text{F}, \text{CH})$  can now be considered in 2,3-difluoro- $\alpha, \alpha$ -diacetoxytoluene. Observed values for  ${}^6J(\text{H}, \text{CH})$  and  ${}^5J(\text{H}, \text{CH})$  are used to find  $\langle \sin^2 \Theta \rangle$  and  $\langle \sin^2(\Theta/2) \rangle$ .

From the results for the analyses of  ${}^1\text{H}$  and  ${}^{19}\text{F}$  nmr spectra for 2,3-difluoro- $\alpha, \alpha$ -diacetoxytoluene in  $\text{CS}_2/\text{C}_6\text{D}_{12}$  solution, shown in Table 5,  ${}^6J_p(\text{H}, \text{CH})$  is -0.185(3) Hz. Therefore the value of  ${}^6J_{90}$  is smaller than is observed for toluene. Since the electronegativity of the acetoxy and methoxy substituents<sup>53</sup> is much the same, a reduction in  ${}^6J_{90}$  of -0.18 Hz relative to toluene should occur<sup>53a</sup>. The introduction of a second acetoxy group to this site should also result in a reduction of  ${}^6J_{90}$ . Assuming this reduction to be half that caused by the addition of the first acetoxy substituent, somewhat arbitrary, results in a  ${}^6J_{90}$  of -0.930(1.15/1.20) or -0.891 Hz. Therefore  $\langle \sin^2 \Theta \rangle$  follows as 0.208. Knowing that  ${}^5J_m(\text{H}, \text{CH})$  is 0.338(3) Hz and making the appropriate substitutions into equation 4 implies that  $\langle \sin^2(\Theta/2) \rangle$  is 0.857. Therefore from equation 13  ${}^5J_m(\text{F}, \text{CH})$  is 0.06 Hz, considering that  $\sin^2(\Theta/2)$  is 1-0.857 where the C-H bond of the sidechain lies predominantly *cis* to the *ortho* C-F bond. In the  ${}^{19}\text{F}$  nmr spectrum of 2,3-difluoro- $\alpha, \alpha$ -diacetoxytoluene, the observed  ${}^5J(\text{F}, \text{CH})$  coupling is a doublet splitting of much less than 10 % of the peak height. This observed splitting of 0.04(1) Hz is compatible with the existence of a small positive  ${}^5J_m(\text{F}, \text{CH})$  at  $\Theta = 0^\circ$ .

For 2,3-difluoro- $\alpha, \alpha$ -diacetoxytoluene in acetone- $\text{d}_6$  solution, as shown in Table 5,  ${}^5J_m(\text{F}, \text{CH})$  is -0.147(2) Hz. Using the same procedure as in the  $\text{CS}_2/\text{C}_6\text{D}_{12}$  solution, a value of -0.180 Hz is predicted, indicating a significant  ${}^5J_0^\sigma$ . Also, from the analysis in acetone- $\text{d}_6$  solution, the observed values for  ${}^5J_m(\text{H}, \text{CH})$  and  ${}^6J_p(\text{H}, \text{CH})$  are 0.357(2) and



-0.202(2) Hz, respectively. The complexity of the above procedure, although logical, raises some question as to the validity of this method. Suppose that values for  $\langle \sin^2 \Theta \rangle$  and  $\langle \sin^2(\Theta/2) \rangle$  could only be obtained from spectral data for toluene and equations 4 and 5. Then for 2,3-difluoro- $\alpha,\alpha$ -diacetoxytoluene in acetone- $d_6$  solution  $\langle \sin^2 \Theta \rangle$  would be -0.202/-1.20 or 0.168 and  $\langle \sin^2(\Theta/2) \rangle$  would be 0.067. As a result equation 13 would give a  $^5J_m(\text{F,CH})$  of -0.216 Hz, again consistent only with a substantial positive value of  $^5J_m(\text{F,CH})$  at  $\Theta = 0^\circ$ .

Empirical equations such as equation 13 appear to be compatible with the conformational properties of 2,3-difluoro- $\alpha,\alpha$ -diacetoxytoluene deduced from the long-range  $^1\text{H}$ - $^1\text{H}$  coupling constants and, therefore, they can be used in conformational analysis. However, the true nature of the coefficient of  $\langle \sin^2 \Theta \rangle$  as a pure  $\sigma$ - $\pi$  term is not certain.

Now a conformational application of equation 13 will be demonstrated using 2-bromo-5-fluoro- $\alpha,\alpha$ -diacetoxytoluene in  $\text{CS}_2/\text{C}_6\text{D}_{12}$  solution. For this compound,  $^5J_m(\text{H,CH})$  is small, 0.04 Hz, and poorly resolved in the  $^1\text{H}$  nmr spectrum. In addition, the NUMARIT analysis indicates a strong correlation between this coupling and the chemical shift of  $\text{H}_3$ , 2238.675 Hz, by 0.51 and with the coupling  $^3J(\text{H}_3, \text{H}_4)$ , 8.770 Hz, by 0.29. Therefore there is a relatively large uncertainty in the correct magnitude of  $^5J(\text{H,CH})$ . However, the observed value for  $^5J(\text{F,CH})$  is 1.037(0) Hz, implying that the predominant conformer has the methine proton near the bromine substituent as shown in figure 33a. If this rigid conformer exists in 2-bromo-5-fluoro- $\alpha,\alpha$ -diacetoxytoluene, then equation 13 implies that  $^5J(\text{F,CH})$  is 1.76 Hz since  $\Theta$  is zero. But a torsion about the  $\text{C}(1)\text{-Csp}^3$  bond as indicated by a  $^6J_p(\text{H,CH})$  of -0.231(0) suggests that this conformer is by no means rigid.

Suppose coupling data for only toluene is available and there are no correlations to  $^6J_p(\text{H,CH})$ , then  $\langle \sin^2 \Theta \rangle$  is -0.231/-1.20 or 0.192. Consequently,  $\Theta$  is  $26^\circ$ , computed using  $\arcsin \langle \sin^2 \Theta \rangle^{1/2}$ , implying a substantial twist out of the plane of the benzene ring. Knowing that for 2-chloro-5-fluorotoluene,  $^6J_p(\text{H,CH}_3)$  is -0.626(3) Hz<sup>54</sup> and that the

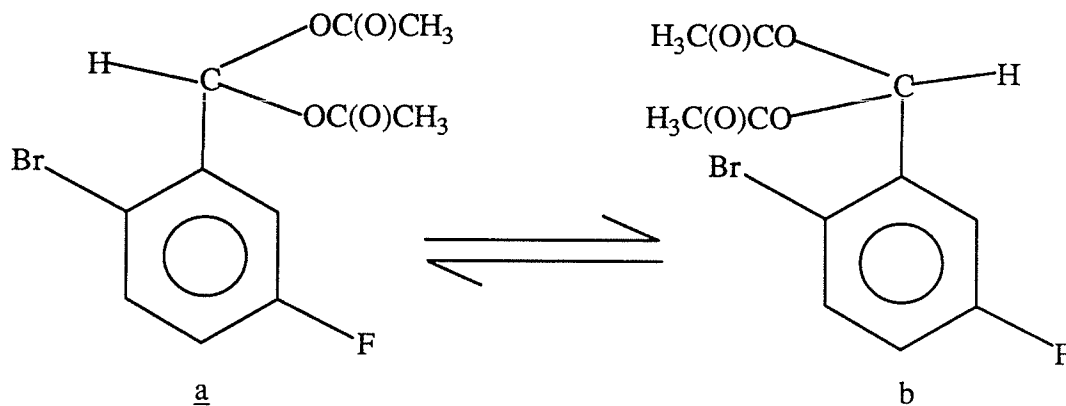


Figure 33

value of  ${}^6J_{90}$  after reduction by the two  $\alpha$  acetoxy substituents is -0.93, leads to a new  ${}^6J_{90}$  value of  $-0.930(1.252/1.204)$  or -0.97 Hz. Then  $\langle \sin^2\Theta \rangle$  follows as 0.238 and consequently  $\Theta$  as  $29^\circ$ . In addition, if this value corresponds to a  $\Theta$  of  $151^\circ$  for the term in  $\sin^2(\Theta/2)$  of equation 13, then  ${}^5J(\text{F},\text{CH})$  is 1.08 Hz, in comparison to the observed value of 1.04 Hz. Therefore,  ${}^6J_p(\text{H},\text{CH})$  gives an estimate of the torsion, but it does not distinguish between two conformers of 2-bromo-5-fluoro- $\alpha,\alpha$ -diacetoxytoluene produced by a  $180^\circ$  rotation about the  $\text{C}(1)\text{-Csp}^3$  bond. Thus, equation 13 and  ${}^5J(\text{F},\text{CH})$  can discriminate between these conformers and, apparently, provide an estimate of the extent of non-planarity of the correct conformer. In some compounds  ${}^6J(\text{H},\text{CH})$  would be unavailable due to substitution at the site under consideration.

## E. SUMMARY AND CONCLUSIONS

The INDO MO FPT values for  ${}^5J_m(\text{F}, \text{CH}_3)$  in 3,5-difluorotoluene are reproduced by  $A + B\sin^2\Theta + C\sin^2(\Theta/2)$  where  $\Theta$  is the angle by which the  $\alpha$  C-H bond rotates out of the plane of the benzene ring. Adjustment of A, B and C to give agreement with experiment for 3,5-difluorotoluene yields an empirical equation. This equation reproduces  ${}^5J_m(\text{F}, \text{CH})$  in 3,5-difluoroethylbenzene and 3,5-difluoroisopropylbenzene where the values of  $\langle \sin^2\Theta \rangle$  are deduced from  ${}^6J_p(\text{H}, \text{CH})$ , the spin-spin coupling constant over six bonds between the  $\alpha$  and *para* ring protons.

This empirical equation is compatible with the conformational properties of 2,3-difluoro- $\alpha, \alpha$ -diacetoxytoluene deduced from the long-range  ${}^1\text{H}$ - ${}^1\text{H}$  coupling constants and therefore,  ${}^5J_m(\text{F}, \text{CH})$  can be used in conformational analysis.

Although  ${}^6J_p(\text{H}, \text{CH})$  gives an estimate of the torsion it does not distinguish between two conformers of 2-bromo-5-fluoro- $\alpha, \alpha$ -diacetoxytoluene produced by a  $180^\circ$  rotation about the  $\text{Csp}^2$ - $\text{Csp}^3$  bond. But the empirical equation and  ${}^5J_m(\text{F}, \text{CH})$  can discriminate between these conformers and, apparently, give an estimate of the extent of non-planarity of the correct conformer. Also, in some compounds,  ${}^6J_p(\text{H}, \text{CH})$  would not be available due to substitution at the site under consideration.

## F. REFERENCES

- 1) H. M. McConnell, J. Mol. Spectrosc., 1 , 11 (1957).
- 2) R. Wasylishen and T. Schaefer, Can. J. Chem., 50 , 1852 (1972).
- 3) T. Schaefer and R. Laatikainen, Can. J. Chem., 61 , 224 (1983).
- 4) M. Barfield, C. J. Fallick, K. Hata, S. Sternhell and P. W. Westerman, J. Am. Chem. Soc., 105 , 2178 (1983).
- 4a) T. Schaefer, R. Sebastian and G. Penner, Can. J. Chem., 63 , 2597 (1985).
- 5) T. Schaefer and R. Laatikainen, Can. J. Chem., 61 , 2785 (1983).
- 6) W. J. E. Parr and T. S. Schaefer, Acc. Chem. Res., 13 , 400 (1980).
- 7) M. Barfield, A. M. Dean, C. J. Fallick, R. J. Spear, S. Sternhell and P. W. Westerman, J. Am. Chem. Soc., 97 , 1482 (1975).
- 8) M. Barfield, R. J. Spear and S. Sternhell, Chem. Rev., 76 , 593 (1976).
- 9) H. Rudolph, H. Dreizler, A. Jaeschke and P. Wendling, Z. Naturforsch., 22A , 940 (1967).
- 10) T. Schaefer, R. Sebastian and T. A. Wildman, Can. J. Chem., 59 , 3021 (1981).
- 11) T. Schaefer, R. Sebastian and T. A. Wildman, Can. J. Chem., 57 , 3005 (1979).
- 12) R. Freeman, Mol. Phys., 6 , 535 (1963).
- 13) S. Forsén and R. A. Hoffman, J. Mol. Spectrosc., 20 , 168 (1966).
- 14) T. Schaefer, S. R. Salman and T. A. Wildman, Can. J. Chem., 58 , 2364 (1980).
- 15) S. Forsén, B. Akermarck and T. Alm, Acta. Chim. Scand., 18 , 2313 (1964).
- 16) G. J. Karabatsos and F. M. Vane, J. Am. Chem. Soc., 85 , 3886 (1963).
- 17) C. J. MacDonald and W. F. Reynolds, Can. J. Chem., 48 , 1002 (1970).
- 18) J. B. Rowbotham and T. Schaefer, Can. J. Chem., 52 , 489 (1974).
- 19) W. J. E. Parr and T. Schaefer, Can. J. Chem., 54 , 3564 (1976).
- 20) J. B. Rowbotham and T. Schaefer, Can. J. Chem., 50 , 2344 (1972).
- 21) R. A. Hoffman, Mol. Phys., 1 , 326 (1958).
- 22) T. Schaefer, T. A. Wildman and R. Sebastian, Can. J. Chem., 60 , 1924 (1982).

- 23) D. J. Blears, S. S. Danyluk and T. Schaefer, *Can. J. Chem.*, 46 , 654 (1968).
- 24) G. Kotowycz and T. Schaefer, *Can. J. Chem.*, 44 , 2743 (1966).
- 25) M. P. Williamson, R. J. Kostelnik and S. M. Costellano, *J. Chem. Phys.*, 49 , 2218 (1968).
- 26) T. Schaefer, W. Danchura and W. Niemczura, *Can. J. Chem.*, 56 , 2233 (1978).
- 27) T. Schaefer, R. Sebastian, R. P. Veregin and R. Laatikainen, *Can. J. Chem.*, 61 , 29 (1983).
- 28) J. B. Rowbotham, M. Smith and T. Schaefer, *Can. J. Chem.*, 53 , 986 (1975).
- 29) T. Schaefer and J. B. Rowbotham, *Chem. Phys. Lett.*, 29 , 633 (1974).
- 29a) T. Schaefer, J. Peeling, G. Penner, A. Lemire and R. Laatikainen, *Can. J. Chem.*, 64 , 1859 (1986).
- 30) R. Wasylishen and T. Schaefer, *Can. J. Chem.*, 49 , 3216 (1971).
- 31) H. D. Rudolph and H. Seiler, *Z. Naturforschung*, 20 , Teil A, 1682 (1965).
- 32) T. Schaefer, W. Danchura, W. Niemczura and J. Peeling, *Can. J. Chem.*, 56 , 2442 (1972).
- 34) C. M. Moore and M. E. Hobbs, *J. Am. Chem. Soc.*, 71 , 411 (1949).
- 35) T. Schaefer and T. A. Wildman, *Can. J. Chem.*, 57 , 450 (1979).
- 36) A. Vogel. Textbook of practical organic chemistry. 4th ed. Longman Group Limited, London, 1978. pp. 600-606.
- 36a) R. P. Veregin, M.Sc. Thesis, University of Manitoba, 1982.
- 37) E. C. Horning (ed). Organic Syntheses Collective Volume III. A revised edition of annual volumes 20-29. John Wiley and Sons, Inc., New York, 1955. pp. 641-643.
- 39) A. R. Quirt and K. E. Worvill. The NMR program library. Daresbury Laboratory, Daresbury, U. K.
- 39a) W. J. Hehre, R. F. Stewart, and J. A. Pople, *J. Chem. Phys.*, 51 , 2657 (1969).
- 40) M. R. Petersen and R. A. Poirier, MONSTERGAUSS, Department of Chemistry, University of Toronto, Toronto, Ontario, 1981.

- 41) J. A. Pople, D. L. Beveridge and P. A. Dobosh, *J. Chem. Phys.*, 47 , 2026 (1967) ;  
P. A. Dobosh and N. S. Ostlund, *QCPE* 11, 281 (1975).
- 42) SAS User's Guide : Statistics, A. A. Ray (ed.), (Statistical Analysis System  
Institute, 1982).
- 43) SAS/Graph User's Guide. K. A. Council and J. T. Helwig (ed.), (Statistical  
Analysis System Institute, 1982).
- 44) T. Schaefer, W. Danchura and W. Niemczura, *Can. J. Chem.*, 56 , 2233 (1978).
- 45) T. Schaefer, R. Sebastian, R. P. Veregin and Reino Laatikainen, *Can. J. Chem.*, 61  
, 29 (1983).
- 46) J. C. Facelli, C. G. Giribet and R. H. Contreras, *Org. Magn. Reson.*, 19 , 138  
(1982).
- 46a) T. Schaefer, W. Danchura and W. Niemczura, *Can. J. Chem.*, 56 , 2233 (1978).
- 47) T. Schaefer, G. H. Penner and R. Sebastian, *Can. J. Chem.*, 65 , 873 (1987).
- 48) T. Schaefer, R. Sebastian and G. H. Penner, *Can. J. Chem.*, 63 , 2597 (1985).
- 49) T. Schaefer and R. Laatikainen, *Can. J. Chem.*, 61 , 2785 (1983).
- 50) T. Schaefer, R. Sebastian and G. H. Penner, *Can. J. Chem.*, 63 , 2597 (1985).
- 52) T. Schaefer, W. Danchura and W. Niemczura, *Can. J. Chem.*, 56 , 2233 (1978).
- 53) S. Marriott, W. F. Reynolds, R. W. Taft and R. D. Topsom, *J. Org. Chem.*, 49 , 959  
(1984).
- 53a) T. Schaefer, R. Sebastian and G. H. Penner, *Can. J. Chem.* 64 , 1372 (1986).
- 54) T. Schaefer, W. Danchura and W. Niemczura, *Can. J. Chem.*, 56 , 2233 (1978).



## PART II

### The Determination of the Nature of the Rotational Barrier In $\alpha,\alpha$ -Diacetoxytoluene Derivatives

## A. INTRODUCTION

The six-bond coupling between the  $\alpha$ -proton of the sidechain and the *para* ring proton,  ${}^6J_p(\text{H},\text{CH})$ , in benzene derivatives has been well studied and found to be useful in the deduction of conformations, and in the determination of internal rotational barriers<sup>1-4</sup>. The magnitude of  ${}^6J_p(\text{H},\text{CH})$  is maximum when the  $\alpha$ -proton of the sidechain lies in a plane perpendicular to the benzene ring plane. This coupling can be expressed as where

$${}^6J_p(\text{H},\text{CH}) = {}^6J_{90}\langle\sin^2\Theta\rangle \quad (1)$$

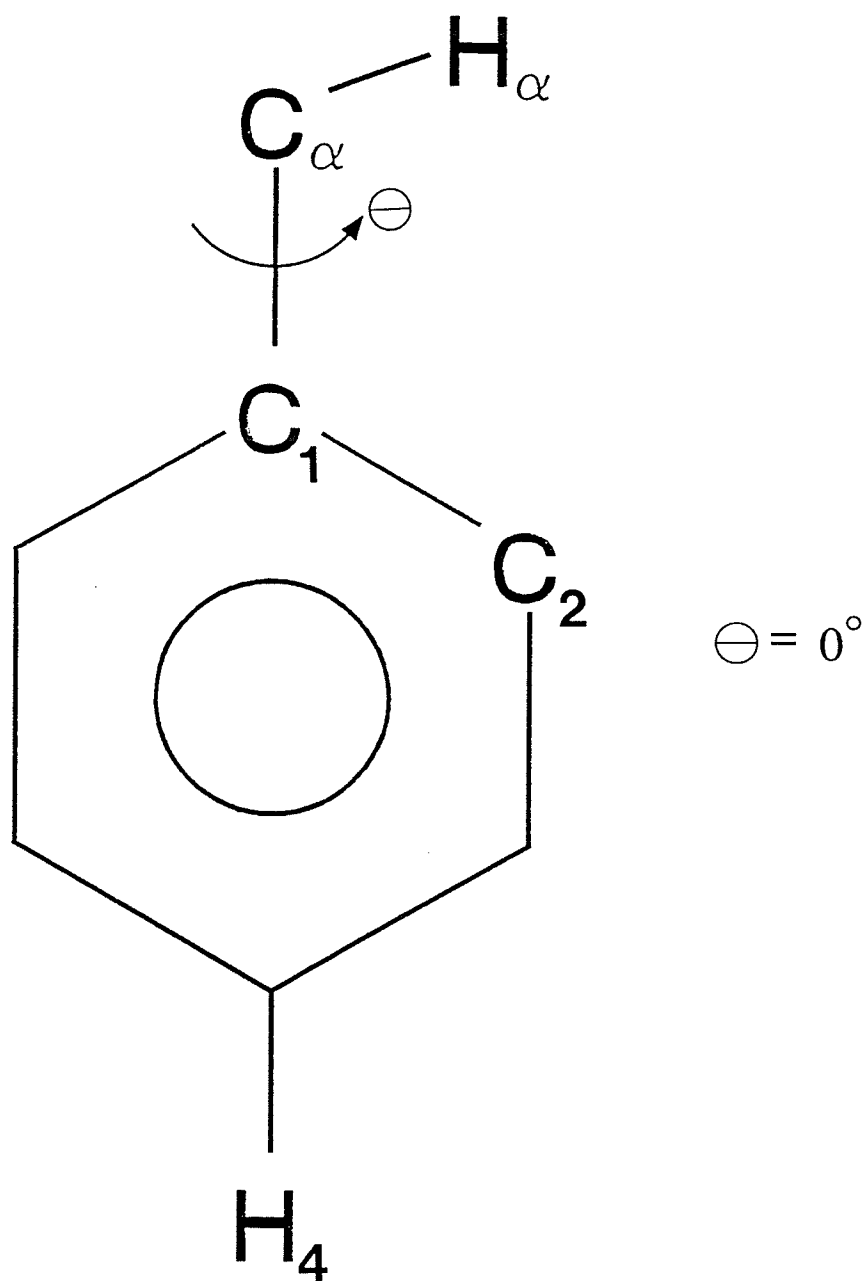
${}^6J_{90}$  is the maximum value of the six-bond coupling, and  $\langle\sin^2\Theta\rangle$  is the expectation value of  $\sin^2\Theta$ . The dihedral angle  $\Theta$  is defined in figure 1. This angle is zero when the  $\alpha$ -proton is in the plane of the benzene ring. If the value of  ${}^6J_{90}$  is known or can be deduced from observed couplings, then a value for  $\langle\sin^2\Theta\rangle$  can be determined from a measurement of the coupling over six bonds, between the methylene protons ( $\text{Ph}-\text{CH}_2\text{X}$ ;  $\text{Ph}=\text{phenyl}$ ) or methine proton ( $\text{Ph}-\text{CHX}_2$ ) and the *para* ring proton. This quantity, in turn, can be related to the internal barrier to rotation by a hindered rotor model<sup>1</sup> or by a classical averaging procedure<sup>5</sup> and to the preferred conformations of the sidechain. Consequently, the preferred conformations of the sidechain can be predicted. The barrier determined using this procedure (J method) is the twofold potential energy barrier,  $V_2$ , which is often considered to be the same as  $\Delta H^\ddagger$ . The J method is presently restricted to benzene derivatives containing sidechains having twofold barriers to internal rotation in the range of 0 to 12.5 kJ/mole.

In toluene  ${}^6J_{90}$  is -1.20 Hz<sup>6</sup>, but electronegative substituents can alter the magnitude<sup>1,3,4</sup> of this value, and consequently introduce some uncertainty into the use of the J method. Further uncertainty originates in the suspicion of the existence of an angle-independent term in equation 1 analogous to that in the Heller-McConnell relationship for  $\beta$ -hyperfine interactions in radicals<sup>7</sup>.

Nevertheless, the J method is one of the few available techniques for the estimation of small barriers in solution and is most reliable for barrier magnitudes much

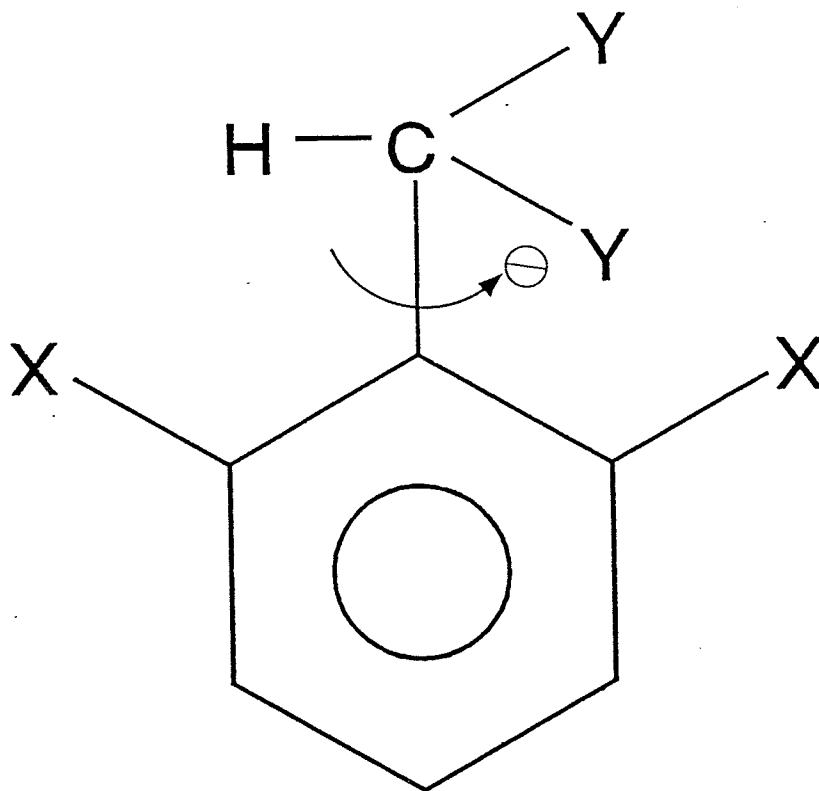
FIGURE 1

Definition of the dihedral angle for the six-bond coupling,  ${}^6J_p(\text{CH}_3, \text{H}_4)$ ;  
the dihedral angle is defined by  $\text{H}_\alpha\text{-C}_\alpha\text{-C}_1\text{-C}_2$



smaller than those accessible to dynamic nuclear magnetic resonance (DNMR) procedures. Consequently it is worthwhile to test its reliability. A previous test involved the overlap of the J method and DNMR in 2,6-difluoroisopropylbenzene<sup>2</sup>, but was not entirely successful with the barrier situated in a region for which both methods are somewhat insensitive. The present work describes another attempt at an overlap of the two methods using  $\alpha,\alpha$ -diacetoxytoluene.

Also, this study has provided additional knowledge of the conformational dependence of the long-range couplings between sidechain protons and ring nuclei in the benzal compounds 2,6-dibromotoluene(1),  $\alpha,\alpha$ -diacetoxytoluene(2) and 2,6-dibromo- $\alpha,\alpha$ -diacetoxytoluene(3) as shown in figure 2.



<u>1</u>	Y = H	X = Br
<u>2</u>	Y = OCOCH <sub>3</sub>	X = H
<u>3</u>	Y = OCOCH <sub>3</sub>	X = Br

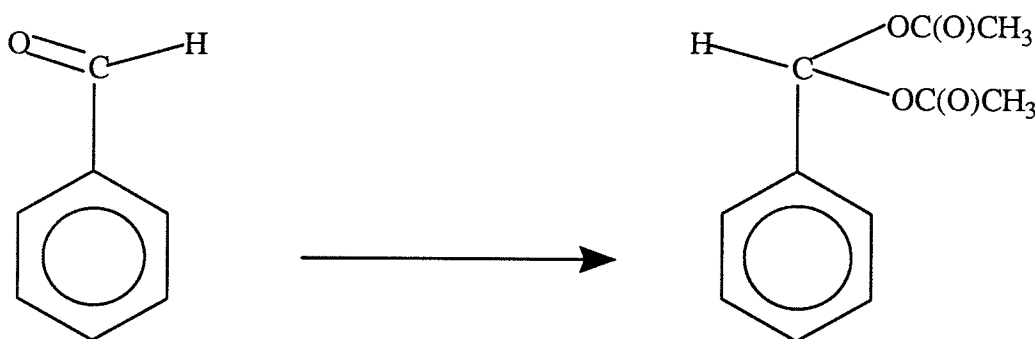
figure 2

## B. EXPERIMENTAL METHODS

## 1. Materials and Syntheses

### A. Preparation of $\alpha,\alpha$ -diacetoxytoluene

The  $\alpha,\alpha$ -diacetoxytoluene was prepared using a standard method as described below.

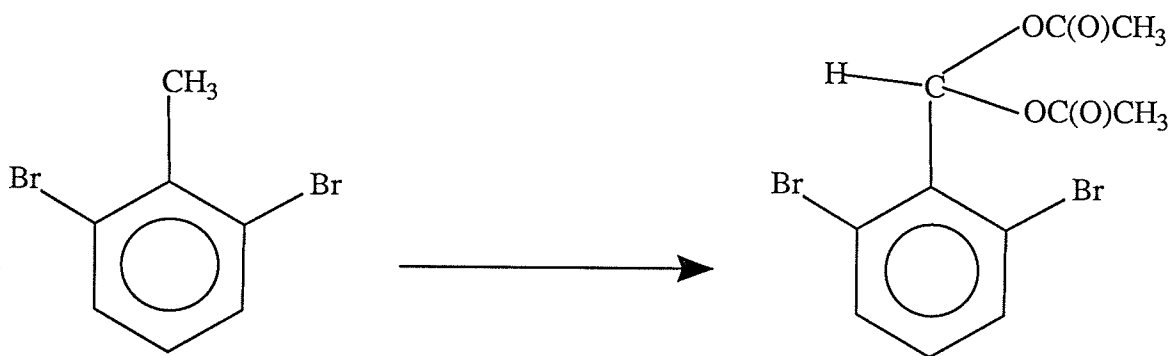


The predistilled benzaldehyde (2.01g) obtained from Fisher Scientific, p-toluene sulfonic acid (0.044g) and 10 ml of acetic anhydride are placed in a 100 ml round bottomed flask and stirred overnight. The resulting solid was washed twice with water to remove excess acetic anhydride and then air dried to give a white crystalline product (3.14g). The product was identified and confirmed by NMR (300 MHz).



### B. Preparation of 2,6-dibromo- $\alpha,\alpha$ -diacetoxytoluene

The 2,6-dibromo- $\alpha,\alpha$ -diacetoxytoluene was prepared using the method<sup>8</sup> as described below.



The 2,6-dibromotoluene (1.01g), obtained from Lancaster, was dissolved in a mixture of 10 ml acetic anhydride, 10 ml glacial acetic acid and 3 ml concentrated sulfuric acid which had previously been well-cooled. When the temperature had fallen to 5°C, 1.7g of chromium trioxide was added in small portions at such a rate that the temperature does not rise above 10°C; the stirring was then continued for 30 min after the addition of chromium trioxide was completed. The contents of the flask were then poured into a 400 ml beaker 1/3-filled with crushed ice and then the beaker was filled to 200 ml with cold water. The resulting solid was then filtered using a Buchner funnel and the product was washed with cold water until the washings were colorless. The solid was then washed with two 20 ml portions of cold 2% sodium bicarbonate solution and finally with 10 ml of cold ethanol. The total yield of product (0.43g) was identified and confirmed by NMR.

## 2. Sample Preparation

NMR samples of  $\alpha,\alpha$ -diacetyltoluene, 2,6-dibromotoluene and 2,6-dibromo- $\alpha,\alpha$ -diacetyltoluene were prepared by weighing the appropriate amounts of the compound and the solvent of choice. 1-5 mole% solutions were prepared in a solvent mixture either consisting of carbon disulfide (Fisher Scientific), 10 mole% cyclohexane- $d_{12}$  (99.5 atom% D from Aldrich Chemical) as an internal locking material, 0.25 mole% tetramethylsilane (Sigma Chemical) as an internal reference for  $^1\text{H}$  nmr spectra and 0.25 mole% hexafluorobenzene (Pierce Chemical) as an internal reference for  $^{19}\text{F}$  nmr spectra or a solvent mixture consisting of acetone- $d_6$ , 1 drop of tetramethylsilane (Sigma Chemical) and 1 drop of hexafluorobenzene (Pierce Chemical). The solutions were then transferred to precision-bore 5 mm sample tubes, fitted with ground glass joints and filtered through a small wad of cotton wool in a Pasteur pipette. The samples were then degassed using the freeze-pump-thaw technique four times. The nmr tubes were then flame-sealed.

### 3. Spectroscopic Method

Proton ( $^1\text{H}$ ) and fluorine ( $^{19}\text{F}$ ) nmr spectra were acquired on a Bruker AM 300 nmr spectrometer at a probe temperature of 300 K. Survey spectra with a sweep width of 6000 Hz were used to reference the compounds with respect to tetramethylsilane (TMS) and hexafluorobenzene ( $\text{C}_6\text{F}_6$ ). Each spectral region was then examined in detail, with sweep width and data region adjusted to give acquisition times of approximately 41 seconds. Proton sweep widths ranged from 50-200 Hz, while fluorine sweep widths were 100-200 Hz. As many as 32 scans were acquired. Zero-filling from 2-4 times the original data region was done before transforming the free induction decay curves (FIDs) using small amounts of gaussian and lorentzian multiplication in order to decrease the linewidth and increase resolution. Intrinsic linewidths at half-height were as small as 0.05 Hz (including spectra where the methyl groups in the sidechain were decoupled) after resolution enhancement, but more often were 0.05 to 0.10 Hz. Partial decoupling experiments were used to determine the sign of  $^6J_p(\text{H},\text{CH})$  in 2,6-dibromo- $\alpha,\alpha$ -diacetoxytoluene.

#### 4. Computations

Spectral analyses and simulations were performed using the program NUMARIT<sup>9</sup> in both the iterative and non-iterative modes and also this program was coupled to a plotting routine.

All curves were statistically fitted to  $\sin^2\Theta$  and  $\sin^2(\Theta/2)$  functions using the SAS nonlinear regression program NLIN.<sup>10</sup> SAS/GRAPH<sup>11</sup> programs were written to plot curves on the computer system plotter. Smooth curves through data points were obtained by using a spline interpolation which is part of the SAS/GRAPH library.

Computations were performed on an Amdahl 470/V8 or Amdahl 580/5850 systems.

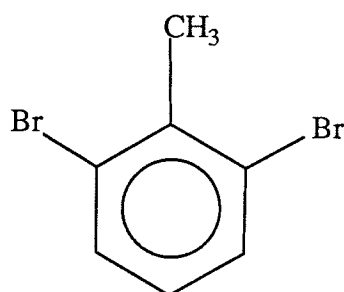
## C. EXPERIMENTAL RESULTS

### 1) 2,6-dibromotoluene

Table 1 gives the results for the analysis of proton spectra for a 2.5 mole % solution of 2,6-dibromotoluene in  $\text{CS}_2/\text{C}_6\text{D}_{12}$  and for a 3.0 mole % solution of 2,6-dibromotoluene in acetone- $\text{d}_6$ . All signs and couplings were taken from an unpublished analysis of 2,6-difluorotoluene. This analysis was straightforward. Figure 3 shows the experimentally observed X part of the  $\text{AB}_2\text{X}_3$  spin system. An estimate of the linewidth at half-height is 0.04 Hz.

TABLE 1

Proton spectral parameters<sup>a</sup> for a 2.5 mole% solution<sup>b</sup> of 2,6-dibromotoluene in CS<sub>2</sub>/C<sub>6</sub>D<sub>12</sub> and a 3.0 mole% solution<sup>c</sup> of 2,6-dibromotoluene in acetone-d<sub>6</sub> at 300K



	CS <sub>2</sub> /C <sub>6</sub> D <sub>12</sub>	Acetone-d <sub>6</sub>
$\nu(\text{CH}_3)$	760.648(1) <sup>d</sup>	764.844(0)
$\nu(\text{H}_3)$	2224.374(1)	2280.602(0)
$\nu(\text{H}_4)$	2051.649(1)	2116.975(0)
$^5J_m(\text{CH}_3, \text{H}_3)$	0.415(1)	0.420(0)
$^6J_p(\text{CH}_3, \text{H}_4)$	-0.627(1)	-0.637(0)
$^3J_o(\text{H}_3, \text{H}_4)$	7.983(1)	8.030(1)
Transitions Calculated	80	80
Transitions Assigned	79	80
Peaks Observed	38	38
Largest Difference	-0.017	-0.010
RMS Deviation	0.005	0.002

## NOTES

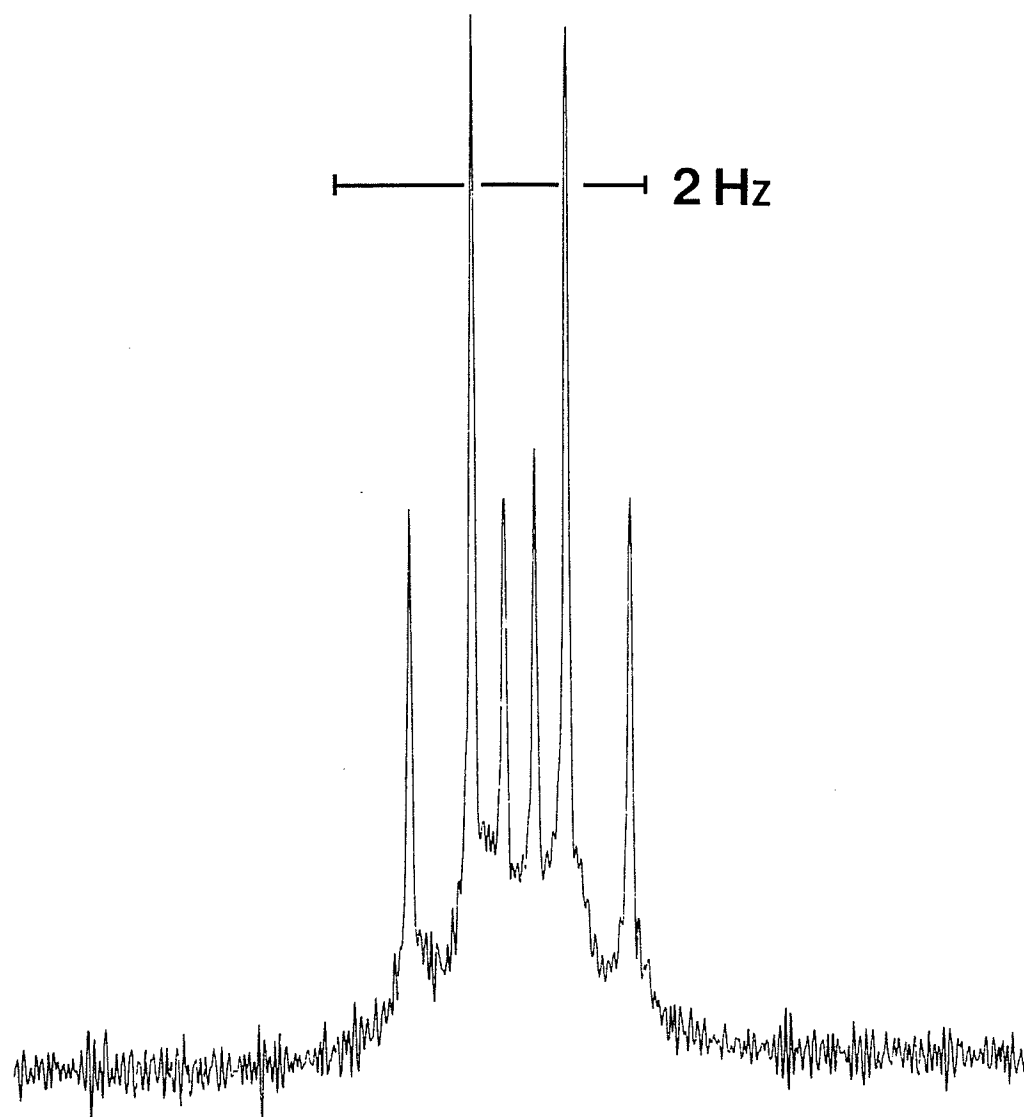
- a In Hertz.  $^1\text{H}$  nmr at 300.135 MHz to high frequency of TMS. Unless otherwise stated, signs of couplings assumed to be as they appear in the table.
- b Approximately 3.0 mole% in solution mixture consisting of  $\text{CS}_2$ , 10 mole%  $\text{C}_6\text{D}_{12}$ , 0.25 mole% TMS and 0.25 mole%  $\text{C}_6\text{F}_6$ .
- c Approximately 3.0 mole% in solution mixture consisting of acetone- $\text{d}_6$  and 1 drop of TMS.
- d Numbers in parentheses are standard deviations in the last significant digit, as given by the NUMARIT analysis.



FIGURE 3

Proton nmr spectrum for the methyl group in 2,6-dibromotoluene

The linewidth at half-height is estimated to be 0.04 Hz.



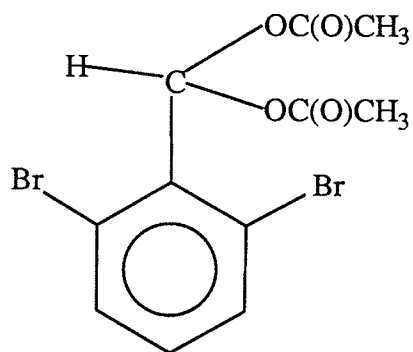
2) 2,6-dibromo- $\alpha,\alpha$ -diacetoxytoluene

Results for the analysis of proton spectra for a 3.0 mole % solution of 2,6-dibromo- $\alpha,\alpha$ -diacetoxytoluene in  $\text{CS}_2/\text{C}_6\text{D}_{12}$  and a 3.1 mole % solution of 2,6-dibromo- $\alpha,\alpha$ -diacetoxytoluene in acetone- $\text{d}_6$  are given in Table 2. The sign of  $^6J_p(\text{H},\text{CH})$  was determined using a double resonance experiment as shown in figure 4. All other signs and couplings between were taken from the previous analysis of 2,6-dibromotoluene.

The proton nmr spectra for the methyl and methine protons are shown in figure 5. For each of the two solutions,  $\text{CS}_2$  and acetone- $\text{d}_6$ , the chemical shift values for both the methyl and methine protons were optimized. The methyl proton region shows a sharp doublet indicating coupling only to the methine proton. The sign for this coupling was not determined. Although the methine proton shift value was optimized, only two peaks in the region were assigned. In contrast to the methyl region, the methine proton not only being coupled to the methyl protons but also to the rest of the ring nuclei gives rise to a rather broad and unresolved proton nmr spectrum. Figure 6 also shows the *meta* and *para* ring proton nmr regions.

TABLE 2

Proton spectral parameters<sup>a</sup> for a 3.0 mole% solution<sup>b</sup> of  
 2,6-dibromo- $\alpha,\alpha$ -diacetoxytoluene in  $\text{CS}_2/\text{C}_6\text{D}_{12}$  and a 3.1 mole% solution<sup>c</sup> of  
 2,6-dibromo- $\alpha,\alpha$ -diacetoxytoluene in acetone- $\text{d}_6$  at 300K



	$\text{CS}_2/\text{C}_6\text{D}_{12}$	Acetone- $\text{d}_6$
$\nu(\text{CH}_3)$	604.004(0) <sup>d</sup>	634.875(0)
$\nu(\text{CH})$	2397.660(1)	2466.041(1)
$\nu(\text{H}_3)$	2248.855(0)	2317.351(0)
$\nu(\text{H}_4)$	2098.784(0)	2182.417(0)
$^5J(\text{CH}_3, \text{CH})$	(+) $0.077(0)^e$	(+) $0.075(0)$
$^5J_m(\text{CH}, \text{H}_3)$	$0.231(0)^e$	$0.233(0)$
$^6J_p(\text{CH}, \text{H}_4)$	$-0.045(1)$	$-0.051(0)^f$
$^3J_o(\text{H}_3, \text{H}_4)$	$8.009(0)$	$8.063(0)$
Transitions Calculated	576	576
Transitions Assigned	269	448
Peaks Observed	245	278
Largest Difference	0.009	0.010
RMS Deviation	0.003	0.003

## NOTES

- a In Hertz.  $^1\text{H}$  nmr at 300.135 MHz to high frequency of TMS. Unless otherwise stated, signs of couplings assumed to be as they appear in the table.
- b Approximately 3.0 mole% in solution mixture of  $\text{CS}_2$ , 10 mole%  $\text{C}_6\text{D}_{12}$ , 0.25 mole% TMS and 0.25 mole%  $\text{C}_6\text{F}_6$ .
- c Approximately 3.1 mole% in solution mixture consisting of acetone- $\text{d}_6$  and 1 drop of TMS.
- d Numbers in parentheses are standard deviations in the last significant digit, as given by the NUMARIT analysis.
- e  $^5\text{J}(\text{CH}_3, \text{CH})$  correlates with  $^5\text{J}_m(\text{CH}, \text{H}_3)$  by 0.447.
- f Sign is determined by double resonance experiments.
- g The number of observed peaks is an estimated value since there are many overlapping transitions and a rather broad proton nmr spectrum found for the methine proton.

a) Determination of the relative sign of  ${}^6J_p(\text{H,CH})$  using double resonance experiments<sup>11a</sup>.

Four peaks of the *para* proton nmr spectrum, figure 4a, in 2,6-dibromo- $\alpha,\alpha$ -diacetoxytoluene are shown for a 3.1 mole% solution in acetone- $d_6$  at 300 MHz and 300K. The small splitting of 0.051 Hz corresponds to  ${}^6J_{AX}$  in the spectrum which originates from an  $AB_2X$  spin system. The doublet on the left represents the two transitions of  $H_4$  where the  $B_2$  protons ( $H_3$  and  $H_5$ ) lie in antisymmetric spin states. In other words, there is a vanishing spin magnetic moment for the  $B_2$  protons. If an  $AM_2X$  spin system were present, then the two pairs of doublets would coincide in frequency.

In figure 4b, the doublets from 4a are shown, but under a very weak radiofrequency field which is applied while coadding<sup>12</sup> 32 FIDs each with an acquisition time of approximately 41 seconds. This weak irradiation is applied to a single transition in the  $B_2$  region, which corresponds to a given spin state of the methine proton X. The peak at low frequency in the doublet on the right side in 4b has been perturbed while the antisymmetric transitions on the left are unaffected by the second radiofrequency field under the conditions here and therefore provide a good reference for resolution conditions and peak frequencies. Since the second radiofrequency field is applied at "high" frequency, this experiment indicates that  ${}^6J_{AX}$  and  ${}^5J_{BX}$  are of opposite sign. The sign was confirmed with three additional experiments where the second radiofrequency field was applied to three other transitions in the  $B_2$  region. Since  ${}^5J_m(\text{H,CH}) > 0$ , then as a result,  ${}^6J_p(\text{H,CH}) < 0$ .

# FIGURE 4

Sign determination of  ${}^6J_p(\text{CH}, \text{H}_4)$  in 2,6-dibromo- $\alpha, \alpha$ -diacetyltoluene using partial decoupling experiments

A) *para* proton region with no decoupling

B) with partial decoupling of the high frequency peak of the *meta* doublet

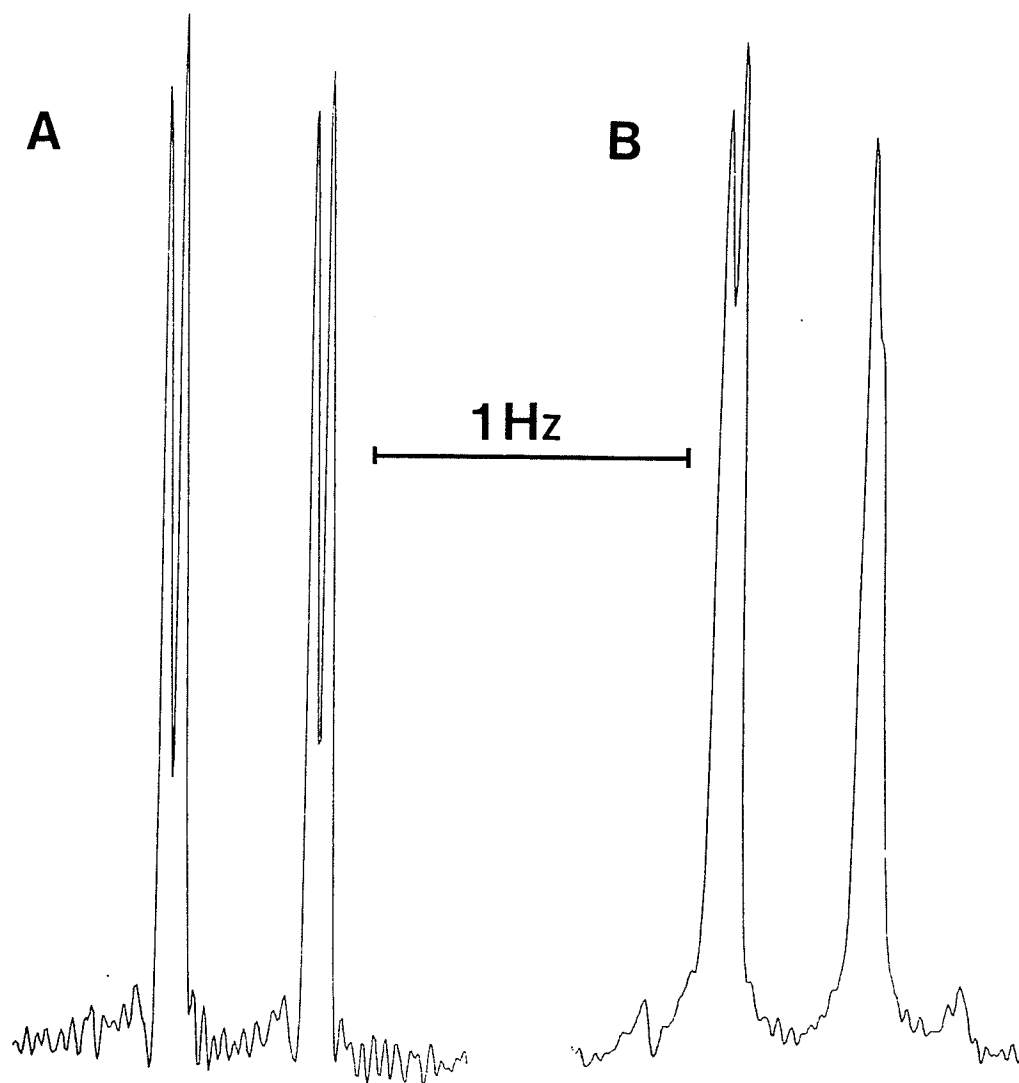




**FIGURE 5**

**The methyl and methine proton regions in 2,6-dibromo- $\alpha,\alpha$ -diacetoxytoluene**

**A) methyl proton region**

**B) methine proton region**

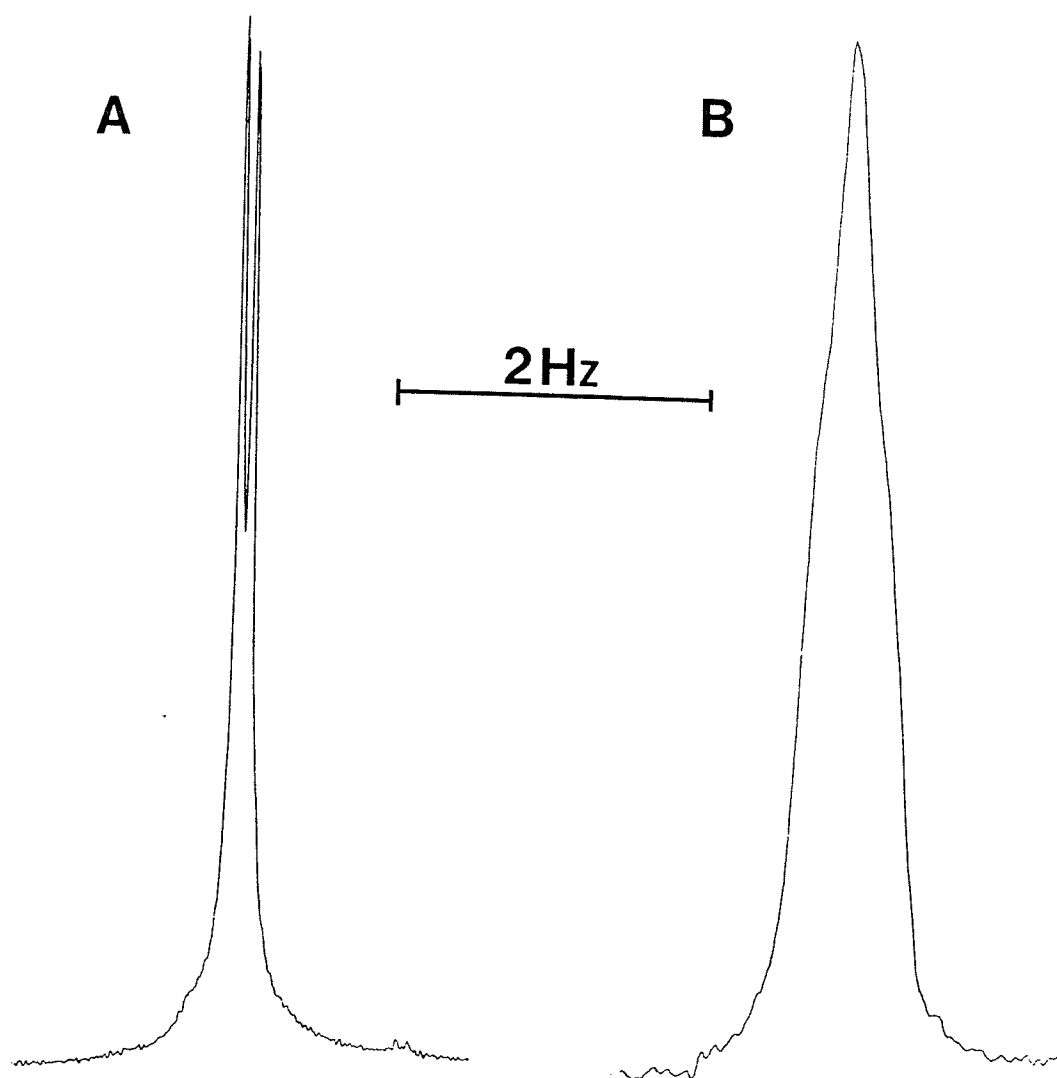


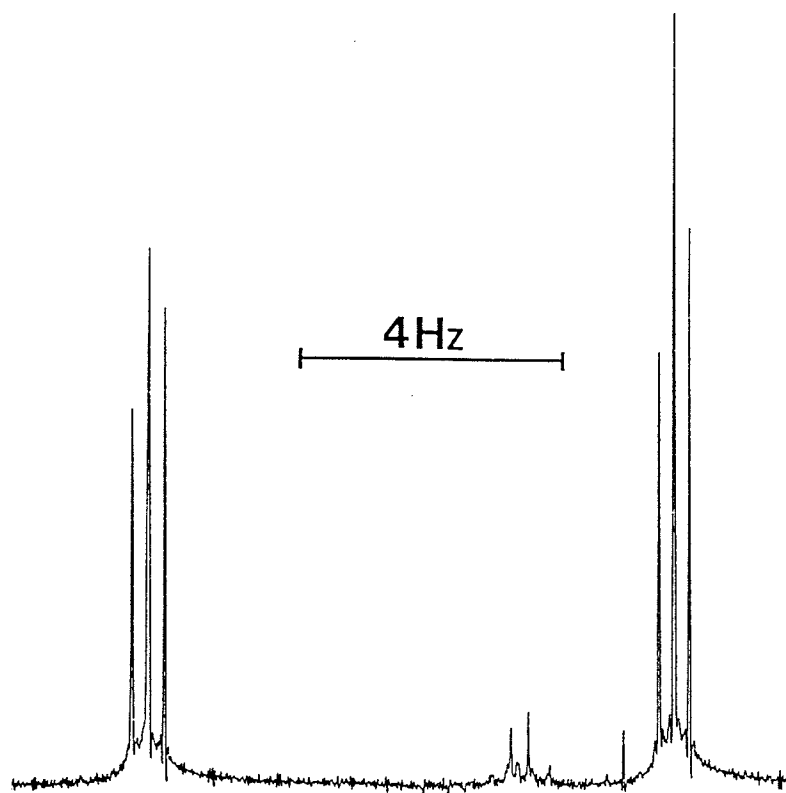
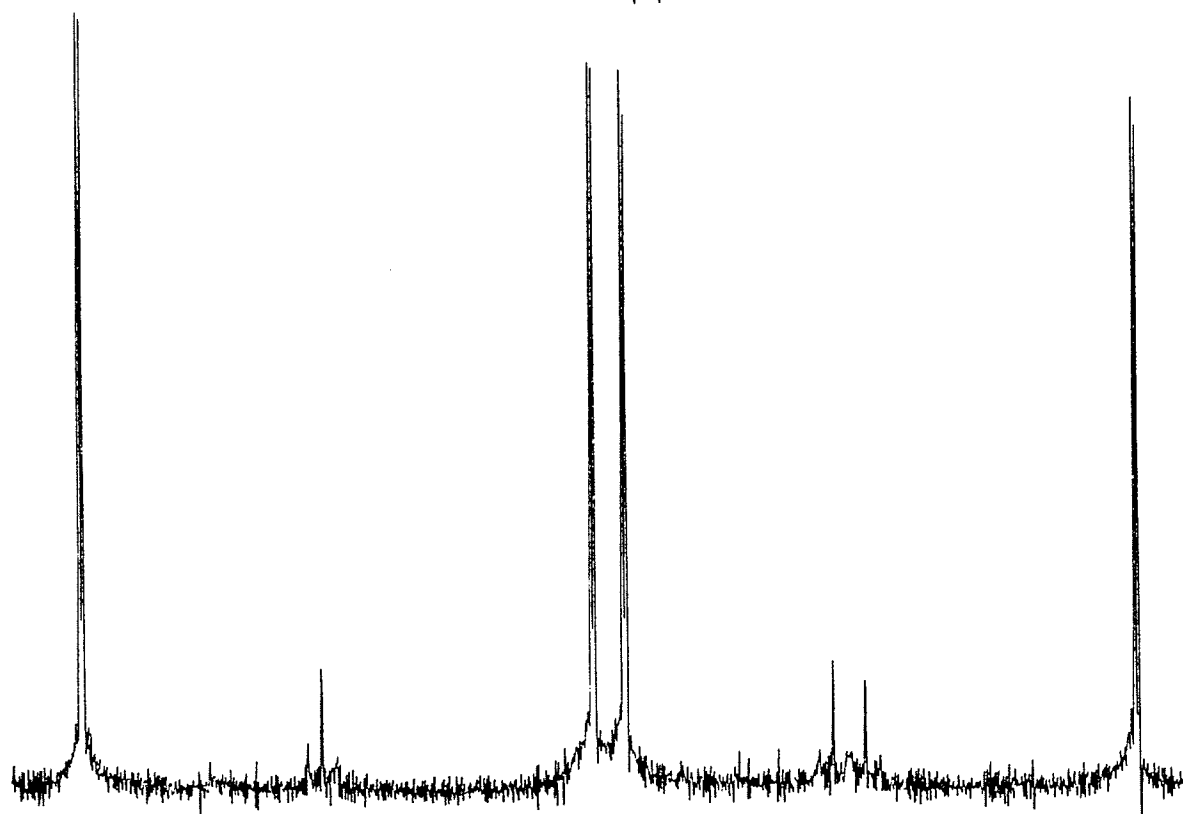
FIGURE 6

The *meta* and *para* ring proton regions in 2,6-dibromo- $\alpha,\alpha$ -diacetoxytoluene

A) *meta* proton nmr spectrum

B) *para* proton nmr spectrum

Note that there are impurity peaks in the experimental spectrum.

**A****B**

### 3) $\alpha,\alpha$ -diacetoxytoluene

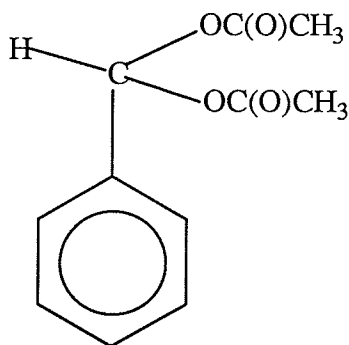
Results for the analysis of the proton spectra for a 2.0 mole % solution of  $\alpha,\alpha$ -diacetoxytoluene in  $\text{CS}_2/\text{C}_6\text{D}_{12}$  and a 2.1 mole % solution of  $\alpha,\alpha$ -diacetoxytoluene in acetone- $\text{d}_6$  are shown in Table 3. All signs and couplings were taken from a recent unpublished analysis in our laboratory of  $\alpha,\alpha$ -dimethoxytoluene.

The methyl and methine proton nmr spectra are shown in figure 7. As in the 2,6-dibromo derivative, the methyl region shows a sharp doublet indicating coupling only to the methine proton in contrast to the methine region which is rather broad and unresolved due to coupling between both the methyl and ring protons. Again, for both  $\text{CS}_2$  and acetone- $\text{d}_6$  solutions, the sign of the coupling between the methyl and methine protons was not determined. Some relatively significant correlations between shift values and coupling constants within the phenyl moiety especially in the  $\text{CS}_2$  can be attributed to the small shift difference encountered between the *meta* and *para* ring protons.

Figure 8 shows the *ortho* ring proton region while figure 9 gives both the *meta* and *para* ring proton regions. Note that for both analyses, in acetone- $\text{d}_6$  and  $\text{CS}_2$  solutions, only observed transitions in the phenyl proton nmr regions were assigned.

TABLE 3

Proton spectral parameters<sup>a</sup> for 2.0 mole% solution<sup>b</sup> of  $\alpha,\alpha$ -diacetoxytoluene in  $\text{CS}_2/\text{C}_6\text{D}_{12}$  and a 2.1 mole% solution<sup>c</sup> of  $\alpha,\alpha$ -diacetoxytoluene in acetone- $\text{d}_6$  at 300K



	$\text{CS}_2/\text{C}_6\text{D}_{12}$	Acetone- $\text{d}_6$	
$\nu(\text{CH}_3)$	586.828 <sup>d</sup>	627.118 <sup>d</sup>	-----P
$\nu(\text{CH})$	2246.000 <sup>d</sup>	2295.500 <sup>d</sup>	2295.481(2)
$\nu(\text{H}_2=\text{H}_6)$	2212.262(1) <sup>e</sup>	2259.647(1) <sup>l</sup>	2259.671(2)
$\nu(\text{H}_3=\text{H}_5)$	2178.543(2) <sup>g</sup>	2230.822(2) <sup>k</sup>	2230.846(2)
$\nu(\text{H}_4)$	2177.577(3) <sup>g</sup>	2227.866(3) <sup>k</sup>	2227.891(3)

TABLE 3 (cont'd)

	CS <sub>2</sub> /C <sub>6</sub> D <sub>12</sub>	Acetone-d <sub>6</sub>	
<sup>5</sup> J(CH <sub>3</sub> ,CH)	(±)0.072 <sup>f</sup>	(±)0.067 <sup>f</sup>	-----P
<sup>4</sup> J <sub>o</sub> (CH,H <sub>2</sub> )	-0.491(3)	-0.529(3)	-0.527(2)
<sup>5</sup> J <sub>m</sub> (CH,H <sub>3</sub> )	0.271(4) <sup>h</sup>	0.275(4)	0.279(3)
<sup>6</sup> J <sub>p</sub> (CH,H <sub>4</sub> )	0.223(6) <sup>h</sup>	-0.264(6)	-0.262(4)
<sup>4</sup> J <sub>m</sub> (H <sub>2</sub> ,H <sub>6</sub> )	1.807(3) <sup>i</sup>	1.934(2)	1.934(3)
<sup>3</sup> J <sub>o</sub> (H <sub>2</sub> ,H <sub>3</sub> )	7.785(2) <sup>j</sup>	7.818(2) <sup>m</sup>	7.822(2)
<sup>4</sup> J <sub>m</sub> (H <sub>2</sub> ,H <sub>4</sub> )	1.276(3) <sup>j</sup>	1.262(3) <sup>m</sup>	1.261(3)
<sup>5</sup> J <sub>p</sub> (H <sub>2</sub> ,H <sub>5</sub> )	0.606(2) <sup>i</sup>	0.605(2) <sup>l</sup>	0.607(2)
<sup>4</sup> J <sub>m</sub> (H <sub>3</sub> ,H <sub>5</sub> )	1.332(3) <sup>i</sup>	1.369(2) <sup>k</sup>	1.367(3)
<sup>3</sup> J <sub>o</sub> (H <sub>3</sub> ,H <sub>4</sub> )	7.386(4) <sup>i</sup>	7.490(3) <sup>l</sup>	7.486(4)
Transitions Calculated	187	183	183
Transitions Assigned	97	111	117 <sup>a</sup>
Peaks Observed	96 <sup>n</sup>	95 <sup>n</sup>	118 <sup>a</sup>
Largest Difference	0.026	-0.034	0.026
RMS Deviation	0.010	0.010	0.010

## NOTES

- a In Hertz.  $^1\text{H}$  nmr at 300.135 MHz to high frequency of TMS. Unless otherwise stated, signs of couplings assumed to be as they appear in the table.
- b Approximately 2.0 mole% in solution mixture of  $\text{CS}_2$ , 10 mole%  $\text{C}_6\text{D}_{12}$ , 0.25 mole% TMS and 0.25 mole%  $\text{C}_6\text{F}_6$ .
- c Approximately 2.1 mole% in solution mixture consisting of acetone- $\text{d}_6$  and 1 drop of TMS.
- d An approximate value for the chemical shift of this proton and this shift value was not optimized in the analysis.
- e Numbers in parentheses are standard deviations in the last significant digit, as given by the NUMARIT analysis.
- f Sign was not determined.
- g  $\nu(\text{H}_3=\text{H}_5)$  correlates with  $\nu(\text{H}_4)$  by -0.233.
- h  $^5J_{\text{m}}(\text{CH},\text{H}_3)$  correlates with  $^6J_{\text{p}}(\text{CH},\text{H}_4)$  by -0.219.
- i  $^4J_{\text{m}}(\text{H}_2,\text{H}_6)$  correlates with  $^5J_{\text{p}}(\text{H}_2,\text{H}_5)$  by 0.380 and with  $^3J_{\text{o}}(\text{H}_3,\text{H}_4)$  by 0.313.  
 $^5J_{\text{p}}(\text{H}_2,\text{H}_5)$  correlates with  $^4J_{\text{m}}(\text{H}_3,\text{H}_5)$  by -0.220.
- j  $^3J_{\text{o}}(\text{H}_2,\text{H}_3)$  correlates with  $^4J_{\text{m}}(\text{H}_2,\text{H}_4)$  by -0.197.
- k  $\nu(\text{H}_4)$  correlates with  $\nu(\text{H}_3)$  and  $^4J_{\text{m}}(\text{H}_3,\text{H}_5)$  by -0.204.
- l  $^5J_{\text{p}}(\text{H}_2,\text{H}_5)$  correlates with  $\nu(\text{H}_2=\text{H}_6)$  by -0.194 and with  $^3J_{\text{o}}(\text{H}_3,\text{H}_4)$  by 0.216.
- m  $^3J_{\text{o}}(\text{H}_2,\text{H}_3)$  correlates with  $^4J_{\text{m}}(\text{H}_2,\text{H}_4)$  by -0.267.
- n Only the observed transitions for the phenyl ring proton nmr regions were assigned.
- p Decoupling of the methyl protons.
- q Ring and methine protons. The two analyses were performed several months apart and independent of each other. A Bloch-Siegert shift of about 0.024 Hz is observed for the ring protons during decoupling of the methyl protons.



**FIGURE 7**

The methyl and methine proton regions in  $\alpha,\alpha$ -diacetoxytoluene

A) methyl proton region

B) methine proton region

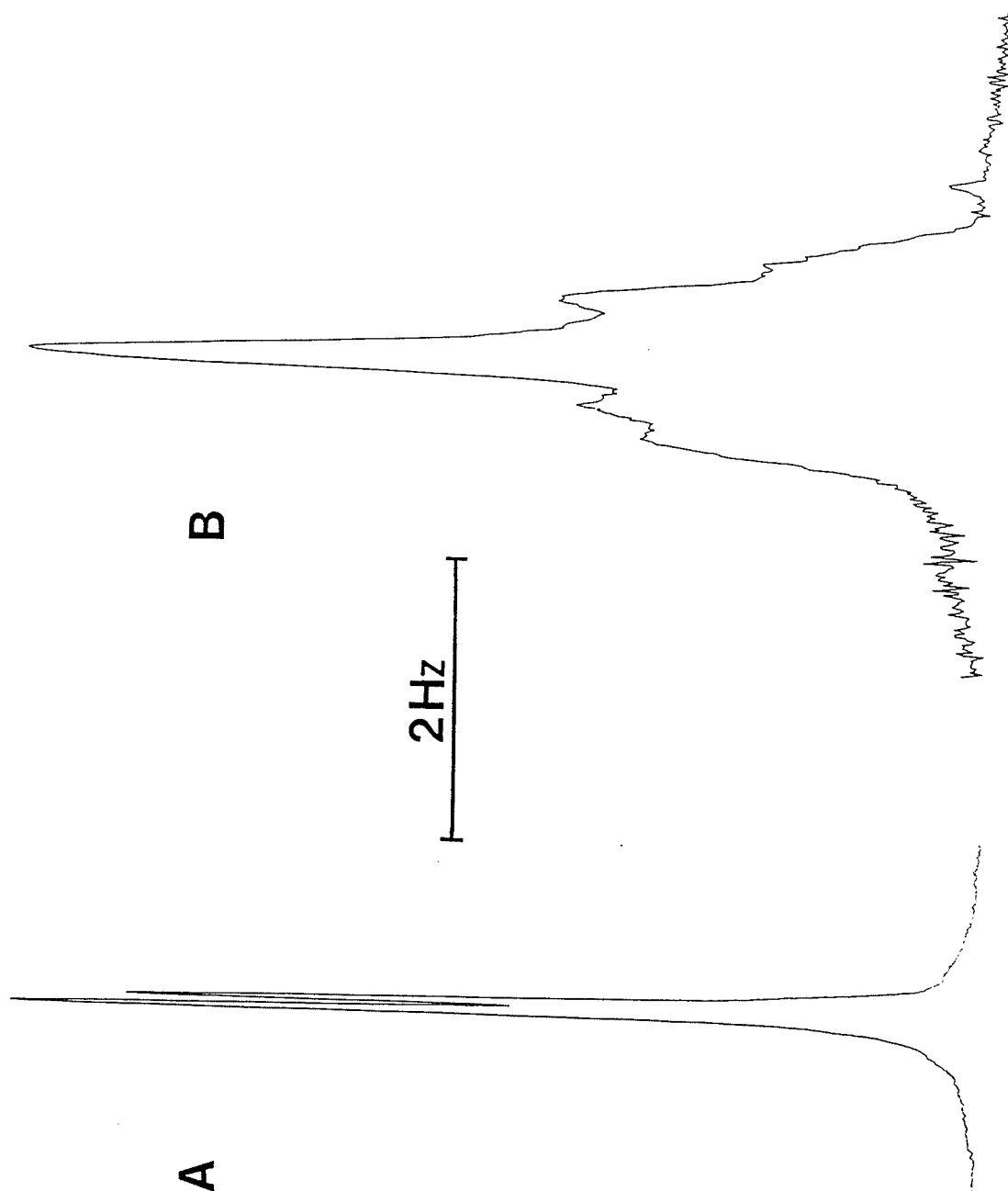


FIGURE 8

The *ortho* ring proton region of  $\alpha,\alpha$ -diacetoxytoluene

A) observed

B) calculated

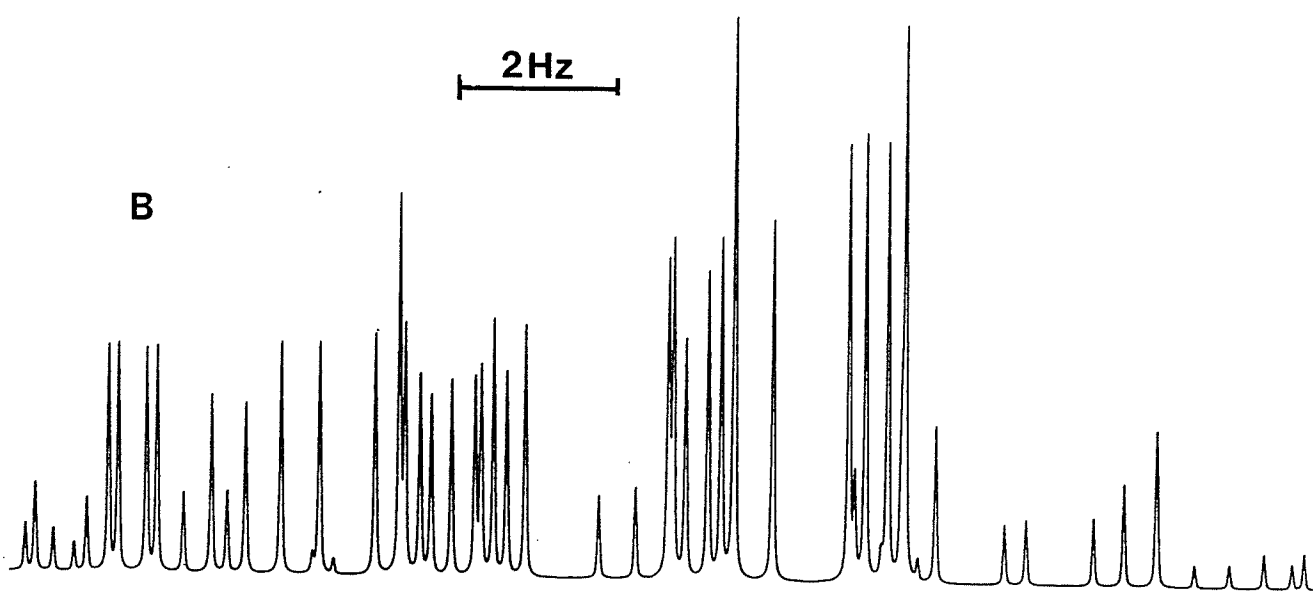
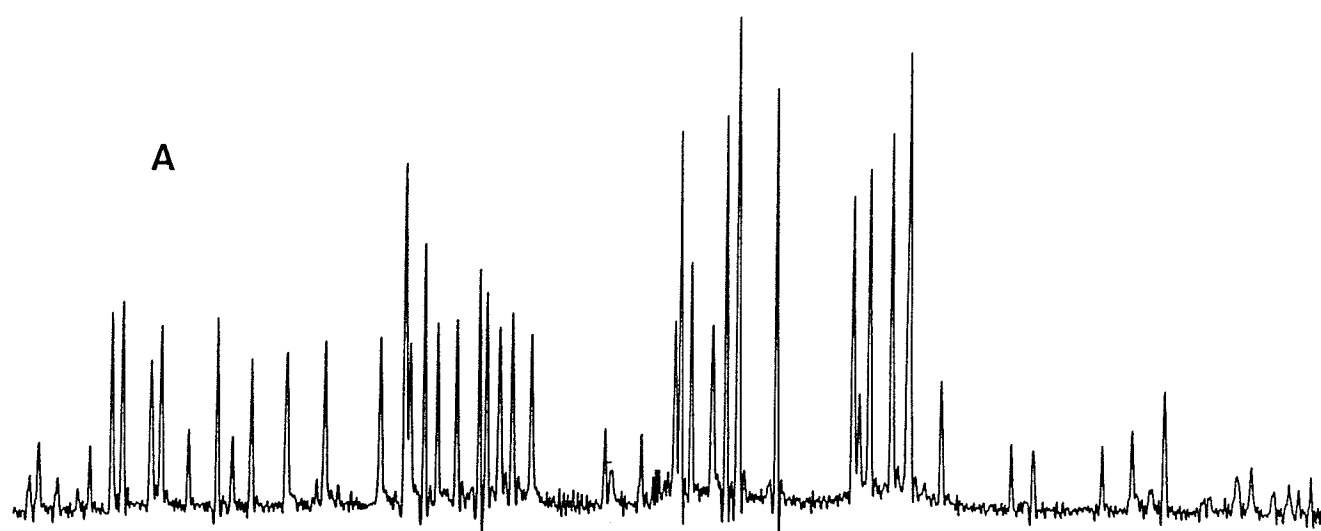


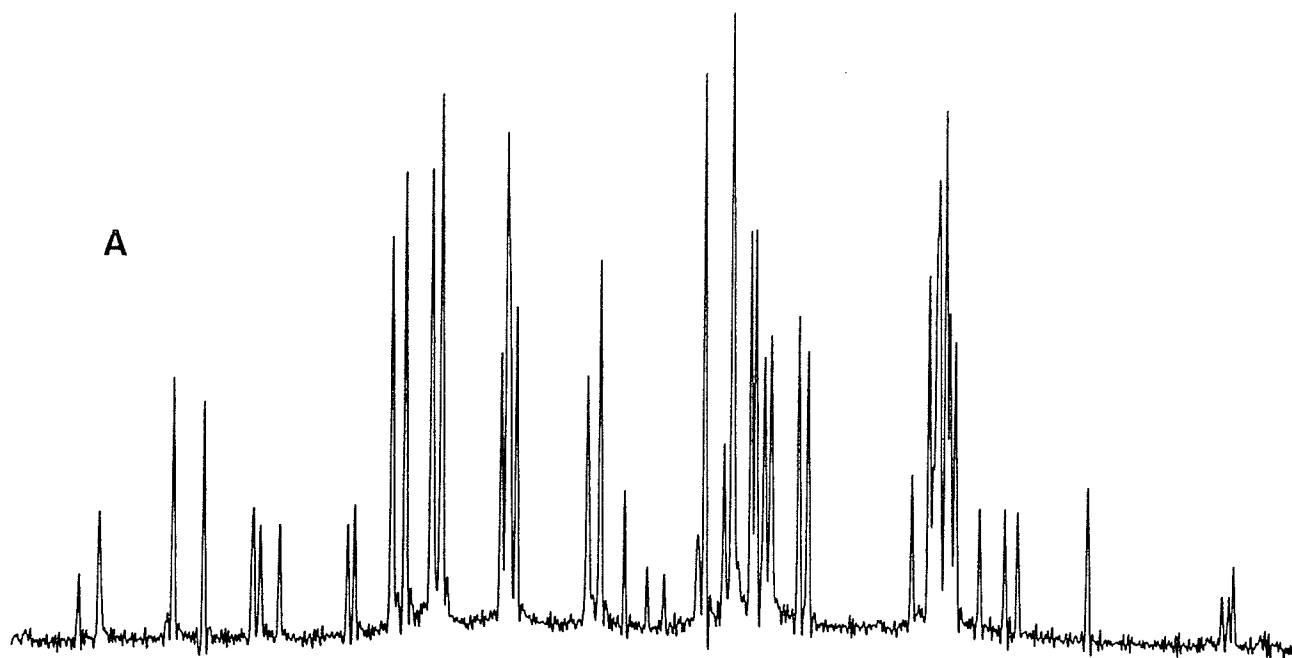
FIGURE 9

The *meta* and *para* proton regions of  $\alpha,\alpha$ -diacetoxytoluene

A) experimental

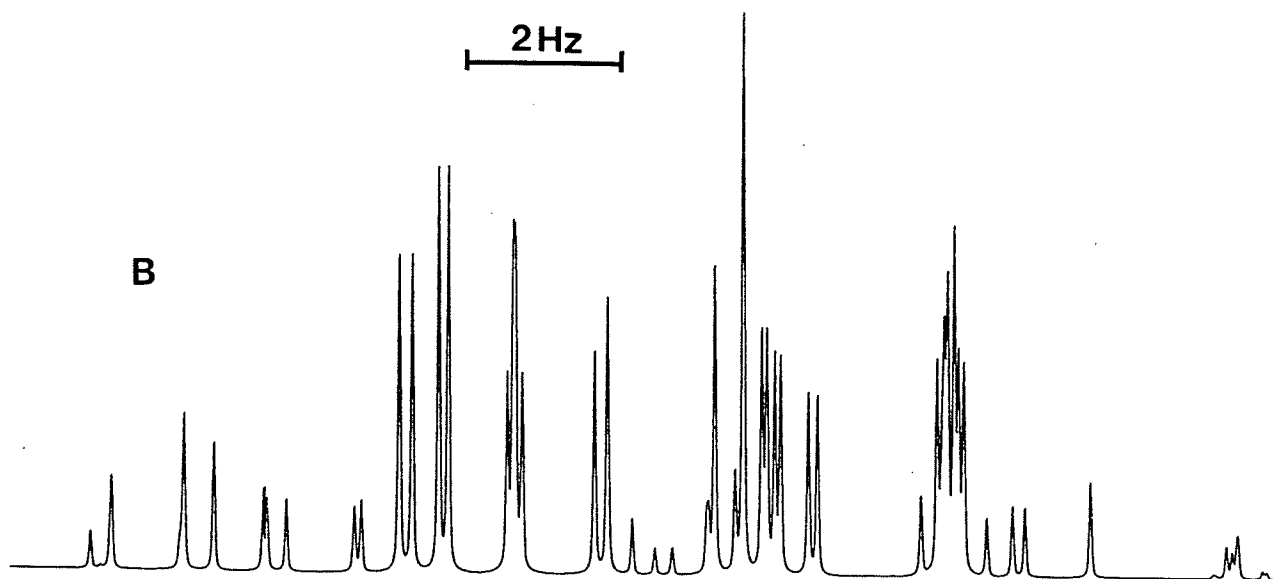
B) calculated

A



2 Hz

B



## D. DISCUSSION

For  $\alpha,\alpha$ -diacetoxytoluene in acetone- $d_6$  solution,  ${}^6J_p(\text{H,CH})$  is found to be  $-0.263(10)$  Hz, the standard deviation being taken as the sum of the standard deviations for the two analyses in Table 3. Assuming  ${}^6J_{90}$  is the same as that for toluene,  $-1.20$  Hz, then  $\langle \sin^2\Theta \rangle$  is  $0.219(8)$ . Also assuming a twofold barrier hindering rotation about the exocyclic  $\text{Csp}^2\text{-Csp}^3$  bond and a hindered rotor model<sup>1</sup> yields a  $V_2$  of  $7.0 \pm 0.3$  kJ/mole. A classical averaging procedure<sup>5</sup> gives the same result at 300K. From the measured value of  ${}^6J_p(\text{H,CH})$ , the lowest energy conformation has the methine C-H bond in the plane of the benzene ring.

However, the electronegativity of the acetoxy group is similar to that of a methoxy group<sup>13</sup>. The latter reduces the magnitude of  ${}^6J_{90}$  to  $-1.02$  Hz<sup>14</sup>. It is not likely that a second acetoxy group would be as effective as the first (saturation effect). If additivity is assumed, then a maximum in  $\langle \sin^2\Theta \rangle$  and a lower limit in  $V_2$  will result. With this principle in mind, a  ${}^6J_{90}$  of  $-0.84$  Hz gives  $\langle \sin^2\Theta \rangle$  as  $0.313(12)$  and an apparent  $V_2$  of  $4.1 \pm 0.4$  kJ/mole. With the alternative assumption, that the second acetoxy group is half as effective as the first in reducing the magnitude of  ${}^6J_{90}$ , then  ${}^6J_{90}$  is  $-0.93$  Hz giving an apparent  $V_2$  of  $4.9 \pm 0.4$  kJ/mole. In conclusion, if the barrier is twofold, then it lies between 4 and 5 kJ/mole.

For this same molecule in  $\text{CS}_2$  solution,  ${}^6J_p(\text{H,CH})$  is  $-0.223(6)$  Hz. The above procedure leads to an apparent  $V_2$  lying between 5 and 6 kJ/mole, an increase of approximately 1 kJ/mole with respect to that found in acetone- $d_6$  solution. This suggests that the perpendicular conformer of  $\alpha,\alpha$ -diacetoxytoluene, where  $\Theta = 90^\circ$ , is stabilized by the polar solvent. A similar stabilization occurs for benzyl chloride, where the acetone stabilizes the conformer having the exocyclic  $\text{Csp}^3\text{-Csp}^2$  bond lying in a plane perpendicular to the plane of the benzene ring. However, in benzyl chloride, since the perpendicular conformer sits at the bottom of the internal rotational potential well, the acetone solvent increases the internal barrier to rotation<sup>15</sup>; that is  ${}^6J_p(\text{H,CH}_2)$  is smaller in



the acetone solution. In contrast, for both benzyl chloride and  $\alpha,\alpha$ -diacetoxytoluene, the coupling constants within the ring are generally larger in the acetone- $d_6$  than in the  $CS_2$  solution. Consequently, it is reasonable to conclude that a solvent dependence of  ${}^6J_p(H,CH)$  in  $\alpha,\alpha$ -diacetoxytoluene suggests that the internal barrier to rotation is also solvent dependent and is not solely indicative of an intrinsic solvent perturbation.

The barrier magnitudes seem reasonable by comparison with those deducible from  ${}^6J_p(H,CH)$  for 2-phenyl-1,3-dioxane and the corresponding dioxolane derivative<sup>16</sup>, for which the present approach using a  ${}^6J_{90}$  value of -0.93 Hz, gives apparent  $V_2$  values of  $1.5 \pm 0.3$  and  $3.1 \pm 0.4$  kJ/mole, respectively. It is worth noting that in the phenyl dioxane, results from molecular mechanics<sup>17</sup> and calorimetric techniques<sup>18</sup> indicate essentially free internal rotation about the  $Csp^2$ - $Csp^3$  bond. An examination of the relative motion between the phenyl and saturated rings shows that the *ortho* C-H bonds of the phenyl group come into the vicinity of the oxygen atoms in the saturated ring, while the remainder of the saturated ring remains distant due to its cyclic structure. Models of  $\alpha,\alpha$ -diacetoxytoluene show that the lowest energy conformation has the  $\alpha$  C-H bond lying in the plane of the benzene ring (as indicated by the magnitude of  ${}^6J_p(H,CH)$ ). Therefore, the acetyl groups of the sidechain must point away from the phenyl group during internal rotational motion. However, whatever the value of  ${}^6J_{90}$ , the  ${}^6J_p(H,CH)$  values in  $\alpha,\alpha$ -diacetoxytoluene, 2-phenyl-1,3-dioxane and 2-phenyl-1,3-dioxolane show that the barrier in  $\alpha,\alpha$ -diacetoxytoluene is much higher than in the remaining two. This seems reasonable since the motions of the acetyl groups must be significant in  $\alpha,\alpha$ -diacetoxytoluene and therefore should lead to a higher barrier to rotation about the  $Csp^2$ - $Csp^3$  bond.

Since the J method assumes a twofold barrier and there is reasonable agreement between the calorimetric and J measurements of the internal barrier to rotation in the phenyl dioxane, it is reasonable to say that for two-ring molecules a twofold component is

dominant. For  $\alpha,\alpha$ -diacetyltoluene, the presence of additional fluctuating groups in the sidechain might introduce more substantial magnitudes of higherfold terms into the internal rotational potential. For example, assume that  $\langle \sin^2\Theta \rangle$  is 0.283 in  $\text{CS}_2$  solution, which corresponds to a  ${}^6J_{90}$  value of -0.93 Hz. At 300K, this value corresponds to a  $V_2, V_4$  combination of 4.0 and 2.0 kJ/mole, rather than a  $V_2$  of 4.9 kJ/mole. If  $V_2$  and  $V_4$  are of opposite sign then selecting typical values from other combinations gives  $V_2$  and  $V_4$  as 11.5 and -7.3 kJ/mole, respectively, or 10.5 and -6.6 kJ/mole. The magnitudes of  $V_4$  are rather high, yet they cannot be excluded solely on the basis of  ${}^6J_p(\text{H,CH})$ .

Finally, further complications would be introduced in the presence of an angle-independent term in equation 1. This term, apparently negative and having a magnitude of approximately 0.1 Hz, may exist in styrene<sup>19</sup>. As a result, the ensuing measurements on 2,6-dibromo- $\alpha,\alpha$ -diacetyltoluene are of interest.

The free energy barrier to internal rotation in 2,6-dibromo- $\alpha,\alpha$ -diacetyltoluene can be deduced from the DNMR data for the dimethyl ether solution. At 150K, the chemical shift difference between the *meta* protons  $\text{H}_3$  and  $\text{H}_5$  is  $12 \pm 2$  Hz at 300 MHz. The coalescence temperature is  $165 \pm 3$  K. A reasonable assumption that the transmission coefficient is unity gives a value for  $\Delta G_{165}^\ddagger$  of  $36.2 \pm 0.9$  kJ/mole. It would be useless<sup>20</sup> to attempt a reliable decomposition of  $\Delta G^\ddagger$  into  $\Delta H^\ddagger$  and  $\Delta S^\ddagger$  for such a small difference in chemical shift for the two *meta* protons because the temperature range over which the lineshape is sensitive to the pre-exchange lifetime is too small.

For 2,6-dibromo- $\alpha,\alpha$ -diacetyltoluene,  ${}^6J_p(\text{H,CH})$  is -0.045(0) and -0.051 Hz in  $\text{CS}_2$  and acetone- $\text{d}_6$  solutions, respectively, as shown in Table 2. The observed  ${}^6J_p(\text{H,CH}_3)$  couplings of -0.627(1) and -0.637(0) Hz for 2,6-dibromotoluene in these same solvents give estimates of  ${}^6J_{90}$  for this substitution pattern.

Since the internal barrier to rotation in 2,6-dibromo- $\alpha,\alpha$ -diacetyltoluene cannot be infinite, then  $|{}^6J_0| < 0.05$  Hz. If  $\Delta S^\ddagger$  is zero, then  $\Delta H^\ddagger$  is equivalent to  $\Delta G^\ddagger$  and is  $36 \pm 1$  kJ/mole in dimethyl ether solution. Making the assumptions that the free energy  $\Delta G^\ddagger$  is

identical in all three solvents, that there is a twofold barrier, that  $0.88 < |^6J_{90}| \leq 1.02$  Hz, that  $^6J_0$  vanishes and that the observed coupling  $^6J_p(\text{H,CH})$  is  $-0.048(3)$  Hz, which is the mean of  $^6J_p(\text{H,CH})$  in  $\text{CS}_2$  and acetone- $d_6$  solutions, leads to a  $\langle \sin^2\Theta \rangle$  of  $0.051(7)$  and therefore gives an apparent  $V_2$  of  $26.5^{+4.0}_{-3.0}$  kJ/mole. If  $^6J_0$  is nonzero, say  $-0.01$  Hz, then  $V_2$  follows as  $33.5^{+6.5}_{-5.0}$  kJ/mole. Since  $^6J_{90}$  may not be affected by  $\alpha$  substituents, then from Table 2,  $^6J_{90}$  would be  $-1.26(1)$  Hz. Using this value together with a  $^6J_p(\text{H,CH})$  of  $-0.048(3)$  Hz and assuming that  $^6J_0$  vanishes leads to an apparent  $V_2$  of  $35.4 \pm 2.1$  kJ/mole. However, it is very unlikely that  $^6J_{90}$  is not of the lower magnitude indicated above.

Now consider the situation where  $\Delta S^\ddagger$  is not zero. In 2,6-difluoroisopropylbenzene,  $\Delta S^\ddagger$  and  $\Delta H^\ddagger$  are  $-21 \pm 4$  J/moleK and  $25.5 \pm 0.4$  kJ/mole<sup>2</sup>, while in  $\alpha,\alpha,2,4,6$ -pentabromotoluene  $\Delta S^\ddagger$  and  $\Delta H^\ddagger$  are  $-2 \pm 2$  J/moleK and  $80 \pm 1$  kJ/mole<sup>21</sup>.

If the former value of  $\Delta S^\ddagger$  applies to 2,6-dibromo- $\alpha,\alpha$ -diacetoxytoluene, then  $\Delta H^\ddagger$  is  $33 \pm 2$  kJ/mole, which again is compatible with a  $^6J_0$  value of  $-0.01$  Hz.

The presence of a fourfold component,  $V_4$ , must also be considered. A negative value for  $V_4$  allows more freedom of motion about the exocyclic  $\text{Csp}^2\text{-Csp}^3$  bond than if only  $V_2$  is present. Therefore, for a given  $V_2$ , a negative  $V_4$  leads to a larger value of  $\langle \sin^2\Theta \rangle$  where  $V_2$  is a measure of the barrier height. Consequently, the existence of a negative  $V_4$  suggests a  $^6J_0$  value of less than  $0.01$  Hz in magnitude.

However, the available data for  $\alpha,\alpha$ -diiodo-2,6-dichlorotoluene implies the presence of a small positive  $V_4$ . Thus, molecular mechanics calculations<sup>22</sup> of the internal energy of this molecule are in agreement with the measured free energy of activation of  $89$  kJ/mole for internal rotation suggesting that  $V_4$  is less than a tenth of  $V_2$ . In such a situation,  $V_2$  is a direct measure of the barrier height. Consider 2,6-dibromo- $\alpha,\alpha$ -diacetoxytoluene at  $300\text{K}$ . If  $V_2$  is  $36$  kJ/mole and  $V_4$  is  $4$  kJ/mole, then  $\langle \sin^2\Theta \rangle$  is  $0.026$ . A  $V_2$  of  $33$  kJ/mole and a  $V_4$  of  $3$  kJ/mole give  $\langle \sin^2\Theta \rangle$  as  $0.030$ . Since the measured value of  $\langle \sin^2\Theta \rangle$  is  $0.051(7)$ , then  $^6J_0$  is approximately  $-0.02$  Hz.

In summary, these illustrative arguments show that with the available information a vanishing  ${}^6J_0$  cannot be established.

Considering a molecule with a higher barrier to internal rotation,  $\alpha,\alpha,2,4,6$ -pentachlorotoluene in  $\text{CS}_2$  solution,  $\Delta H^\ddagger$  is  $57.3 \pm 1.1$  kJ/mole<sup>23</sup> and is expected<sup>21,23,24</sup> to be much the same in  $\alpha,\alpha,2,6$ -tetrachlorotoluene. For a dilute solution of the  $\alpha,\alpha,2,6$ -tetrachlorotoluene in  $\text{CS}_2$ , containing also a smaller amount of  $\alpha,2,6$ -trichlorotoluene, the outer peaks of the *para* proton  $\text{H}_4$  correspond to  $\alpha\alpha$  and  $\beta\beta$  spin states of the *meta* protons  $\text{H}_3$  and  $\text{H}_5$ . As a result, these peaks are not broadened by the internal rate process. At 300K, the peak at lowest frequency has a linewidth of 0.06 Hz, while the triplets of the *para* proton  $\text{H}_4$  in  $\alpha,2,6$ -trichlorotoluene have a linewidth of 0.03<sub>3</sub> Hz. The larger linewidth is attributed to an unresolved  ${}^6J_p(\text{CH},\text{H})$  coupling in  $\alpha,\alpha,2,6$ -tetrachlorotoluene. Simulations accounting for the partially gaussian character of the resolution-enhanced experimental spectra, show that a  ${}^6J_p(\text{CH},\text{H})$  of just over 0.025 Hz, but certainly less than 0.030 Hz, in magnitude will account for the lineshapes of the measured peaks.

In benzyl chloride,  ${}^6J_{90}$  is deduced as -1.06 Hz<sup>15</sup>. The assumption of additivity implies a  ${}^6J_{90}$  value of -0.92 Hz for benzal chloride. In 2,6-dichlorotoluene,  ${}^6J_p(\text{H},\text{CH}_3)$  is -0.630(1) Hz, implying  ${}^6J_{90}$  as -1.26 Hz compared to -1.20 Hz in toluene. Assuming additivity,  ${}^6J_{90}$  for  $\alpha,\alpha,2,6$ -tetrachlorotoluene is -0.98 Hz. But if the second  $\alpha$  chlorine substituent is only half as effective as the first in reducing the magnitude of  ${}^6J_{90}$ , then the value of  ${}^6J_{90}$  appears to be -1.05 Hz. From all these considerations,  $\langle \sin^2\Theta \rangle$  is estimated as 0.027(3). For 300K, the hindered rotor approach<sup>1</sup>, using 51 basis functions, together with a  $V_2$  of 57.3 kJ/mole leads to a  $\langle \sin^2\Theta \rangle$  value of 0.030. A molecular mechanics calculation<sup>25</sup> gives a barrier height of 55.2 kJ/mole for  $\alpha,\alpha,2,6$ -tetrachlorotoluene and implies the presence of a small fourfold component of the internal potential. If this contribution is as large as 10 % of  $V_2$ , then  $\langle \sin^2\Theta \rangle$  is 0.024. For  $\alpha,\alpha,2,6$ -tetrachlorotoluene,  ${}^6J_0$  is negligibly small. There seems to be no a priori reason

why the situation should be any different in  $\alpha,\alpha$ -diacetoxytoluene or 2,6-dibromo- $\alpha,\alpha$ -diacetoxytoluene.

## E. SUMMARY AND CONCLUSIONS

The  $^1\text{H}$  nmr spectral parameters are given for  $\alpha,\alpha$ -diacetoxytoluene in  $\text{CS}_2$  and acetone- $\text{d}_6$  solutions. The long-range spin-spin coupling constant over six bonds,  $^6J_p(\text{H},\text{CH})$ , can be used to determine twofold barriers to rotation about the exocyclic  $\text{Csp}^2\text{-Csp}^3$  bond in the two solutions. The conformation of lowest energy has the  $\alpha$  C-H bond in the plane of the benzene ring. The barrier is higher in  $\text{CS}_2$  than in acetone- $\text{d}_6$ , in contrast to benzyl chloride. In 2,6-dibromo- $\alpha,\alpha$ -diacetoxytoluene, the free energy of activation for rotation about the  $\text{Csp}^2\text{-Csp}^3$  bond is 36 kJ/mole at 165 K in dimethyl ether solution. This barrier implies a small  $^6J_p(\text{H},\text{CH})$  coupling since the latter is proportional to the expectation value of  $\sin^2\Theta$ . The angle  $\Theta$  is zero when the  $\alpha$  C-H bond lies in the plane of the benzene ring. For 2,6-dibromo- $\alpha,\alpha$ -diacetoxytoluene both a maximum magnitude of 0.02 Hz and a magnitude of zero at  $\Theta = 0^\circ$  are compatible with the measured free energy barrier. For  $\alpha,\alpha,2,6$ -tetrachlorotoluene, a compound with a higher internal barrier, the experimental results suggest a negligibly small  $^6J_p(\text{H},\text{CH})$  at  $\Theta = 0^\circ$ .

## F. REFERENCES



- 1) W. J. E. Parr and T. Schaefer, *Acc. Chem. Res.*, 13 , 400 (1980).
- 2) T. Schaefer, R. P. Veregin, R. Laatikainen, R. Sebastian, K. Marat and J. L. Charlton, *Can. J. Chem.*, 60 , 2611 (1982).
- 3) T. Schaefer, J. Peeling and R. Sebastian, *Can. J. Chem.*, 65 , 3219 (1985).
- 4) T. Schaefer, G.H. Penner and R. Sebastian, *Can. J. Chem.*, 65 , 873 (1987).
- 5) G. H. Penner, *Can. J. Chem.*, 65 , 538 (1987).
- 6) T. Schaefer, R. Sebastian and G. H. Penner, *Can. J. Chem.*, 63 , 2597 (1985).
- 7) C. Heller and H. M. McConnell, *J. Chem. Phys.*, 32 , 1535 (1960).
- 8) A.I. Vogel. *Practical organic chemistry*. Longmans, London, 1956. 3rd ed. p. 769.
- 9) A. R. Quirt and K. E. Worvill. *The NMR program library*. Daresbury Laboratory, Daresbury, UK.
- 10) *SAS User's Guide : Statistics*; A. A. Ray (ed.), (Statistical Analysis System Institute, 1982).
- 11) *SAS/Graph User's Guide*. K. A. Council and J. T. Helwig (ed.) , (Statistical Analysis System Institute, 1982).
- 11a) W. A. Anderson and R. Freeman, *J. Chem. Phys.*, 37 , 83 (1962).
- 12) R. R. Ernst, E. Bodenhausen and A. Wokaun. *Principles of nuclear magnetic resonance in one and two dimensions*. Oxford University Press, Oxford, 1987. Section 4.7.
- 13) S. Marriott, W. F. Reynolds, R. W. Taft and R. D. Topsom, *J. Org. Chem.*, 49 , 959 (1984).
- 14) R. Laatikainen, *Magn. Reson. Chem.*, 24 , 588 (1986).
- 15) T. Schaefer, R. Sebastian and G. H. Penner, *Can. J. Chem.*, 64 , 1372 (1986).
- 16) T. Schaefer, W. Niemczura and W. Danchura, *Can. J. Chem.*, 57 , 355 (1979).
- 17) N. L. Allinger and D. Y. Chung, *J. Am. Chem. Soc.*, 98 , 6798 (1976).
- 18) W. F. Bailey, H. Connon, E. L. Eliel and K. B. Wiberg, *J. Am. Chem. Soc.*, 100 ,

2202 (1978).

- 19) R. Laatikainen and E. Kolehmainen, *J. Magn. Reson.*, 65, 89 (1985).
- 20) G. Binsch and H. Kessler, *Angew. Chem. Int. Ed. Engl.*, 19, 411 (1980).
- 21) J. Peeling, L. Ernst and T. Schaefer, *Can. J. Chem.*, 52, 849 (1974).
- 22) J. Peeling, J. B. Rowbotham, L. Ernst and T. Schaefer, *Can. J. Chem.*, 52, 2414 (1974).
- 23) H. G. Gyulai, B. J. Fuhr, H. M. Hutton and T. Schaefer, *Can. J. Chem.*, 48, 3877 (1970).
- 24) T. Schaefer, R. Schwenk, C. J. Macdonald and W. F. Reynolds, *Can. J. Chem.*, 46, 2187 (1968).